UNIVERSITÀ DEGLI STUDI DI NAPOLI
"FEDERICO II"

Tesi di Dottorato

"New perspectives in the mechanisms of aging in animals"

Coordinatore	**Candidato**	**Tutor**
Ch.mo Prof. Giuseppe Cringoli	Dott. Davide De Biase	Ch.mo Prof. Orlando Paciello

To my tutor, Orlando

"*The mediocre teacher tells. The good teacher explains. The superior teacher demonstrates. The great teacher inspires*."

Thank you for constantly inspiring me. You made me possible.

To my family and friends,

"*Always the years between us. Always, the years. Always, the love. Always, the hours*"

Thank you for giving me the *hours*. You have made a sense of me.

To my colleagues of "XXX ciclo",

"*It has been a privilege playing with you*."

To myself,

"*Ti insegneranno a non splendere. E tu splendi, invece*"

Table of Contents

List of Abbreviations

AD Alzheimer's disease
ALS Amyotrophic Lateral Sclerosis
APAmyloid plaques
APP Amyloid-β protein precursor
Aβ Amyloid-β
BACE1 β-secretase 1
BER base excision repair
CA Cornu Ammonis region
CAACerebral amyloid angiopathy
CMA chaperone-mediated autophagy
CNS Central Nervous System
COX cytochrome oxidase
DP Diffuse or Amorphous Plaque
EP endogenous peroxidase
ET Engel trichrome
GVDGranulovacuolar degeneration
HE haematoxylin and eosin
HIER Heat Induced Epitope Retrieval
HR homologous recombination
IHC Immunohistochemistry
IL-1β interleukin-1 β
IL-6 interleukin-6
LC3 Microtubule-associated protein 1 light chain 3
LRP1low-density lipoprotein-like receptor
MAP microtubule-associated protein
MHC I Major Histocompatibility Complex I
MHC II Major Histocompatibility Complex II
MMR mismatch repair
NADH-TR reduced nicotinamide adenine dinucleotide tetrazolium reductase
NER nucleotide excision repair
NFT Neurofibrillary tangles
NHEJ non-homologous end joining

List of Abbreviations

NLRP3nucleotide-binding domain, leucine-rich-containing family, pyrin domain-containing-3
NP Neuritic Plaque
OH Hydroxyl radicals
PAMP pathogen associated molecular patterns
PAS Periodic acid–Schiff
PBS Phosphate-buffered Saline
PD Parkinson Disease
PK Proteinase K
PrP^c Cellular prion protein
PVDF PolyVinylidene DiFluoride
RAGE advanced glycation endproducts
ROS reactive oxygen species
RRF ragged red fibers
SAC Spindle assembly checkpoint
SDH succinate dehydrogenase
SDS PAGE Sodium Dodecyl Sulphate - PolyAcrylamide Gel Electrophoresis
s-IBM sporadic inclusion body myositis
SN substantia nigra
SOD1 Superoxide dismutase 1
TBS Tris-buffered saline
TLS translesion synthesis
TNF-α tumor necrosis factor α
TRITC Tetramethylrhodamine
TTBS Tween Tris-Buffered Saline
WMD white matter degeneration
DAMP damage-associated molecular patterns

List of Figures

List of Tables

Abstract

In recent years, the study of aging process in humans and animals has progressed rapidly, mainly due to the advent of new research instruments and our increasing liability to assemble large, complex data sets acquired across several approaches into an integrated representation of neural and muscular function at the molecular, cellular, and systemic levels. The overall aim of my Ph.D. thesis was to describe the age-related morphological changes in brain and skeletal muscle of cattle and to investigate some of the mechanisms and pathways underlying the aging process of Central Nervous System. First, I describe morphological changes of brain tissue and skeletal muscle associated with old age. Second, I report our studies on autophagy, a highly regulated process involving the bulk degradation of cytoplasmic macromolecules and the possible consequences of the intraneuronal accumulation of lipofuscin, amyloid precursor protein (APP) and increased reactive oxygen species (ROS) on autophagy machinery. Finally, I present the results of our researches concerning one on the most recognized effects of aging: the "*immunosenescence*", the dysregulation of the immune system as a result of defects in both initiation and resolution of immune responses. Specifically, we investigated the expression of one of the major "culprits" of neuroinflammation, the NALP3 inflammasome and its association with autophagy and increased ROS production. Our results indicate that changes such as *satellitosis*, *lipofuscin accumulation* and *central chromatolysis* are quite consistent in bovine brains, although it is still debatable whether call them pathologic lesions or simply physiologic age-related alteration. Moreover, we confirm the presence of age-related morphologic changes in skeletal muscle of cows similar to human *sarcopenia* and underline the possible role of amyloid deposition and subsequent inflammation in muscle senescence. In aged bovine, autophagy is significantly impaired if compared to young animals. In our opinion, this data suggest that the increased age-related intraneuronal deposition of APP and lipofuscin may have an important role on the age-related autophagy impairment. Consistent with the recent scientific literature, our findings showed an increased expression of NLRP3 inflammasome in neurons and

microglial cells of aged brains when compared with younger, indicating that the NLRP3 inflammasome is up-regulated in the brain as a result of aging. We also report a direct association between NLRP3 inflammasome, Superoxide Dismutase 1 (SOD1) and autophagy marker Beclin 1. The consequences of the autophagy and inflammasomes interplay are still poorly understood. Our results led us to hypothesize that the increased ROS production may activate inflammasomes provoking a low-grade inflammation thus accelerating the aging process. Furthermore, the activation of inflammasomes may lead to an induction of autophagy that work to limit inflammasome activity by physical engulfment. This Ph.D thesis is the outcome of several experiments, all aimed to elucidate the molecular mechanisms resulting in morphologic and/or clinical age-related alterations of brain and skeletal muscle in cows. Our ultimate goal is to improve our understanding of aging with more detailed studies and, possibly, include bovine as a valuable animal model for the study of brain aging, sarcopenia and other age-related alterations.

General Background

Hallmarks of aging

Aging, by definition, is the ineluctable, time-dependent, gradual and progressive impairment in physiological organ function and tissue homeostasis that eventually leads to death (Aunan, 2016). Paraphrasing what Peter Pan said: “getting older is inevitable” (but growing up is a choice!) and a universal process, common among the species despite differences in lifespan. Thus, researchers have suggested the possible existence of a similarly universal mechanism of aging regulation. In a pivotal and very important paper, Lòpez-Otin et al (2013) have perfectly delineated nine hallmarks of aging also summarizing new crucial insights underlying the molecular mechanisms of the aging process. The nine hallmarks can be grouped into three main categories: primary hallmarks, antagonistic hallmarks and integrative hallmarks (Fig. 1) (Lòpez-Otin, 2013). **Primary hallmarks** are the principal culprit, responsible of the damage to cellular functions and comprise *genomic instability, telomere attrition, epigenetic alterations* and *loss of proteostasis*. **Antagonistic hallmarks** represent the response to cellular damage and comprise *deregulated nutrient sensing*, *mitochondrial dysfunction* and *cellular senescence*. Last, but not least, **integrative hallmarks** contribute to the clinical effects of ageing, therefore responsible of the clinical phenotype of aging characterized by physiological loss of reserve, organ decline and reduced function. Integrative hallmarks include *stem cell exhaustion* and *altered intercellular communication*.

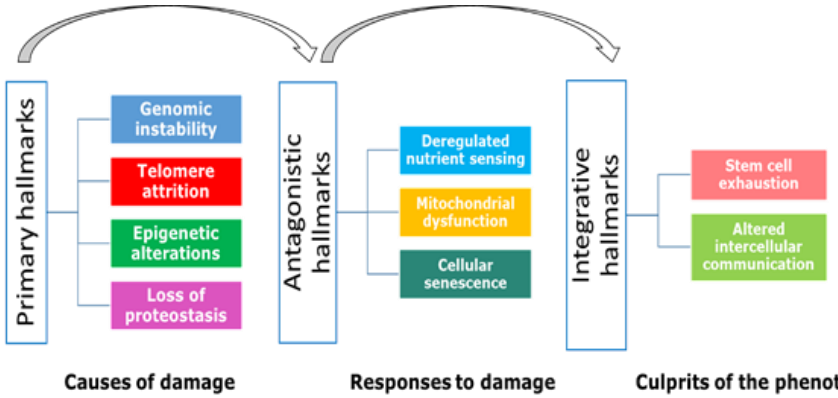

Fig. 1. Functional Interconnections between the Hallmarks of Aging *(modified Lòpez-Otin, 2013)*

Primary hallmarks

Genomic instability

Accumulation of genetic damage throughout life is a common denominator of aging (Moskalev et al., 2012). Accumulated DNA damage is implicated directly in carcinogenesis and other age-associated disorders, such as neurodegenerative diseases (Kryston et al., 2011). The integrity and stability of DNA are constantly exposed to all kinds of possible threats, both exogenous (physical, chemical and biological) and endogenous (DNA replication errors, spontaneous hydrolytic reactions and reactive oxygen species) (Hoeijmakers, 2009). Genetic lesions arising from extrinsic or intrinsic damages are usually fixed by a powerful cellular DNA repair machinery (Friedberg, 2003). Genetic instability may range from small point mutations to large chromosome breaks and translocations, so implications may vary from silent mutation that codes for the same amino acid, to the more severe activation of oncogenes or silencing of tumour suppressor genes (Aunan, 2016).

Telomere attrition

Normal aging is accompanied by telomere attrition in mammals (Lòpez-Otin, 2013). Telomeres are repetitive nucleotide sequences that protect the ends of chromosomes maintaining genomic stability. Telomeres are particularly susceptible to age-related deterioration and their dysfunction and genomic instability appear to be of critical importance for aging at a cellular level (Pusceddu, 2015; Xie, 2015). Telomere shortening is observed during normal aging both in human and mice (Blasco, 2007), but also to age-related diseases and premature ageing syndromes. In 1961, Hayflick and Moorhead noted that human diploid cells lines had limited proliferative capacity *in vitro* (Hayflick and Moorhead, 1961). With their fundamental experiments, Hayflick and Moorhead postulated the so-called "*telomerase theory of ageing*" and the *Hayflick limit.* This theory founds on the observation that most human somatic cells do not express *telomerase*, an enzyme capable of extending the telomere ends of human DNA. Human DNA polymerase is actually incapable to fully replicate the telomere ends of DNA. Thus, each cell division leads to progressive shortening of the DNA strands. Therefore, the cells enter replicative senescence after a certain number of divisions and associated telomere shortening (the Hayflick limit) in order to avoid coding parts of the DNA. In the absence of telomerase, telomeres are progressively shortened. However, even in the presence of telomerase, the infliction of exogenous DNA damage to telomeres becomes invisible to the DNA repair machineries producing a persistent type of DNA damage that leads to deleterious cellular effects including senescence and/or apoptosis (Fumagalli et al., 2012).

Epigenetic alterations

Epigenetic alteration refers to changes in gene expression that are achieved without mutating the original base sequence of the affected genes (Aunan,

2016). Epigenetic alteration patterns vary frequently in an age-dependent manner. Epigenetic changes involve alterations in mechanisms such as DNA methylation, post-translational modification of histones, chromatin remodeling and non-coding RNA. *DNA methylation* is a process by which methyl groups are added to the DNA molecule. DNA methylation seems not only to be a predictor of human age (Bocklandt, 2011; Hannum, 2013; Koch, 2011), but it also represent a risk measure other than chronological age itself. A study of Marioni et al. (2015) correlated increased risk of death with methylation status, which was independent of other known risk factors, such as smoking, diabetes, hypertension and chronological age alone. *Histone modifications* are a variety of covalent, reversible chemical reactions (acetylations, mono-, di- and tri-methylations and phosphorylations are the most common) that add or subtract moieties to amino acid residues of the histone protein octamers (Aunan, 2016). In a process similar to genetic instability patterns in cancer, chromatin and gene expression are destabilized when there is loss or gain of specific histone-modifier proteins such as histone deacetylases or histone methyltransferases (Aunan, 2016). Global depletion is the first histone-associated mechanism affecting ageing (Das et al, 2013). *Non-coding RNAs* also play an important role in gene silencing and regulation. MicroRNAs (miRNAs) are short single-stranded RNAs (about 22 nucleotides) that may regulate up to 80% of all expressed genes (Kozomara, 2011; Lu, 2012). miRNAs are believed to play a really important role in aging. They are involved in regulation of senescence-related genes and pathways (Bonifacio, 2010), the modulation of insulin/insulin-like growth factor (IGF) 1 signalling and target of rapamycin (TOR) signalling pathways, whose conserved role in ageing is well established (Barzilai, 2012; Kenyon, 2010; Lòpez-otìn, 2013). Furthermore, miRNAs are also involved in immunosenescence, the age-reated decline of the immune system, another hallmark of human ageing (Aalaei-Andabili, 2015). Epigenetic alterations have often been linked to detrimental effects that may cause ageing or accelerate ageing processes. It has to be further investigated whether epigenetic alterations represent the

cause or the consequence of ageing, and how they affect the ageing process and age-related diseases.

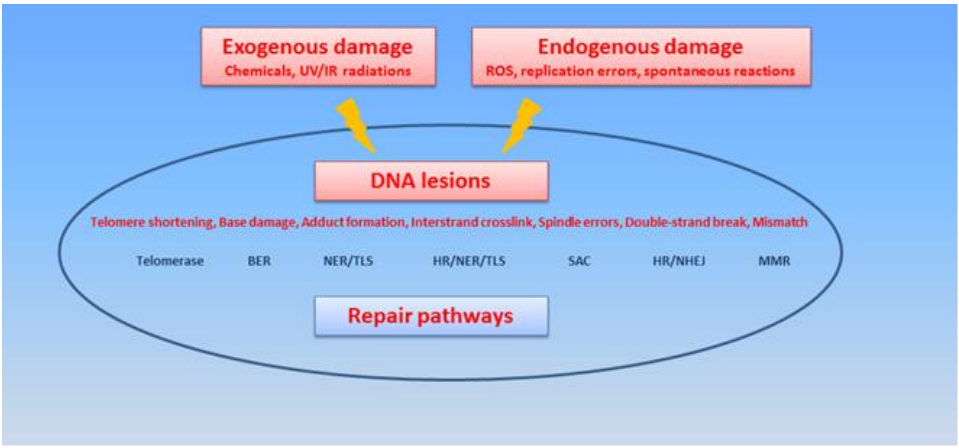

Fig. 2 Genomic instability and telomere attrition. *Endogenous or exogenous agents can stimulate a variety of DNA lesions. Such lesions can by repaired by a variety of mechanisms. Excessive DNA damage or insufficient DNA repair favors the aging process. BER, base excision repair; HR, homologous recombination; NER, nucleotide excision repair; NHEJ, non-homologous end joining; MMR, mismatch repair; ROS, reactive oxygen species; TLS, translesion synthesis; SAC, spindle assembly checkpoint (modified from Lòpez-Otin, 2013).*

Loss of proteostasis

The word *"proteostasis"* encompasses cellular mechanisms involved in maintaining the homeostasis of the proteome, the stabilization of correctly folded proteins and mechanisms for the degradation of proteins by the proteasome or the lysosome system (Eisenstein et al, 2014). The accumulation and aggregation of misfolded proteins is the principal cause of some of the most common age-associated modifications and diseases in humans and animals (Labbadia et al, 2015; Youssef et al, 2016). The proteostasis network consists of *chaperone-mediated folding, proteasomal degradation* and *autophagy*. All these systems works to remove and degrade misfolded polypeptides either preventing the accumulation of damaged components or completely restoring their structure, thus assuring

the continuous renewal of intracellular proteins. Several studies have demonstrated a progressive cellular impairment in maintaining homeostasis of the proteome with age, leading to protein aggregation and inclusions in almost all tissues of the aged organism (Koga et al., 2011). *Molecular chaperones* are small proteins that assist native polypeptide chains in the folding into functional protein structures and their activity is significantly impaired in aging (Calderwood et al., 2009). The autophagy-lysosomal system and the ubiquitin-proteasome are two principal proteolytic systems implicated in protein quality control. *Proteasome activity* was found to be high in centenarians, and it has been postulated to be one of the main mechanisms for their healthy aging (Chondrogianni, 2000). *Autophagy* is a highly regulated process involving non-specific degradation of cytoplasmic macromolecules and organelles via the lysosomal system. The activities of the autophagy-lysosomal system and the ubiquitin-proteasome system, decline with aging (De Biase et al, 2017; Rubinsztein et al., 2011; Tomaru et al., 2012), supporting the idea that collapsing proteostasis constitutes a common feature of old age.

Antagonistic hallmarks

Antagonistic hallmarks comes to the rescue as a response to molecular and cellular damage mechanisms in the form of *deregulated nutrient sensing*, *mitochondrial dysfunction* and induction of *cellular senescence*. At low intensity, these antagonistic forms may be beneficial (for example, senescence protect the cell from carcinogenic transformation) whereas at high intensity they can induce the aging process and also play a role in disease development (Aunan, 2016).

Deregulated nutrient sensing

The ability to use nutrients and fluids in metabolic processes is vital at the cellular level and guarantee the growth and maintenance of bodily

functions throughout life of both humans and animals. *Nutrient sensing* is a cellular process within an organism that ensures proper levels of nutrition for optimal metabolic function. Namely, glucose is one of the most important substrate for homeostatic mechanisms and different hormones and nutrients are involved in maintaining its levels in blood within a physiological range (Aunan, 2016). In old age, many of these sensors and molecular targets that monitors and regulate nutrition are lost or downregulated, thus they become unable to function properly (Aunan, 2016). Consistent with the relevance of deregulated nutrient-sensing as a hallmark of aging, *dietary restriction* (DR) increases lifespan or healthspan in eukaryote species, including unicellular and multicellular organisms and also non-human primates (Colman et al., 2009; Fontana et al., 2010; Mattison et al., 2012). Calorie restricted diets are unfortunately difficult to manage, particularly in humans (Scheen et al., 2008). However, several authors are currently investigating possible pharmacological substitutes that could induce the same beneficial metabolic response (Ingram et al, 2015). Finally, the ability of an organism to respond or adapt according to changes in metabolic or energy demand as well as the prevailing conditions or activity is known as *metabolic flexibility* (Goodpaster and Sparks, 2017). According to the "metabolic flexibility theory of aging", that longevity is dependent on metabolic health and on functional, healthy mitochondria that are able to use carbohydrates, proteins and fatty acids for energy production. Upon disruption of mitochondrial integrity the cell is unable to maintain flexible metabolic homeostasis and, subsequently, respond to metabolic demand (Nunn et al., 2009).

Mitochondrial Dysfunction

Over three decades ago Harman was one of the first to propose that mitochondrial dysfunction plays a central role in aging (Harman, 1972). Harman's "free radical theory of aging" suggested that reactive oxygen species (ROS) can have deleterious effects on various cell components. Levels of reactive oxygen species are increased in old age and have been

associated with a decline in mitochondrial integrity as the mitochondria are the main producers of these radicals (Harman, 1972). More recently, a growing body of evidence pointed to the new emerging concept that high levels of reactive oxygen species do not aggravate the aging process, but rather slow it down (Yang et al., 2010; Yee et al, 2014). Reactive oxygen species may, in fact, function as signaling molecules that trigger pathways involved in cellular homeostasis. Above a certain threshold, reactive oxygen species are therefore tolerable and may also extend lifespan or reduce cell death (Hekimi et al., 2011). Such hormetic reactions are known as "*mitohormesis*" and they may consist in the induction of adaptive compensatory processes and protective mechanisms within the cells either in the same tissue in which mitochondria are defective or even in distant tissues (Lòpez-Otin et al., 2013). However, the timing of mitochondrial perturbation seems to be essential with regard to the extent to which it affects cellular metabolism. This is exemplified by the fact that many diseases associated with old age are related to mitochondrial dysfunction and deregulation of the mitochondrial biomass (Aunan, 2016).

Cellular senescence

Cellular senescence can be defined as an irreversible process characterized by stable arrest of the cell cycle coupled to stereotyped phenotypic alterations, including chromatin and secretome changes (Campisi and d'Adda di Fagagna, 2007; Collado et al., 2007; Kuilman et al., 2010). Senescent cells are usually removed by immune surveillance and phagocytosis, but seem to accumulate with age (Hoenike et al., 2012; Kang et al., 2011; Sagiv et al., 2013). The age-related accumulation of senescent cells can be associated to an increase in the rate of generation of senescent cells and/or a decrease in their rate of clearance (Lòpez-Otin et al., 2013). In aged organisms, this an efficient cell replacement system may become inefficient or may exhaust the regenerative capacity of progenitor cells, eventually resulting in the accumulation of senescent cells aggravating the damage and contributing to aging. It has been recently observed that

senescent cells manifest dramatic alterations in their *secretome*, referred to as the totality of secreted organic molecules and inorganic elements by cells. Secretome of senescent cells is particularly enriched in pro-inflammatory cytokines, interleukins, growth factors and matrix metalloproteinases (Kuilman et al., 2010; Rodier and Campisi, 2011). It is believed that the accumulation of senescent cells and their associated secretome constitutes one of the mechanisms of ageing and age-related diseases (Aunan, 2016).

Integrative hallmarks

Finally, stem cell exhaustion and altered intercellular communication represent the rate-limiting intrinsic alterations responsible for the clinical signs of aging.

Stem cell exhaustion

The decline in the regenerative potential of tissues is one of the most obvious characteristics of aging. For example, haematopoietic stem cell exhaustion leads to anaemia resulting in *immunosenescence*, a diminished production of adaptive immune cells and in an increased incidence of anemia and myeloid malignancies (Shaw et al., 2010). Mesenchymal stem cell decline leads to osteoporosis and fractures; and intestinal epithelial stem cell depletion causes decreased intestinal function (Lòpez-Otin et al., 2013). Muscle stem cells or satellite cell dysfunction have also been implicated in *sarcopenia*, the muscle loss associated with ageing. Stem cell exhaustion unfolds as the integrative consequence of multiple types of aging-associated damages and likely constitutes one of the ultimate culprits of tissue and organismal aging. Recent promising studies suggest that stem cell rejuvenation may reverse the aging phenotype at the organismal level (Rando and Chang, 2012).

Altered intercellular communication

Beyond cell-autonomous alterations, effects of aging also involve changes in intercellular communication, including endocrine, neuroendocrine, neuronal and inflammatory signalling. A prominent age-related alteration in intercellular communication is is the dysregulation of the immune system as a result of defects in both initiation and resolution of immune responses (*immunosenescence*) and chronic low-grade inflammation (*inflammaging*) (Franceschi et al., 2007; Montecino-Rodriguez et al., 2013). Inflammaging may result from multiple causes such as the accumulation of pro-inflammatory tissue damage, the failure of an ever more dysfunctional immune system to effectively clear pathogens and dysfunctional host cells, the propensity of senescent cells to secrete pro-inflammatory, the enhanced activation of the NF-κB transcription factor, or the occurrence of a defective autophagy response (Salminen et al., 2012). These alterations result in an enhanced activation of the NLRP3 inflammasome and other pro-inflammatory pathways, finally leading to increased production of IL-1ß, tumor necrosis factor and interferons (Green et al., 2011; Salminen et al., 2012). Inflammaging is associated with frailty, morbidity and mortality in elderly people (Capri et al., 2014).

Specific Background

The severity of aging and age-related deterioration varies greatly between individuals and it varies also in a tissue specific manner (Youssef et al., 2016). Many of the degenerative changes in tissue are usually encountered in veterinary medicine in the geriatric population of companion animals (dog, cat and horse). With respect to the Central Nervous System (CNS) and neuromuscular system, a statement can be made that applies equally to all diseases of humans and animals: some disorders are highly comparable, some share some points of similarity and others are limited to humans or to individual animal species.

The aging brain

Brain is probably the most vulnerable tissue affected by aging because of its high oxygen requirement, low synthetic capacity of endogenous antioxidants, and limited regeneration capability (Dror et al., 2014). Brain aging is associated not only with molecular and morphological changes but also with declining cognitive functions that cannot be attributed to other medical conditions. Cognitive dysfunction disorders are described in dogs and recently in cats and horses (Youssef et al., 2016). However, the correlation between these conditions and age-related neurologic lesions is not completely understood. Various age-associated neuronal lesions are found in humans and animals, and some of them are considered to be the hallmarks of several human neurodegenerative disorders.

Neuronal lesions

Necrotic or apoptotic processes induced by mitochondrial or endoplasmic reticulum stress or the disturbance of autophagy or ubiquitin/proteasome systems are responsible of *neuronal cell loss*, one of the most common

lesions associated with aging (Ghavami et al., 2014). Significant neuronal loss leads to a reduction in neuronal density and ultimately *brain atrophy* that is defined as the gradual reduction in brain volume and size after reaching its mature size (Youssef et al., 2016). Grossly, brain atrophy is characterized by decreased volume and weight, a darker gray-yellow discoloration being and it may be firmer than normal. The meninges are usually thickened (due to fibrosis and/or mineralization) and become partially adherent to the skull. The gyri or folds are narrowed and wrinkled and the sulci become shallow and widened. The ventricles are mildly to moderately dilated (Maxie et al., 2007). The *neurofibrillary tangles* (NFTs) are intraneuronal filamentous inclusions within the perikaryal region of pyramidal neurons composed of hyperphosphorylated and misfolded insoluble tau protein that become extraneuronal ("ghost" tangles) when tangle-bearing neurons die (Serrano-Pozo et al., 2011). In humans, NFT are a major microscopic hallmark of Alzheimer's disease (AD). NFTs have a stereotypical spatiotemporal progression that correlates with the severity of the cognitive decline. The first NFTs consistently appear in the transentorhinal (perirhinal) region (stage I) along with the entorhinal cortex proper, followed by the CA1 region of the hippocampus (stage II). Next, NFTs develop and accumulate in limbic structures such as the subiculum of the hippocampal formation (stage III) and the amygdala, thalamus, and claustrum (stage IV). Finally, NFTs spread to all isocortical areas (isocortical stage), with the associative areas being affected prior and more severely (stage V) than the primary sensory, motor, and visual areas (stage VI) (Serrano-Pozo et al., 2011). The NFTs are argyrophilic and can be shown by silver impregnation methods such as the Gallyas technique, with fluorescent dyes such as Thioflavin-S which recognize the β-sheet pleated structure of the paired helical filaments (De Biase and Paciello, 2015) or by immunostaining with anti-tau antibodies. NFTs are rarely found in animal brains, although they frequently form senile plaques with aging (Chambers et al., 2012). Interestingly, there is evidence of increased phosphorylated tau in some animal species even if typical NFTs have not been identified (Youssef et al., 2016). Typically, these tau changes tend to be sporadic and do not adopt the full blown features of intracellular

NFTs and are usually not associated with neuronal loss (Chambers et al., 2012). Age-dependent pigment accumulation, principally *lipofuscin*, is one of the most consistent features of aging. Lipofuscin is a yellowish, autofluorescent, pigment found in postmitotic cells, such as neurons and cardiomyocytes (De Biase et al., 2017). Lipofuscin can be stained with periodic acid–Schiff (PAS), Luxol fast blue, Sudan black B, and Ziehl-Neelsen acid fast stain (De Biase and Paciello, 2015). Lipofuscin granules are detectable in a small percentage of neurons in young brains, but become progressively and markedly more abundant with age (Bonavides et al., 2002). The rate of lipofuscin accumulation is the highest in the hippocampus and cerebral cortex among brain regions (Brunk and Terman, 2002). Lipofuscin was generally thought to be an innocent end product of oxidation which has no significant influence on cellular activities (Rubin and Farber, 1999). Conversely, recent evidences suggest that lipofuscin accumulation may decrease the cellular autophagic capacity (Brunk and Terman, 2002b), impair normal cellular functions (Mizushima, 2007) also promoting the accumulation of misfolded proteins or ensuing apoptosis (Powell et al., 2005). *Neuromelanin*, a dark brown pigment that is not autofluorescent, is an organic polymer produced by dopamine metabolism. It is primarily found in the neurons of the substantia nigra (SN) and the pinealocytes of the pineal glands in various animal species as well as humans (Yussef et al., 2016). In humans, the neurons of the SN contain large amounts of neuromelanin and the concentration of neuromelanin increases with age, while it is markedly decreased in Parkinson Disease (PD) patients. In dogs, the number of neuromelanin-bearing neurons in the SN tends to increase with age (Yussef et al., 2016). *Granulovacuolar degeneration* (GVD) is characterized by the intraneuronal accumulation of large (up to 5 μm diameter) membrane-bound vacuoles harbouring a central granule. GVD is tipically observed in Alzheimer's disease (AD), and classically detected in hippocampal pyramidal neurons. GVD also affects additional brain regions and is found increased in other adult-onset dementias including forms of frontotemporal lobar degeneration (Funk et al., 2011). Although there have been a few studies of hippocampal GVD in

aged animals, its morphological and immunohistochemical features have not been described in detail (Youssef et al., 2016).

Neuropilar lesions

Amyloid plaques (AP) are extracellular deposits of amyloid beta in the grey matter of the brain. Amyloid-β (Aβ) is a secreted peptide produced through sequential cleavage of the amyloid-β protein precursor (APP), a transmembrane protein widely expressed in the brain (Vallino-Costassa et al., 2016). Processed through the amyloidogenic pathway, the majority of cleaved Aβ peptides are 40 residues in length (Aβ40), and a minority is composed of the 42 residue variant (Aβ42), which is more hydrophobic and more prone to fibril formation (Vallino-Costassa et al., 2016). APs have been histologically classified into 2 types: the Mature or Neuritic Plaque (NP) and the Diffuse or Amorphous Plaque (DP). DPs are spherical extracellular deposits of Aβ that are up to 100 microns diameter and are negative for both Congo red and Thioflavin S (Youssef et al., 2016). DPs are typically not associated with a glial reaction, or neuronal and synaptic loss. DPs seems to not have a specific role in AD or any neuropathologic condition, since they are commonly found in cognitively intact elderly people (Youssef et al., 2016). NPs are spherical structures primarily composed of a core of extracellular amyloid fibrils surrounded by degenerating or dystrophic neurons and argyrophilic cholinergic neurites containing hyperphosphorylated tau. NPs are positive for both Congo red and thioflavin S (De Biase and Paciello, 2015) and they are usually accompanied by reactive astrocytes and microgliosis, and associated with synaptic loss. Amino acid sequence of Aβ is relatively conserved among mammalian species and age-related Aβ deposits have been detected in the brains of birds, primates, carnivores, bears, and some other mammalian species including bovine (Youssef et al., 2016; Vallino-Costassa et al., 2016). Other neuropilar changes comprise *neuroaxonal dystrophy* and *white matter degeneration*. Neuroaxonal dystrophy is characterized by spheroid formation due to axonal swelling. Neuronal dystrophy can be

congenital (not related to aging) or acquired (age-related) and it may be also seen in animals without any neurological signs. The distribution and diameter of swollen axons differs between each type of the condition (Youssef et al., 2016). In aged dogs, spheroids are often observed in the brain stem, especially in the dorsal column nuclei of the medulla oblongata as well as in the spinal cord (Youssef et al., 2016). Age-dependant white matter degeneration (WMD) consisting mostly in white matter atrophy has been observed in dogs (Chambers et al., 2012b). WMD is associated, in humans, to several neurodegenerative disoders such as Alzheimer's disease. However, WMD importance and pathogenetic significance in animals is yet to be completely understood.

Vascular Lesions

The aged canine is considered to be a unique model to study the cerebrovascular features of aging and AD due to the spontaneous nature of these same neuropathological features in older animals. *Cerebral amyloid angiopathy* (CAA) refers to the deposition of β-amyloid in the media and adventitia of small and mid-sized arteries (and, less frequently, veins) of the cerebral cortex and the leptomeninges (Pezzini et al., 2009). In humans, CAA has been recognized as one of the morphologic hallmarks of Alzheimer disease (AD), but it is also often found in the brains of elderly patients who are neurologically healthy. While often asymptomatic, CAA may lead to dementia, intracranial hemorrhage (ICH), or transient neurologic events (Weller et al., 2009). CAA is common in aged dogs and there is increasing recognition that it can be a significant contributor to clinical signs of cognitive dysfunction in this species. In dogs, Aβ is mainly deposited in the vascular walls of meningeal arterioles and/or capillaries in the deep cortex (Youssef et al., 2016). Age-dependent CAA is also reported in the cerebral blood vessels of cats and nonhuman primates, but not in horses (Youssef et al., 2016). Spontaneous *vascular degeneration* such as atherosclerosis is extremely rare in animals with the exception of aged pigs and birds, and also it occurs in dogs in association

with hypothyroidism. *Vascular mineralization* (calcification, siderocalcinosis) not pertaining to generalized vascular diseases is well documented in humans, monkeys, cows, mice, rats, cats, dogs and horses (Youssef et al., 2016). Mineral deposits generally stain positively with PAS, von Kossa, and Perl's stains, indicating the presence of mucopolysaccharides, calcium, and iron salts (De Biase and Paciello, 2015). Vascular mineralization has been considered an age-dependent incidental finding with an undetermined clinical significance, even if several authors referred neurological signs and areas of infarction with neovascularization in association with severe siderocalcinosis and vascular occlusion (Capucchio et al., 2010; Maxie and Yousseff, 2007; Martinez et al., 2012).

Glial Lesions

Glia, also called Neuroglia or Glial cells, are non-neuronal cells that comprise oligodendrocytes, astrocytes, ependymal cells and microglia (the guard machrophages-like cells of the CNS) in the Central Nervous System. In the peripheral nervous system glial cells include Schwann cells and satellite cells. Glial cells have a fundamental role in maintain homeostasis, form myelin, and provide support and protection for neurons both in the central and peripheral nervous systems. Damage to the central nervous system result in a non-specific reactive change of glial cells known as *gliosis*. *Reactive astrogliosis* is the most common form of gliosis and involves the proliferation of astrocytes, while microgliosis consists in the alteration of the morphology, surface phenotype and gene expression and increased number of microglial cells. Age-related astrocytosis or microgliosis not related to these conditions are poorly documented in humans and animals. Age-related astrocytosis and/or microgliosis have been reported in cattle and dogs (Youssef et al., 2016).

The aging muscle

Sarcopenia is a word used for the first time by Irwin Rosenberg (1997) to define the age related loss of muscle mass and strength. At present, sarcopenia has been defined as the condition of muscle wasting strictly linked to aging, characterized by loss of skeletal muscle mass and function, which may affect both animals and humans, at different stages of severity. Sarcopenia is a multifactorial condition that occurs in a variety of species and represents a major healthcare concern for older adults in human medicine (Pagano et al., 2015). The age-related alterations in skeletal muscle are mainly attributed to several factors, including neuromuscular junction, muscle structure (architecture and fiber composition), and metabolism (Pagano et al., 2015; Ryall et al., 2008; Sakuma et al., 2012). The loss of muscle mass and strength results from the progressive atrophy and loss of single muscle fibers, along with loss of both types of motor units (slow and fast). The pathogenesis of these alterations is associated with specific biological processes, such as oxidative stress (Sullivan-Gunn et al., 2013). Oxidative metabolism generates reactive oxygen species (ROS), which accumulate over time and are responsible for damaging and altering cell components, particularly mitochondria and DNA sequences (Carrì et al., 2015; Wang et al., 2012). Mitochondrial dysfunction is also involved in the pathogenesis of degenerative diseases, predisposing skeletal muscle to the accumulation of APP) (Schuh et al., 2014). Several studies have demonstrated that the age-related reduction in the synthesis of specific muscle proteins with a concurrent increase in proteolysis may result in the decline of muscle protein content and, subsequently, of muscle mass (Proctor et al., 1998; Nair, 2005; Augustin and Partridge, 2009). Skeletal muscle has four main proteolytic systems, namely, lysosomal, caspase, calpain and ubiquitin–proteasome, all of which could potentially contribute to age-related muscular atrophy. Our group has recently described the increased of autophagic markers such as Beclin-1 and LC3 in skeletal muscles of geriatric dogs, associated with several histochemical features of myopathy suggesting that enhanced autophagy might be one of

the factors underlying muscle atrophy in dogs as they age (Pagano et al., 2015).

Bovine as animal model of human diseases: a big animal for big resources

Translational medicine is focused on ensuring strategies for disease treatment and prevention and is constantly evolving through the improvement of well-established *in vitro* and *in vivo* models and the development of original paradigms (Peruffo and Cozzi, 2014). Animal models represent convenient and clinically relevant tools in the research on many human diseases. Animal models are essential for three main reasons: explore the underlying pathology and molecular mechanisms of disorders; evaluate the potential efficacy of therapeutic interventions; and provide an initial estimate of the safety margin and human dosing parameters of a drug candidate (McGonigle, 2014). Rodents (mostly mouse and rat) are the most commonly used animal models among the vertebrate species because of their ease of management and handling, fast reproduction, and low maintenance cost. However, the use of rodents in research has some limitations due mostly to the challenge associated with attempting to model complex and still poorly understood human disorders in a lower species (McGonigle, 2014). Thus, it has been suggested that larger mammals may also be a valuable tool because their more complex anatomy and physiology make them more directly comparable to humans in some respects (Gregory et al., 2012). Large animals are more similar to humans in relation to brain size and lifespan and could be therefore essential to investigate complex patho-physiological mechanisms relating to neurodegenerative diseases and infectious neuropathologies (Guildimann, 2012) or even, possibly, muscular disorders. The bovine species *Bos taurus* is a widespread domestic mammal, raised worldwide for meat and milk production. The bovine possesses a relatively large (approximately 600 g), highly gyrencephalic brain, in comparison to the smooth-surfaced brain of laboratory rodents (Hofman et al., 1985). A

number of studies have validated in vitro models based on neural primary cultures obtained from fetal bovine hypothalamus, cerebral cortex, and cerebellum, allowing examinations of neurons and/or glial cells under controlled and reproducible conditions. Furthermore, the CNS and muscle of bovine can be easily collected in large quantities at the slaughterhouse allowing a considerable reduction in the sacrifice of laboratory animals (Peruffo and Cozzi, 2014).

Objectives

The overall aim of this Ph.D. thesis was to investigate age-related morphological changes and molecular alterations in brain and skeletal muscle of aged bovine. Our ultimate goal was to provide a broader understanding and documentation of these alterations that may enhance the cultural awarness for veterinary pathologists and enrich future studies on bovine as animal model of human aging.

The specific objectives were:

1. Describe the age-related changes of brain and skeletal muscle in Podolica cows in order to highlight a new model of brain aging and sarcopenia for comparative studies.
2. Investigate the expression of autophagic markers such as Beclin 1 and LC3 and the accumulation lipofuscin and pathologic proteins such as APP in aged bovine brains.
3. Investigate the expression of NLRP3 inflammasome in bovine brains and its association with autophagy and oxidative stress.

REFERENCES

1. Aalaei-Andabili SH, Rezaei N. **MicroRNAs (MiRs) precisely regulate immune system development and function in immunosenescence process.** Int Rev Immunol 2015; [Epub ahead of print].
2. Aunan JR, Watson MM, Hagland HR, Søreide K. **Molecular and biological hallmarks of ageing.** Br J Surg. 2016 Jan; 103(2):e29-46. doi: 10.1002/bjs.10053.
3. Barzilai N, Huffman DM, Muzumdar RH, Bartke A. **The critical role of metabolic pathways in aging**. Diabetes 2012; 6: 1315–1322.
4. Bocklandt S, Lin W, Sehl ME, Sánchez FJ, Sinsheimer JS, Horvath S et al.**Epigenetic predictor of age.** PLoS One 2011; 6:e14821.
5. Benavides SH, Monserrat AJ, Farina S, Porta EA. **Sequential histochemical studies of neuronal lipofuscin in human cerebral cortex from the first to the ninth decade of life.** Arch. Gerontol. Geriatr. 2002;34:219-231
6. Bonifacio LN, JarstferMB. **MiRNA profile associated with replicative senescence, extended cell culture, and ectopic telomerase expression in human foreskin fibroblasts**. PloS One 2010; 5: e12519.
7. BrunkUT, Terman A. **Lipofuscin: Mechanisms of age-related accumulation and influence on cell functions**. Free Radic. Biol. Med. 2002;33:611–619
8. BrunkUT, Terman A. **The mitochondrial-lysosomal axis theory of aging: accumulation of damaged mitochondria as a result of imperfect autophagocytosis.** Eur J Biochem. 2002;269(8):1996-2002.
9. CalderwoodSK, Murshid A, Prince T. **The shock of aging: molecular chaperones and the heat shock response in longevity and aging--a mini-review.**Gerontology. 2009;55:550–558.
10. Capri M, Yani SL, Chattat R, Fortuna D, Bucci L,Lanzarini Cet al. **Pre-operative, high-IL-6 blood level is a risk factor of post-**

operative delirium onset in old patients. Front Endocrinol (Lausanne) 2014; 5: 173.

11. Capucchio MT, Márquez M, Pregel P, et al. **Parenchymal and vascular lesions in ageing equine brains: histological and immunohistochemical studies.**J Comp Pathol . 2010; 142(1):61–73.
12. CarrìMT, Valle C, Bozzo F. **Oxidative stress and mitochondrial damage: importance in non-SOD1 ALS**. Front Cell Neurosci. 2015; 9:41.
13. Chambers JK, Uchida K, Harada T, Tsuboi M, Sato M, Kubo M, et al. (2012) **Neurofibrillary Tangles and the Deposition of a Beta Amyloid Peptide with a Novel N-Terminal Epitope in the Brains of Wild Tsushima Leopard Cats**. PLoS ONE 2012; 7(10): e46452.
14. Chambers JK, Uchida K, Nakayama H.**White matter myelin loss in the brains of aged dogs**.Exp Gerontol. 2012 Mar;47(3):263-9.
15. Chondrogianni N, Petropoulos I, Franceschi C, Friguet B, Gonos ES. **Fibroblast cultures from healthy centenarianshave an active proteasome.** Exp Gerontol 2000; 35:721–728.
16. Colman RJ, Anderson RM, Johnson SC, Kastman EK, Kosmatka KJ, Beasley TM, Allison DB, Cruzen C, Simmons HA, Kemnitz JW, Weindruch R **Caloric restriction delays disease onset and mortality in rhesus monkeys.** Science. 2009 Jul 10; 325(5937):201-4.
17. Das C, Tyler JK. **Histone exchange and histone modifications during transcription and aging**. Biochim Biophys Acta 2013; 1819: 332–342.
18. De Biase D and Paciello O. **Essential and current methods for a practical approach to comparative neuropathology**Folia Morphol.Vol. 74, No. 2, pp. 137–149
19. De Biase D, Costagliola A, Pagano TB, Piegari G, Wojcik S, Dziewiątkowski J, Grieco E, Mattace Raso G, Russo V, Papparella S, Paciello O. **Amyloid precursor protein, lipofuscin accumulation and expression of autophagy markers in aged**

bovine brain BMC Vet Res. 2017 Apr 13;13(1):102. doi: 10.1186/s12917-017-1028-1.

20. Dror Y, Stern F, Gomori MJ**. Vitamins in the prevention or delay of cognitive disability of aging**. Curr Aging Sci 2014;7(3):187–213.
21. Eisenstein M. **Molecular biology: remove, reuse, recycle.** Nature 2014;514:S2–S4.
22. Fontana L, Partridge L, Longo VD **Extending healthy life span--from yeast to humans.**Science. 2010 Apr 16; 328(5976):321-6.
23. Franceschi C., Capri M., Monti D., Giunta S., Olivieri F., Sevini F., et al. **Inflammaging and anti-inflammaging: a systemic perspective on aging and longevity emerged from studies in humans.** Mech. Ageing Dev. 2007; 128: 92–105. doi: 10.1016/j.mad.2006.11.016
24. Friedberg EC. **DNA damage and repair.** Nature 2003; 421:436–440.
25. Fumagalli M, Rossiello F, Clerici M, Barozzi S, Cittaro D, Kaplunov JM, Bucci G, Dobreva M, Matti V, Beausejour CM, et al. **Telomeric DNA damage is irreparable and causes persistent DNA-damage-response activation.** Nat Cell Biol. 2012;14:355–365.
26. Funk KE, Mrak RE, Kuret J. **Granulovacuolar Degeneration Bodies of Alzheimer's Disease Resemble Late-stage Autophagic Organelles.** Neuropathology and applied neurobiology. 2011;37(3):295-306.
27. Ghavami S, Shojaei S, Yeganeh B, et al. **Autophagy and apoptosis dysfunction in neurodegenerative disorders**. Prog Neurobiol. 2014;112:24–49.
28. Goodpaster BH, Sparks LM. **Metabolic Flexibility in Health and Disease.**Cell Metab. 2017 May 2;25(5):1027-1036.
29. Green DR, Galluzzi L, Kroemer G**Mitochondria and the autophagy-inflammation-cell death axis in organismal aging**.Science. 2011 Aug 26; 333(6046):1109-12.

30. Gregory MH, Capito N, Kuroki K, Stoker AM, Cook JL, Sherman SL. **A review of translational animal models for knee osteoarthritis**. Arthritis 2012; 764621.
31. Guldimann C, Lejeune B, Hofer S, Leib SL, Frey J, Zurbriggen A, et al**. Ruminant organotypic brain-slice cultures as a model for the investigation of CNS listeriosis. Int J Exp Pathol** 2012; 93:259–68.
32. Hannum G, Guinney J, Zhao L, Zhang L, Hughes G, Sadda S et al. **Genome-wide methylation profiles reveal quantitative views of human aging rates.** Mol Cell 2013; 49:359–367.
33. Harman D. **The biologic clock: the mitochondria?** J Am Geriatr Soc 1972; 20: 145–7.
34. Hayflick L, Moorhead PS. **The serial cultivation of human diploid cell strains.** Exp Cell Res. 1961;25:585–621.
35. Hekimi S, Lapointe J, Wen Y. **Taking a 'good' look at free radicals in the aging process.** Trends Cell Biol 2011; 21:569–576.
36. Hoeijmakers JH. **DNA damage, aging, and cancer.** N Engl J Med. 2009; 361:1475–1485.
37. Hoenicke L, Zender L. **Immune surveillance of senescent cells – biological significance in cancer- and non-cancer pathologies**. Carcinogenesis 2012; 33: 1123–1126.
38. Hofman MA. **Size and shape of the cerebral cortex in mammals**. I. The cortical surface. Brain Behav Evol 1985; 27:28–40.
39. Ingram DK, Roth GS. **Calorie restriction mimetics: can you have your cake and eat it, too?** Ageing Res Rev 2015; 20:46–62.
40. Kenyon CJ. **The genetics of ageing**. Nature 2010; 464:504–512.
41. Kryston TB, Georgiev AB, Pissis P, Georgakilas AG. **Role of oxidative stress and DNA damage in human carcinogenesis.** Mutat Res 2011; 711:193–201.
42. Kang TW, Yevsa T, Woller N, Hoenicke L, Wuestefeld T, Dauch D et al. **Senescence surveillance of pre-malignant hepatocytes limits liver cancer development**. Nature 2011; 479: 547–551.
43. Koch CM, Wagner W. **Epigenetic-aging-signature to determine age in different tissues.** Aging (AlbanyNY) 2011;3: 1018–1027.

44. Koga H, Kaushik S, Cuervo AM. **Protein homeostasis and aging: The importance of exquisite quality control.** Ageing Res Rev. 2011;10:205–215.
45. Kozomara A, Griffiths-Jones S. **miRBase: integrating microRNA annotation and deep-sequencing data.** Nucleic Acids Res 2011; 39: D152–D157.
46. Kuilman T, Michaloglou C, Mooi WJ, Peeper DS **The essence of senescence.** Genes Dev. 2010 Nov 15; 24(22):2463-79.
47. Labbadia J, MorimotoRI. **The biology of proteostasis in aging and disease.**Annu Rev Biochem 2015; 84: 435–464.
48. Lòpez-Otin C, Blasco MA, Partridge L, Serrano M, Kroemer G. **The hallmarks of aging.** Cell 2013; 153:1194–1217.
49. Lu J, Clark AG. **Impact of microRNA regulation on variation in human gene expression.** Genome Res 2012; 22: 1243–1254.
50. Maxie MG, Youssef S. **Nervous system**. In: Maxie MG, ed. Jubb, Kennedy, and Palmer's Pathology of Domestic Animals. 5th ed, vol.1. Philadelphia, PA:Elsevier; 2007:281–457
51. Marioni RE, Shah S, McRae AF, Chen BH, Colicino E, Harris SE et al. **DNA methylation age of blood predicts all cause mortality in later life.** Genome Biol 2015; 16:25.
52. Martınez J, Montgomery DL, Uzal FA. **Vascular mineralization in the brain of horses.** J Vet Diagn Invest. 2012; 24(3):612–617.
53. Mattison JA, Roth GS, Beasley TM, Tilmont EM, Handy AM, Herbert RL, Longo DL, Allison DB, Young JE, Bryant M, Barnard D, Ward WF, Qi W, Ingram DK, de Cabo R **Impact of caloric restriction on health and survival in rhesus monkeys from the NIA study.** Nature. 2012 Sep 13; 489(7415):318-21.
54. McGonigle P. **Animal models of CNS disorders**. 2014 Biochem Pharmacol 87:140–9
55. Mizushima N. **Autophagy: Process and function**. Genes Dev. 2007;21:2861–2873.
56. Montecino-Rodriguez E., Berent-Maoz B., and Dorshkind K. **Causes, consequences, and reversal of immune system aging**. J. Clin. Invest. 2013; 123,:958–965. doi: 10.1172/JCI64096

57. Moskalev AA, Shaposhnikov MV, Plyusnina EN, Zhavoronkov A, Budovsky A, Yanai H, Fraifeld VE. **The role of DNA damage and repair in aging through the prism of Koch-like criteria**. Ageing Res Rev. 2012
58. Nunn AVW, Bell JD, Guy GW. **Lifestyle-induced metabolic inflexibility and accelerated ageing syndrome: insulin resistance, friend or foe?** Nutr Metab (Lond) 2009; 6:16
59. Peruffo A and Cozzi B **Bovine brain: an in vitro translational model in developmental neuroscience and neurodegenerative research**Front. Pediatr. 2:74.
60. Pezzini A, Del Zotto E, Volonghi I, Giossi A, Costa P, Padovani A. **Cerebral amyloid angiopathy: a common cause of cerebral hemorrhage.** Curr Med Chem. 2009;16(20):2498-513.
61. Powell SR, Wang P, Divald A, Teichberg S et al. **Aggregates of oxidized proteins (lipofuscin) induce apoptosis through proteasome inhibition and dysregulation of proapoptotic proteins**. Free Radic Biol Med. 2005;38(8):1093-101.
62. Pusceddu I, Farrell CJ, Di Pierro AM, Jani E, Herrmann W, Herrmann M. **The role of telomeres and vitamin D in cellular aging and age-related diseases.** Clin Chem Lab Med 2015; 53: 1661–1678.
63. Rando TA, Chang HY **Aging, rejuvenation, and epigenetic reprogramming: resetting the aging clock**. Cell. 2012 Jan 20; 148(1-2):46-57.
64. Rodier F, Campisi J **Four faces of cellular senescence**. J Cell Biol. 2011 Feb 21; 192(4):547-56.
65. Rosenberg IH. **Sarcopenia: origins and clinical relevance.** J Nutr . 1997; 127 (5):990S–991S.
66. Rubin E, Farber JL. **Cell injury**. In Rubin E, Farber JL, eds Pathology, Lippincott–Raven, Philadelphia; 1999:1–34
67. RubinszteinDC, Marino G, Kroemer G. **Autophagy and aging.** Cell. 2011; 146:682–695.

68. Ryall JG, Schertzer JD, Lynch GS. **Cellular and molecular mechanisms underlying age-related skeletal muscle wasting and weakness.** Biogerontology. 2008;9(4):213–228.
69. Sagiv A, Krizhanovsky V. **Immunosurveillance of senescent cells: the bright side of the senescence program.** Biogerontology 2013; 14: 617–628.
70. Sakuma K, Yamaguchi A. **Molecular and cellular mechanism of muscle regeneration**. In: Cseri J, ed. Skeletal Muscle: From Myogenesis to Clinical Relations.Rijeka, Croatia: InTech; 2012: 3–18.
71. Salminen A, Kaarniranta K, Kauppinen A**Inflammaging: disturbed interplay between autophagy and inflammasomes.**Aging (AlbanyNY). 2012 Mar; 4(3):166-75.
72. Scheen AJ. **The future of obesity: new drugs versus lifestyle interventions**. Expert Opin Investig Drugs 2008; 17:263–267.
73. Schuh RA, Jackson KC, Schlappal AE, et al. **Mitochondrial oxygen consumption deficits in skeletal muscle isolated from an Alzheimer's disease–relevant murine model.** BMC Neurosci. 2014;15:24.
74. Serrano-Pozo A, Frosch MP, Masliah E, Hyman BT. **Neuropathological Alterations in Alzheimer Disease**. Cold Spring Harbor Perspectives in Medicine: 2011;1(1):a006189.
75. Shaw AC, Joshi S, Greenwood H, Panda A, Lord JM. **Aging of the innate immune system.**Curr Opin Immunol. 2010 Aug; 22(4):507-13.
76. Sullivan-Gunn MJ, Lewandowski PA. **Elevated hydrogen peroxide and decreased catalase and glutathione peroxidase protection are associated with aging sarcopenia**. BMC Geriatr. 2013; 13:104
77. Tomaru U, Takahashi S, Ishizu A, Miyatake Y, Gohda A, Suzuki S, Ono A, Ohara J, Baba T, Murata S, et al. **Decreased proteasomal activity causes age-related phenotypes and promotes the development of metabolic abnormalities.** Am J Pathol. 2012; 180:963–972.

78. Vallino Costassa E, Fiorini M, Zanusso G, et al. **Characterization of Amyloid-β Deposits in Bovine**. J Alzheimers Dis. 2016;51(3):875–87.
79. Yang W, Hekimi S. **A mitochondrial superoxide signal triggers increased longevity in Caenorhabditis elegans**. PLoS Biol 2010; 8: e1000556.
80. Yee C, Yang W, Hekimi S. **The intrinsic apoptosis pathway mediates the pro-longevity response to mitochondrial ROS in C. elegans.** Cell 2014; 157: 897–909.
81. Youssef SA, Capucchio MT, Rofina JE, Chambers JK, Uchida K, Nakayama H, Head E. **Pathology of the Aging Brain in Domestic and Laboratory Animals, and Animal Models of Human Neurodegenerative Diseases.**Vet Pathol. 2016 Mar;53(2):327-48.
82. Xie Z,Jay KA,Smith DL,Zhang Y,Liu Z,Zheng J et al. **Early telomerase inactivation accelerates aging independently of telomere length.** Cell 2015; 160: 928–939.
83. Wang JL, Wang PC. **The effect of aging on the DNA damage and repair capacity in 2BS cells undergoing oxidative stress**. Mol Biol Rep. 2012; 39(1):233–241.
84. Weller RO, PrestonSD, Subash M, Carare RO.**Cerebral amyloid angiopathy in the aetiology and immunotherapy of Alzheimer disease**. Alzheimers Res Ther. 2009 Oct 12;1(2):6.

Chapter 1

Age-related changes in brain and skeletal muscle of cattle

Based on manuscripts:
Costagliola A, Wojcik S, Pagano TB, De Biase D, Russo V, Iovane V, Grieco E, Papparella S, Paciello O ***Age-Related Changes in Skeletal Muscle of Cattle***. Vet Pathol. 2016 Mar;53(2):436-46.
De Biase D and Paciello O. ***Essential and current methods for a practical approach to comparative neuropathology*** Folia Morphol. 2015 Vol. 74, No. 2, pp. 137–149

1.1 INTRODUCTION

The understanding of mechanisms underlying the aging process in humans and in animals has progressed rapidly in recent years, mainly due to the advent of new research instruments and our increasing liability to assemble large, complex data sets acquired across several approaches into an integrated representation of neural and muscular function at the molecular, cellular, and systemic levels. Nevertheless, morphology always represents the essential approaches that are crucial for any kind of interpretation of the lesions or to explain new molecular pathways of the diseases. A wide variety of age-related changes have been extensively described in the nervous system of many species (Youssef et al., 2016) and also *sarcopenia*, the age-related loss of skeletal muscle mass and function, has been extensively described in several animal species, from nematodes, flies, rodents, domestic and wild animals, and nonhuman primates to humans (Costagliola et al., 2016). However, no information is available about sarcopenia in farm animals and only few studies have investigated age-related changes in the brain of cattle (Gavier-Widen et al., 2001; Yanay et al., 1994).

The first year of my Ph.D has been dedicated to describe the age related changes of the brain and muscle of Podolica cattle. We also investigated the expression of cellular prion protein (PrP^{c}) in aged bovine brains, in order to evaluate if theaging process may alter PrP^{C} biochemical properties, influencing its propensity to convert into its conformational and pathogenic isoform, the prion (or PrP^{Sc}). Part of the experiments on brain tissue have also been designed to illustrate the newest and also well-established principal methods for the nervous tissue collection and processing as well as to describe the histochemical and immunohistochemical staining tools that are currently most suitable for a neuropathological assessment of the central nervous system.

1.2 MATERIALS AND METHODS

1.2.1 Animals

For this study, brains were collected from thirty Podolic dairy cattle (1–20 years old) (Table 1) in an abattoir in CampaniaRegion, Italy, during post mortem inspection. Permission to obtain the samples was granted from the owner of the abattoir and from the veterinary inspector responsible for the sanitary surveillance. Each animal underwent a physical examination that did not report any apparent clinical illness or neurological sign (gait abnormalities, weakness and decreased mental status). Afterward, the animals were slaughtered in strictly accordance with European slaughter regulations (CE n° 1099/2009). Animals were divided in two groups: group A (old) comprised bovine aged more than ten years (n=19) and group B (young) comprised bovine aged up to five years (n=11) (table 1).

Bovine n°	Breed	Sex	Age (years)
1	Podolic	F	20
2	Podolic	F	16
3	Podolic	F	16
4	Podolic	F	13
5	Podolic	F	13
6	Podolic	F	13
7	Podolic	F	13
8	Podolic	F	13
9	Podolic	F	13
10	Podolic	F	13
11	Podolic	F	13
12	Podolic	F	12
13	Podolic	F	12
14	Podolic	F	12
15	Podolic	F	12
16	Podolic	F	11
17	Podolic	F	11
18	Podolic	F	11
19	Podolic	F	11
20	Podolic	F	5
21	Podolic	F	5
22	Podolic	F	5
23	Podolic	F	4
24	Podolic	F	3
25	Podolic	F	2
26	Podolic	F	3
27	Podolic	F	2
28	Podolic	F	1
29	Podolic	F	1
30	Podolic	F	1

Table 1. *Age, sex, and breed of the old (Nos. 1– 19) and young (Nos. 20–30) animals employed for the neuropathology study.*

Skeletal muscle samples from 60 elderly Podolica-breed cows (aged 15–23 years) and 10 young controls (3–6 years old) were randomly selected during the arrival to the abattoir, and all old cows presented muscle atrophy, which is a clinical finding that can be observed in Podolica cattle >15 years of age. Animals were subdivided in 3 groups (n=20 each) and 1 control group (n=10):

Group 1: 15–17 years old (15 years, n=7; 16, n=7; 17,n=6)
Group 2: 18–20 years old (18 years, n=7; 19, n=7; 20,n=6)
Group 3: 21–23 years old (21 years, n=6; 22, n=8; 23,n=6)
Control group: 3–6 years old (3 years, n=3; 4, n=2; 5,n=3; 6,n=2)

Clinically, cattle showed moderate to severe muscle atrophy associated with weakness and difficulty in walking. All cows were tested for several chronic diseases (brucellosis, tuberculosis, paratuberculosis, and leukosis) by serologic tests and skin test and then regularly slaughtered according to the European law 852/04 and 853/04 guidelines and procedures.For every single animal of the study, a complete postmortem evaluation of carcass and organs was carried out by gross examination. No macroscopic alterations of adrenal and thyroid glands or other lesions commonly related to chronic wasting diseases were observed, including tuberculosis, paratuberculosis, leucosis, brucellosis, parasitosis (intestinal, pulmonary, or hepatic), renal disease, and neoplasia.The muscle atrophy was evident after the slaughtering, in comparison of the old cows with the young ones (Figs. 1, 2).

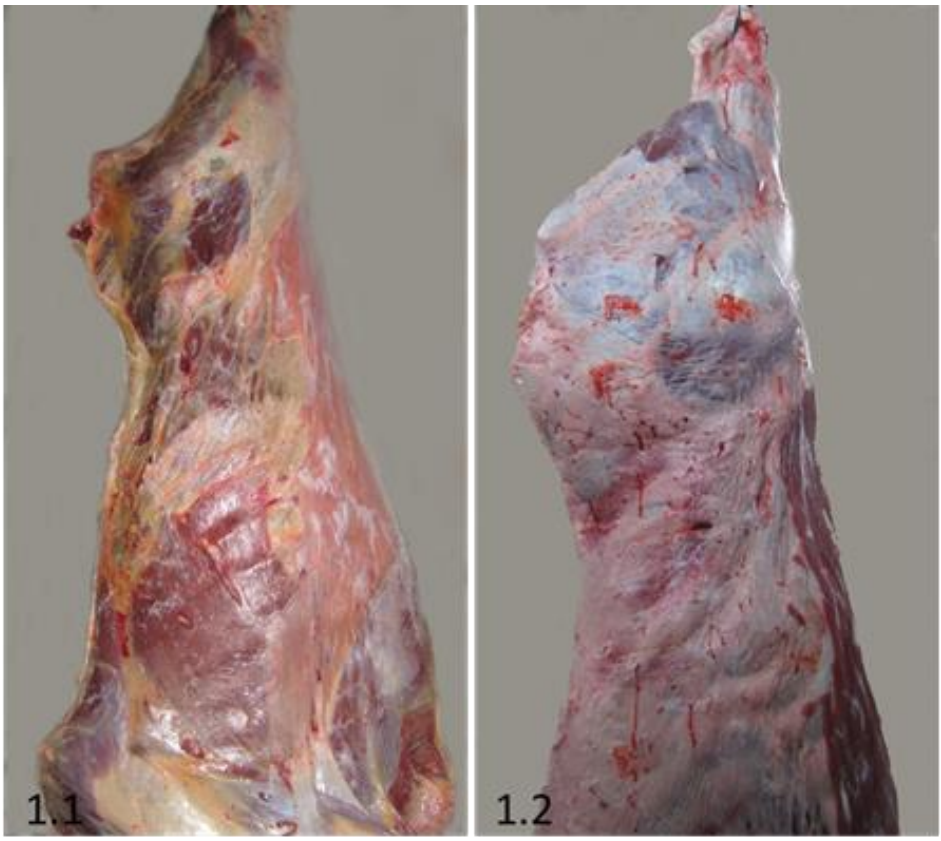

Fig 1.1. ***Carcass; aged cow.*** *Severe, diffuse muscle atrophy in an old cow is more evident in the longissimus dorsi, quadriceps, and gluteus muscles.* ***Figure 1.2. Carcass; young cow.*** *Normal aspect of the skeletal muscle mass in a young control.*

1.2.2 Morphology

Neuropathology techniques (removal of the brain, fixation procedures, macroscopic examination and sampling) were carefully followed as broadly described (De Biase and Paciello, 2015) in order to avoid the many possible resultant artefactual changes. For this study, the brain was immediately removed at slaughterhouse and divided into two parts by a sagittal paramedian cut. The small part was frozen at -80°C until further

processing while the other part was fixed for 15 days in 10% neutral buffered formalin for histological and immunohistochemical examination.
Coronal slices of the frontal and temporoparietal cerebral cortex, basal nuclei area, hippocampus, thalamus, midbrain, cerebellum, pons and medulla oblongata were embedded in paraffin wax. Sections (5 μm) were stained with haematoxylin and eosin (HE), Periodic acid–Schiff (PAS) for lipofuscin and Congo red for amyloid. Additionally, 8 μm sections were stained with Luxol fast blue/Cresyl violet (Code 04-200812 Bio-Optica, Milan) for the evaluation of chromatolysis and demyelination and Bielschowsky stain for plaques and neurofibrillary tangles detection (Code 04-040805 Bio-Optica, Milan). Histological specimens were examined and photographed with a light microscope (Nikon eclipse E600) associated to a microphotography system (Nikon digital camera DMX1200). Unstained sections from all cases were also evaluated with a fluorescence microscope (AxioSkop2 MOT, Zeiss) associated to a microphotography system (AxioCam MRc5, Zeiss) using blue light excitation (FITC filter; excitation, 455–500 nm emission, 500–570 nm) in order to detect lipofuscin autofluorescence.
The severity of microscopical lesions was graded using criteria from Capucchio et al.(2010) by two independent observers (Dott. De Biase and Prof. Paciello) with a concordance rate of 95%:

a) no lesions (0);
b) low number of focal to multifocal lesions (1);
c) a moderate number of lesions disseminated through one or more areas (2);
d) diffuse and severe lesions (3).

For skeletal muscle, samples (1x1x1 cm in size) were immediately collected after slaughtering, from *triceps brachii* and s*emitendinosus*, snap frozen in liquid nitrogen as previously described (Doherty, 2003) and stored at –80° C.
For histologic and histochemical examination, sections were cut in a transverse plane at 10 mm with a cryostat (–20°C) and stained according to

our routinely performed extensive laboratory stains (Paciello and Papparella, 2009; Pagano et al., 2015). Specifically, we performed:

1) hematoxylin and eosin (HE) and Engel trichrome (ET) for a basic morphologic evaluation and mitochondria distribution;
2) reduced nicotinamide adenine dinucleotide tetrazolium reductase (NADH) to observe distribution of mitochondria;
3) succinate dehydrogenase (SDH) and cytochrome oxidase (COX) to evaluate activity and distribution of mitochondria;
4) nonspecific esterase for the evaluation of the neuromuscular junctions and lipofuscins;
5) ATPase at pH 9.4 and 4.3 for histochemical fiber type I and II subtyping, respectively; and
6) Congo red with fluorescence microscopy with an excitation filter suitable for fluorochromes such as Texas red for amyloid detection (Askanas et al., 1993).

Approximately 20 fields at 20x magnification were evaluated for each section by 2 independent pathologists (Dott. Alessandro Costagliola, Prof. Orlando Paciello) with a concordance rate of 95%.

1.2.3 Immunohistochemistry

1.2.3.1 Immunohistochemistry on brain tissue

Immunohistochemistry (IHC) experiments were performed in order to evaluate the expression of βAPP and Prion protein (PrP^{sc}). For IHC, 4-μm-thick sections of frontal cortex and hippocampus were mounted on positively charged glass slides (Bio-Optica, Milan). For βAPP detection, we used a well-established protocol described elsewhere (Pagano et al., 2015). Briefly, antigen retrieval pretreatments were performed using a HIER citrate buffer pH 6.0 (Bio-Optica, Milan, Italy) for 20 minutes at 98 °C. Following, endogenous peroxidase (EP) activity was quenched with

3% hydrogen peroxide (H2O2) in methanol and sections were blocked with a protein block (MACH1, Biocare Medical LLC, Concord, California, USA) for 30 minutes each. Slides were sequentially incubated overnight at 4 °C with primary mouse monoclonal β–amyloid 1-16 (6E10) antibody (SIG-39320, BioLegend, San Diego, California, US) diluted 1:600 in PBS. Antibody deposition was visualized using the DAB chromogen diluted in DAB substrate buffer and the slides were counterstained with hematoxylin. Between all incubation steps, slides were washed two times (5 minutes each) in PBS. In the corresponding negative control sections, the primary antibody was either omitted or replaced with normal serum from the same species of primary antibody (mouse).

IHC for the PrP distribution profiling was performed as described previously by Seuberlich et al.(2007). The protocol was optimized as follows: two slides of 4-µm-thick for each tissue sections were deparaffinized and, subsequently, only one of them was treated with Proteinase K (PK) to see if PK digestion enhances the signal or Prion protein. Slides were then immersed in 98% formic acid (30 min) and after citrated autoclaving (121 °C, 30 min), the endogenous peroxidase activity was blocked (H2O2 in methanol, 10 min) and slides placed in distilled water overnight at 4 °C. After incubation with 5% normal goat serum (Dako, Denmark) for 20 min, PrP was detected with the monoclonal antibody F99/97.6.1 (2 µg/ml; VMRD). Subsequent steps were performed with the peroxidase/DAB Dako Envision detection kit (Dako). Cerebellum of a sheep with scrapie was used as positive control. Thepercentage of βAPP and PrP immunolabeled cells was scored semi-quantitatively as it follows:

- Absent/none: negative (0);
- 1%-25%: mild (1);
- 26%-50%: moderate (2) and
- > 50%: high (3).

The percentage of positively stained cells was scored by two independent observers (O.P., S.P.) in each specimen, for each antibody and under blinded conditions as performed in a previous study (Pagano et al., 2015).

1.2.3.2 Immunohistochemistry on muscle cryosections

In brief, the cryosections where incubated with primary antibodies (diluted in phosphate-buffered saline) overnight at 4°C. After 2 washes in phosphate-buffered saline, MACH 1 mouse probe (Biocare Medical, LLC, Concord, CA, USA) was applied for 20 minutes at room temperature. After, MACH-1 Universal HPR-Polymer (Biocare Medical) was added for 30 minutes at room temperature. The reaction was detected by DAB chromogen diluted in DAB substrate buffer. Finally, sections were counterstained in hematoxylin.
The primary antibodies used were directed against mouse monoclonal β-amyloid 1-16 (6E10, 1:300, SIG-39300; Signet, Dedham, MA, USA), anti-human CD79α mouse monoclonal antibody (1:200, clone JCB117; Dako, Milan, Italy), anti-human CD3 polyclonal rabbit antibody (1:200; Dako), anti-bovine CD4 (1:200) and CD8α (1:200) monoclonal mouse antibodies (clones GC50A1 and CACT80C; VMRD, Pullman, WA, USA), and MHC I (1:300) monoclonal mouse antibody (clone H58A; VMRD). All the antibodies were well established for the use on bovine tissue as described previously (De Biase and Paciello, 2015).
We used specific controls for each immunohistochemistry assay as follows: for antibodies directed against lymphocytes and plasma cell antigens, we used sections from bovine lymphnodes belonging to the archive of Veterinary Medicine Department of University of Naples Federico II. Blood vessel endothelial cells within sections were used as internal control for MHC I expression. For ß-amyloid, we used sections from brain of old chimpanzee with ß-amyloid deposition.
In the corresponding negative control sections, the primary antibody was either omitted or replaced with normal serum from the same species of primary antibody (rabbit or mouse).

To quantify the histologic and immunohistochemical findings, score systems were performed for each parameter; the percentage of atrophic fibers per section, the percentage of necrotic fibers per section, the percentage of ragged red fibers (RRFs)per section, the percentage of vacuolated fibers, the percentage of MHC I–positive fibers, and the percentage of 6E10 (amyloid)–positive fibers were scored as follows:

- 0 = absent/none
- 1%–25% = mild
- 26%–50% = moderate
- >50% = severe

The atrophic fibers, considered smaller than normal, were usually easy to identify given the variability and change in fiber size by simple inspection of the biopsy under the microscope. Sometimes we used a measurement of the diameter of the smallest and largest fibers with an eyepiece micrometer to establish the range of sizes (Dubowitz and Sewry, 2003).
Necrotic fibers were detected at H&E or ET as pale “liquefied” or hyaline-stained fibers (Dubowitz and Sewry, 2003). RRFs were detected as coarsely granular fibers showing prominent peripheral accumulations of abnormal mitochondria, which stains bluish with H&E and red with ET stain (Dubowitz and Sewry, 2003).
Predominantly angular atrophy, the presence of lymphocytic infiltrate, the presence of fiber-type grouping, and the presence of type II selective atrophy were scored as follows:

0 = absent
1 = present

Angular atrophic fibers were detected at H&E stain considering, on cross section, fibers that have lost the polygonal shape and have angulated profiles. Fiber-type grouping was evaluated on ATPase stains at pH 4.3 and 9.4 as groups of fibers of the same type (>2 fibers) closer to each other

and consisting in an aspect of reinnervation from collateral sprouting nerves of denervated fibers.

1.2.4 Velocity sedimentation in sucrose step gradient

For velocity sedimentation in sucrose step gradient, a well-established protocol was used (Serra et al., 2017). Briefly, bain homogenates (10% [w/v]) were prepared in PBS with 1% sarcosyl. The supernatant was recovered after pre-centrifugation at 1000xg for 5 min and was loaded on top of sucrose gradient, prepared by superimposing 350µl layers of 45%, 40%, 35%, 30%, 25%, 20%, 15%, and 10% sucrose solutions from bottom to top. The gradients were centrifuged at 200,000xg (46,000 rpm) for 65min at 4°C using a P55ST2 rotor and a Hitachi CP100NX centrifuge. After centrifugation, the contents of the centrifuge tubes were sequentially removed from the bottom to the top to collect 13 fractions of approximately 250µl each. Half of each fraction was subjected to PK digestion (50 µg/ml) for 1 hour; the second half remained undigested. The samples were subjected to Western blot analysis to detect PrPc/PrPsc in the individual fractions.

1.2.5 Western blot analysis

For Western blot, the muscle tissues from elder cows and controls were cut at the cryostat at 20 µm and then lysed at 4°C in 200 µL of lysis buffer (Tris-buffered saline, 20mM Tris-HCl, pH 7.6, 140mM NaCl, 30mM sodium pyrophosphate, 5mM EDTA, 0.55% Nonided P40, 1% Triton X-100, 50mM NaF, 0.1mM Na3VO4, 1mM PMSF, 1mM benzamidine, 1mM iodoacetamide, 1mM phenanthroline). Protein concentration in the supernatant was determined by BCA protein assay (Pierce, Rockford, IL, USA), and lysates were adjusted to equivalent concentrations with lysis buffer. Aliquots of 30 µg of total muscle lysate were then separated on SDS-PAGE. Proteins were transferred to PVDF membranes that were

blocked overnight at 4°C with 5% nonfat milk in TTBS (TBS with 0.05% Tween 20) and immunoprobed with primary mouse monoclonal β-amyloid 1-16 (6E10, 1:1000, SIG-39300; Signet), as well as horseradish peroxidase–conjugated secondary antibodies performed in blocking solution for 1 hour at room temperature. Immunoreactive bands were visualized by SuperSignal West Pico Chemiluminescent Substrate Kit (Pierce). The same blots were stripped and reprobed with anti-β-actin monoclonal antibody provided by Sigma-Aldrich (A3853, 1:2000) to confirm equal loading of proteins in all lines.
Quantification of immunoreactivity was performed by densitometric analysis via the Kodak Gel Logic 440 Imaging System (EastmanKodak Company, Rochester, NY, USA).

1.2.6 Statistical Methods

For measuring the association between age and studied parameters, data from immunohistochemistry and the morphology were compared with the gamma statistic G. To establish the relation of present association, Somers d statistic was performed. Data obtained from Western blots were analyzed with StatView software (Abacus Concepts, Piscataway, NJ, USA) by Student's t test. Blots were revealed by ECL and autoradiography with ß-actin as a loading control. The autoradiographs shown are representative of 4 independent experiments. Bars represent the mean ± SD of 4 independent experiments. P values <.05 were considered statistically significant.

1.3 RESULTS

1.3.1 Brain changes

No gross, pathologic changes were observed in the brain of any of the bovine (fig. 1.3 and 1.4). Histologically, no significant differences were

found between the two groups (aged and young), except for the presence of lipofuscinosis, satellitosis and chromatolysis.

In all the aged bovine, microscopic evaluation revealed a moderate to severe increase of the number of glial cells around neurons (satellitosis) with a wide distribution particularly in frontal cerebral cortex and hippocampus (fig 1.5 a and b). A moderate satellitosis was observed in occipital cortex and basal ganglia, while mild degree was present in cerebellar cortex. In young controls, a mild degree satellitosis was observed sporadically in cortical areas: hippocampus, frontal and occipital cortex. Satellitosis was significantly more noticeable among the older animals ($p<0.001$). There was a statistically significant positive association between age and increase in severity of satellitosis ($G=0.7516$; $p<0.01$) and this relation was moderate (d Sommer's statistics = 0.5374; $p<0.001$). In 12 cases (60%) of aged animals small foci of neuronophagia were observed. In frontal cerebral cortex, occipital cortex and hippocampus of the brains of aged animals we observed scattered, strongly eosinophilic and shrunken neurons with nuclear pyknosis of a centrally placed nucleus. The striking and constant finding in all the aged bovine was the accumulation of small perinuclear and granular yellow-brown, PAS-positive (fig 1.5 d) and autofluorescent deposits consisting of lipofuscin within the perikarya and sometimes the proximal dendritic tree of neurons. No evidence of lipofuscin accumulation was observed in the neurons of young controls (fig 1.5 c). The amount of lipofuscin was moderate to severe, with a wide distribution in cerebral cortex, basal nuclei, hippocampus, cerebellar cortex, and occipital cortex. Lipofuscin accumulation was significantly more noticeable among the older animals ($p<0.001$). There was a statistically significant positive association between age and increase in severity of lipofuscin accumulation ($G=0.7980$; $p<0.001$) and this relation was strong (d Sommer's statistics = 0.6611; $p<0.001$).

Cresyl violet stain showed a high degree, widespread central chromatolysis - the disintegration of the Nissl bodies of a neuron that may occur after exhaustion of the cell or damage to its peripheral process (fig 1.5 e and f). Other changes considered part of chromatolysis included swelling of the

perikaryon and shifting of the nucleus from its central position to the periphery. The high degree central chromatolysis was observed mostly in the neurons of hippocampus, cerebral frontal cortex and basal nuclei of all aged animals. A moderate degree chromatolysis was observed in occipital cortex, while mild degree and less diffuse chromatolysis was present in the cerebellar cortex neurons. Also in the brains of the young controls a mild degree and less diffuse chromatolysis was observed in all studied telencephalic structures. Modified Bielschowsky stain didn't detect any flame-shaped accumulation of argyrophilic fibrillary material (neurofibrillary tangles) (fig 1.6 a and b). Congo red stain didn't detect any β-amyloid central core of senile plaques nor congophilic angiopathy using both a light microscope and polarized light (fig 1.6 c and d). Other microscopic changes such as meningeal calcification and fibrosis, white matter spongiosis, vascular degeneration and vascular mineralization were not observed in aged or young animals.

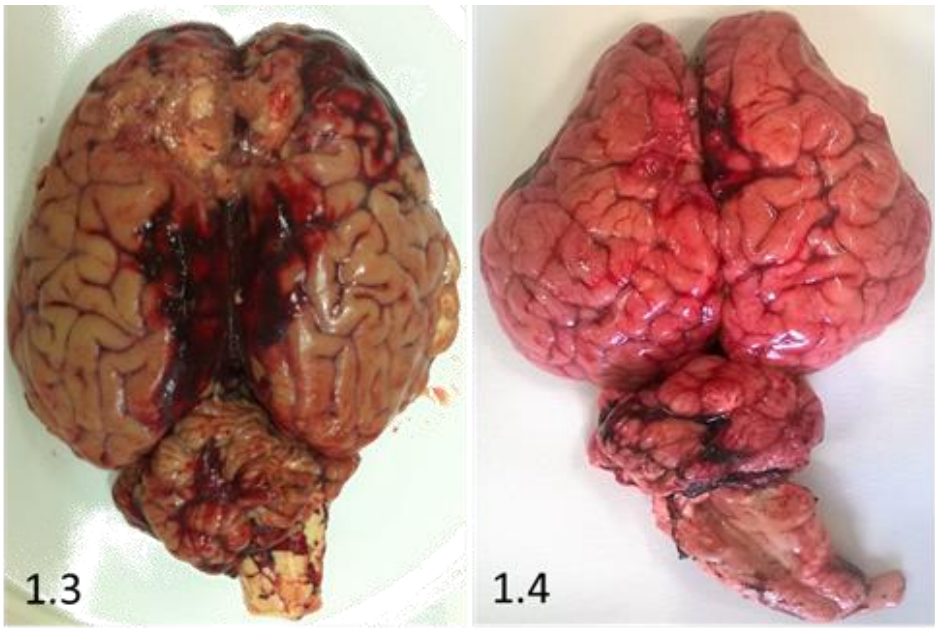

Fig. 1.3 Aged brain. *Brains from aged bovine didn't show marked macroscopic and pathologic changes, except for the age-related darker color of meninges. Hemorrhagic area was due to the slaughtering.* ***Fig. 1.4 Young brain****. Brains from young animals were normal without any pathologic changes.*

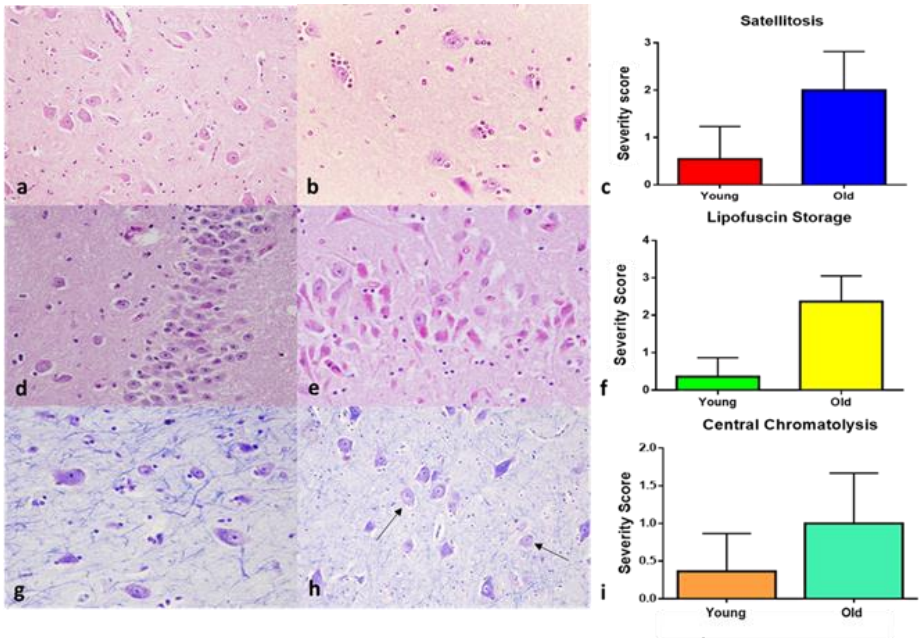

Fig. 1.5 Microscopic changes in bovine brains, hippocampus, dentate gyrus. (a) *Normal brain tissue from a young animal. HEHematoxylin and eosin (H&E) stain. (b) Brain from an aged animal with a severe satellitosis. Hematoxylin and eosin (H&E) stain. (c) severity score for satellitosis. Each value is* the mean ± SEM*(p<0,001). Periodic Acid – Schiff (PAS) stain from a young (d) and an aged animal (e). Lipofuscin storage is marked in the old cattle. (f) severity score for lipofuscin storage. Each value is* the mean ± SEM*(p<0,001) Luxol fast blue/Cresyl violet stain didn't detect chromatolysis in young animals (g) while some neurons in aged brain (h) showed moderate central chromatolysis (arrows). severity score for central chromatolysis. Each value is* the mean ± SEM*(p<0,001)*

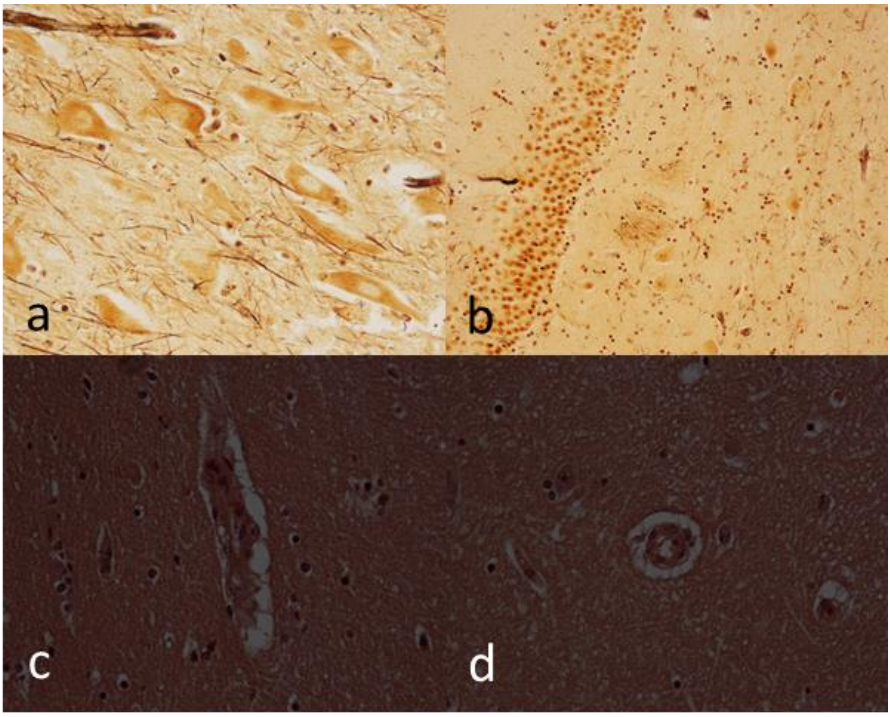

Fig. 1.6 Histochemical staining in aged and young bovine brains, hippocampus. *Neurofibrillary tangles were not detected in young nor in aged bovine brain (a and b). Bielschowsky silver stain. Congo red with polarized light didn't highlight amyloid plaques or congophylic angiopathy in young nor in aged animals (c and d).*

1.3.1.1 Immunohistochemistry

β-amyloid 1-16 positive immunoreaction was detected as intraneuronal granules in the hippocampus and cerebral frontal cortex of all the old cows but never in young control animals (fig. 1.6). Percentage of β–amyloid immunopositive cells were significantly more noticeable among the older animals ($p<0.001$) and there was a statistically significant positive association between age and increase in severity of β-amyloid 1-16 positive immunoreaction ($G=1$; $p<0.001$) and this relation was moderate (d Sommer's statistics = 0.5230; $p<0.001$). PrP^c was normally expressed both

in young and aged animals and no labelling for PrP^{sc} was detected in any brain (fig. 1.7).

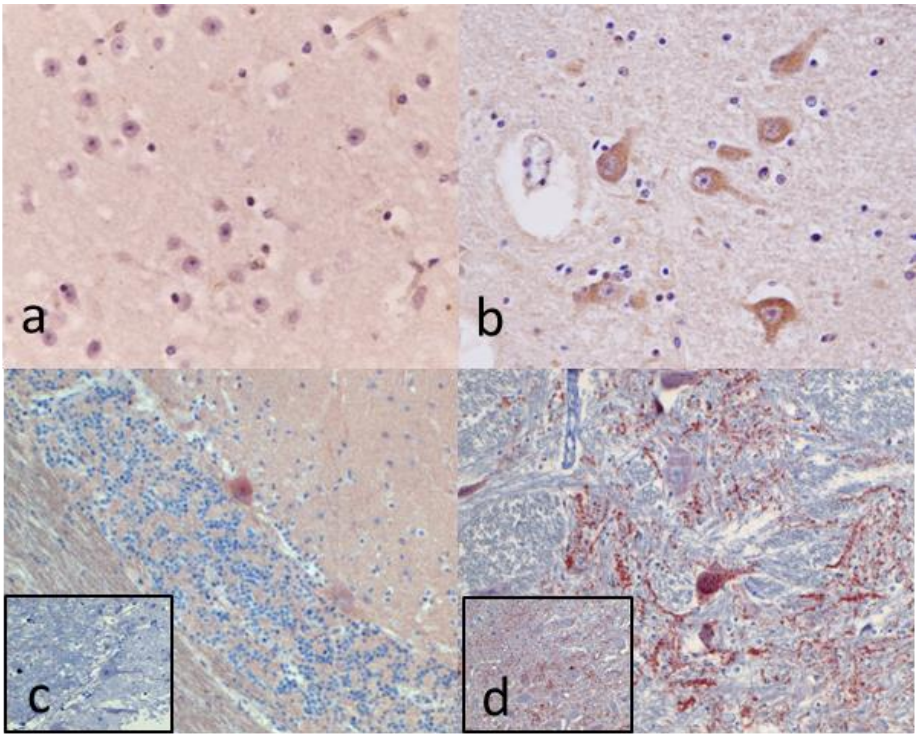

Fig. 1.7 Immunohistochemical analysis in aged and young bovine brains, hippocampus. *Immunoreactivity to Amyloid precursor protein (APP) was absent in young (e) brains, but it was present in old animals as a granular and intraneuronal accumulation. HRP method, haematoxylin counterstain. (g) PrP^{c} expression in aged animals was normal. PrP^{sc} wasn't detectable after Proteinase K (PK) digestion (inset). (h) Positive control from an ovine brain with Scrapie. PrP^{sc} was evident even after PK digestion (inset)*

1.3.1.2 Velocity sedimentation in sucrose step gradient

In contrast to PrP^{c} the TSE associated $PrP^{sc}$is insoluble in non-denaturing detergent and recovered in the pellet following ultracentrifugation at 115,000xg for 1h at 4°C. Thus, we analyzed the solubility of the prion

protein species in aged and young bovine by ultracentrifugationand PK digestion. Brain homogenates were subjected to high-speed centrifugation through a sucrose-gradient ranging from 10% sucrose (fraction 12, top) to 45 % sucrose (fraction 1, bottom). Individual fractions were analysed for prion protein by Western blot. PrP^{sc} was not detected in none of the samples. As expected, aged cow revealed larger amounts of PrP^{c} aggregates than in younger and with a wide range of sizes. (fig. 1.8)

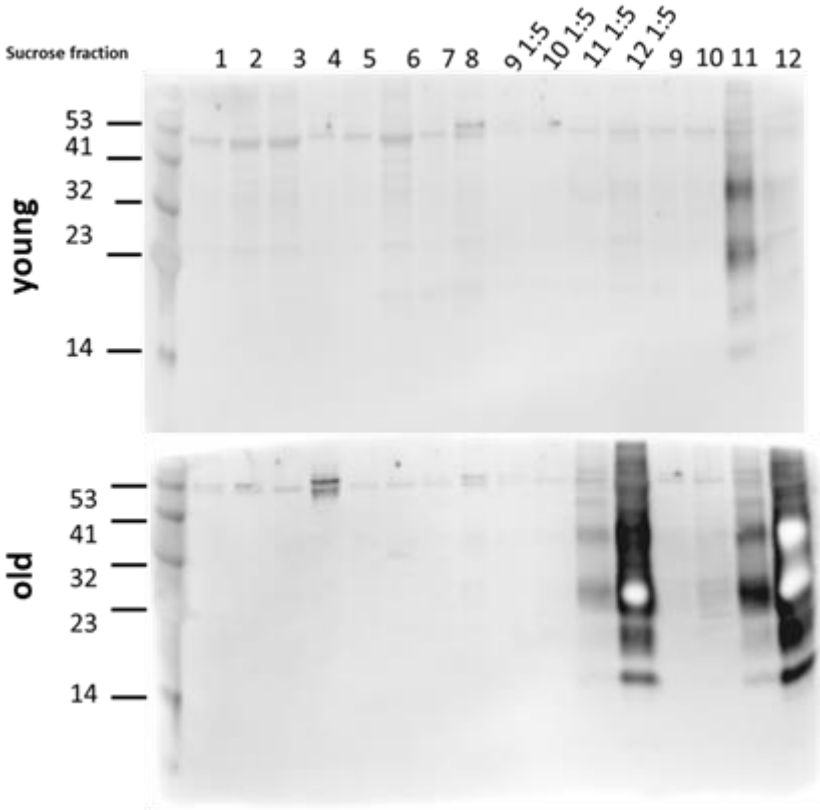

Fig 1.8 Velocity sedimentation in sucrose step gradient. *As expected, PrP starts to be visible at fraction 11 1:5 in the brain of the old animal and at fraction 11 in the young animal.*

1.3.2 Muscle changes

H&E staining of all muscle biopsies from old cows showed variability in diameter size of muscle fibers and mild to severe fiber atrophy. Percentage distribution of fiber atrophy in studied groups was as follows:

Group 1: 40% mild, 30% moderate, 30% severe
Group 2: 20% mild, 30% moderate, 50% severe
Group 3: 20% moderate, 80% severe

In the control group, no muscle fiber atrophy was observed.There was a statistically significant positive association between age and presence of muscle atrophy (G = 0.7836; P< .001), and this relation was moderate (Somers d = 0.5956; P< .001).

Angular atrophy (Fig. 1.9 a) was observed in 90% of aged animals. Percentage distribution of angular atrophy in studied groups was as follows: group 1, 80%; group 2, 95%; group 3, 95%. There was a statistically significant positive association between age and presence of angular atrophy (G = 0.8108; P< .001), and this relation was small (Somers d = 0.3000; P< .001).

Presence of lymphocytic infiltrates (evidences of inflammation) was not observed on the biopsies of the control group. Lymphocytic infiltrates (Fig. 1.9 b) were observed in 40% of biopsies from aged animals. Percentage distribution of inflammation in studied groups was as follows: group 1, 25%; group 2, 35%; group 3, 60%. There was a statistically significant positive association between age and presence of inflammation (G = 0.6176; P< .001), and this relation was small (Somers d = 0.2889; P< .001).

Necrotic muscle fibers (Fig. 1.9 c) were observed in 80% of biopsies from aged animals. Percentage distribution of fiber necrosis in studied groups was as follows: group 1, 5%; group 2, 55%; group 3, 90%. In the control group, no necrosis of muscle fibers was observed (Fig. 1.9 d). There was a statistically significant positive association between age and presence of

necrotic muscle fibers (G = 0.8904; P< .001), and this relation was moderate (Somers d = 0.4606; P< .001).

RRFs (Fig. 1.9 e) and demyelinated nerve axons (Fig. 1.9 f) were observed in ET stain. They were observed in 70% of biopsies from aged animals. Percentage distribution of RRFs in studied groups was as follows: group 1, 50% mild; group 2, 80% mild; group 3, 60% mild and 20% moderate. There was a statistically significant positive association between age and presence of RRFs (G = 0.6860; P< .001), and this relation was moderate (Somers d = 0.3933; P< .001).

Vacuolated fibers (Fig. 1.9 g) were observed in 75% of biopsies from aged animals stained with ET. Presence of rimmed vacuoles within muscle fibers was not observed on the biopsies of the control group (Fig. 1.9 h). Percentage distribution of vacuolated fibers in studied groups was as follows: group 1, 65% mild; group 2, 50% mild and 15% moderate; group 3, 50% mild and 40% moderate. There was a statistically significant positive association between age and presence of vacuolated fibers (G = 0.7065; P< .01), and this relation was moderate (Somers d = 0.4628; P< .001).

Succinic dehydrogenase stain showed increased staining in muscle fibers with mitochondrial proliferation-defined ragged blue fibers in a percentage of cases similar to RRFs observed in ET stain (Fig. 1.10 a) and compared with control (Fig. 1.10 b).

Abnormal internal architecture of the myofibers was studied with the nicotinamide adenine dinucleotide tetrazoliumreductase stain, which showed moth-eaten fibers in only a few studied cases (Fig. 1.10 c; control, Fig. 1.10 d).

All the studied biopsies from aged animals showed alterations of the cytochrome C oxidase enzyme activity, such as moth-eaten fibers, subsarcolemmal mitochondrial collection, and partially or totally negative fibers (Fig. 1.10 e), which were observed in 60% of biopsies. Percentage distribution of COX-negative fibers in studied groups was as follows: group 1, 45% mild; group 2, 50% mild and 10% moderate; group 3, 50% mild and 25% moderate. In muscle biopsies from control group animals, no alteration of cytochrome C oxidase enzyme activity was observed (Fig.

1.10 f).There was a statistically significant positive association between age and presence of COX-negative fibers (G = 0.6375; P< .01), and this relation was moderate (Somers d = 0.3850; P< .001).

Nonspecific esterase showed, in 80% biopsies of aged cows, less and smaller neuromuscular junctions (Fig. 1.10 g) versus controls (Fig. 1.10 h). Percentage of small neuromuscular junctions in studied groups was as follows: group 1, 20%; group 2, 30%; group 3, 50%.There was a statistically significant positive association between age and presence of small neuromuscular junctions (G = 0.5851; P< .05), and this relation was small (Somers d = 0.2444; P< .05). Nonspecific esterase was suitable also for the identification of lipofuscin in almost all muscle biopsies of aged cows.

The ATP-ase stains performed at pH 4.3 and 9.4 was used to evaluate which type of muscle fibers undergoes atrophy. Type II fiber selective atrophy was not observed on the biopsies in control group but was observed on 40% of biopsies from aged animals (Fig. 1.10 i; control, Fig. 1.10 j). Percentage distribution of type II fiber selective atrophy in studied groups was as follows: group 1, 30%; group 2, 40%; group 3, 50%. No statistically significant association between age and presence of type II selective atrophy was observed (G = 0.4854; P = .053).

ATP-ase stains also revealed fiber-type grouping in 83% of biopsies from aged animals (Fig. 1.10 k), which was not observed on the biopsies in control group (Fig. 1.10 l). Percentage distribution of fiber-type grouping in studied groups was as follows: group 1, 65%; group 2, 85%; group 3, 95%. There was a statistically significant positive association between age and presence of fiber-type grouping (G = 0.8410; P< .001), and this relation was moderate (Somers d = 0.4056; P< .001).

Multiple intrasarcoplasmatic deposits of amyloid identified by Congo red fluorescence visualized through Texas red filters were evident within approximately 30% of biopsies (Fig. 1.11 a; control, Fig. 1.11 b).

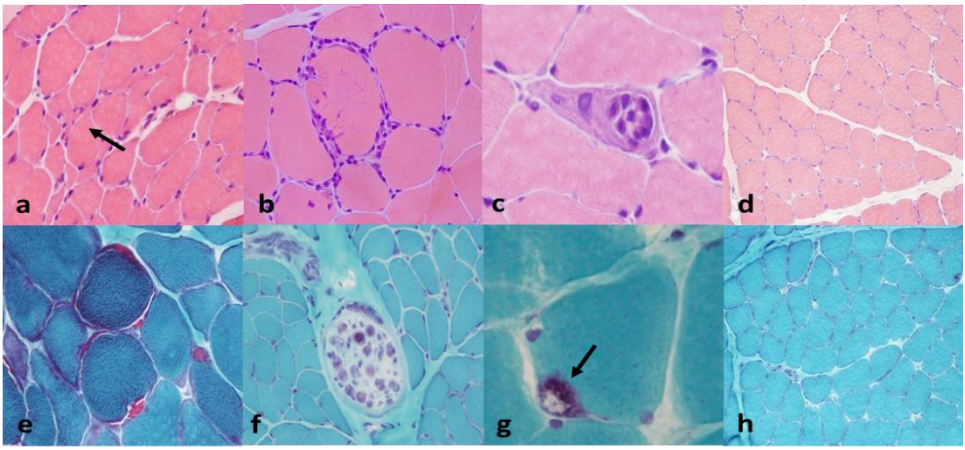

Figure 1.9. Morphological changes in muscle a. *Muscle; aged cow (group 2). Moderate variability in muscle fiber size, with atrophic fibers occasionally showing angular profile (arrow). Hematoxylin and eosin (H&E) stain.* ***b.****Muscle; aged cow (group 3). Lymphoplasmacytic inflammatory infiltrate within the endomysium. H&E stain.****c.*** *Muscle; aged cow (group 3). Muscle fiber necrosis associated with sarcoclastosis (arrow). H&E stain.****d.*** *Muscle; young cow (group 1). Normal muscle fibers. H&E stain.****e****.Muscle; aged cow (group 2). Muscle fibers showing subsarcolemmal mitochondrial accumulations (ragged red fibers) stained in red. Engel trichrome (ET) stain.****f.****Muscle; aged cow (group 2). Demyelinated peripheral nerve. ET stain.****g.****Muscle; aged cow (group 2). Muscle fiber showing rimmed vacuole within the sarcoplasm (arrow). ET stain.****h.*** *Muscle; young cow (group 1). Normal muscle fibers. ET stain.*

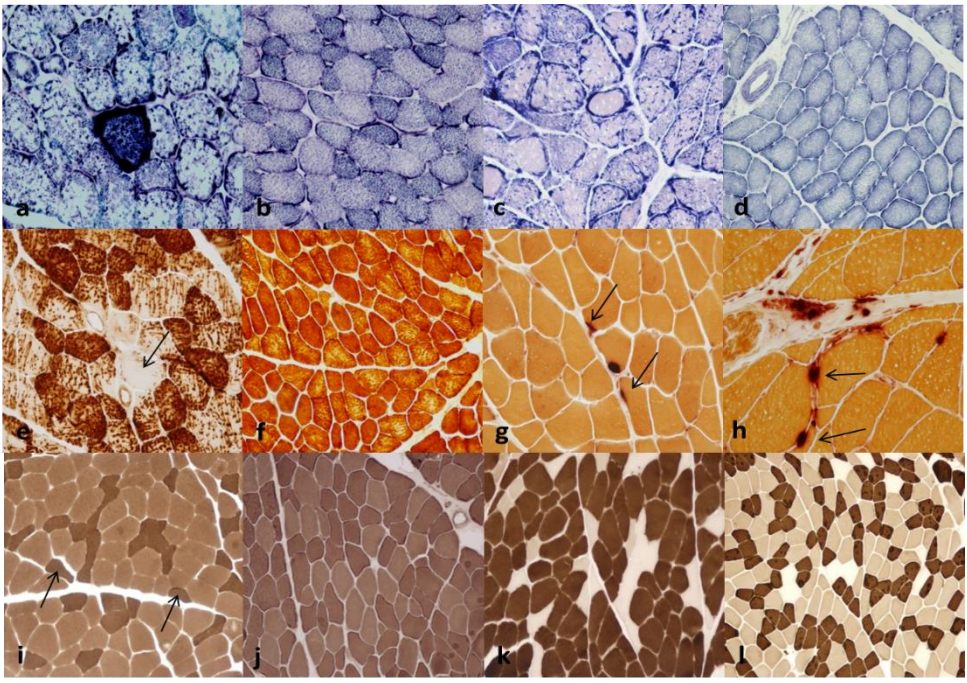

Figure 1.10 Histoenzymatic stains, sketal muscle, cow a*Muscle; aged cow (group 2). Ragged blue fiber deeply stained in blue. Succinate dehydrogenase stain.*
b.*Muscle; young cow (group 1). Normal muscle fibers. Succinate dehydrogenase stain.*
c.*Muscle; aged cow (group 2). Moth-eaten fibers showing irregular disruption of myofibrillar network. Nicotinamide adenine dinucleotide tetrazolium reductase stain.*
d.*Muscle; young cow (group 1). Normal muscle fibers. Nicotinamide adenine dinucleotide tetrazolium reductase stain.*
e.*Muscle; aged cow (group 2). Completely cytochrome oxidase (COX)–negative fiber and many others showing a sensible decrease of COX activity (arrow). COX stain.*
f.*Muscle, cow (group 1). Normal muscle fibers. COX stain.*
g.*Muscle; aged cow (group 2). Muscle fibers showing small, pale, and multisegmented neuromuscular junctions (arrows). Nonspecific esterase stain.*
h.*Muscle; cow. Normal muscle fibers from young cow of group 1 showing normal-size neuromuscular junctions (arrows). Nonspecific esterase stain.*
i.*Muscle; aged cow (group 2). Transverse sections showing atrophy restricted to darkly stained type 2 fibers (arrows). ATPase (pH 9.4) stain.*
j.*Muscle; young cow (group 1). Normal muscle fibers. ATPase (pH 9.4) stain.*
k.*Muscle; aged cow (group 2). Grouping of type II muscle fiber types (arrow). ATPase (pH 4.3) stain.*
l.*Muscle; young cow (group 1). Normal muscle fibers. ATPase (pH 4.3) stain.*

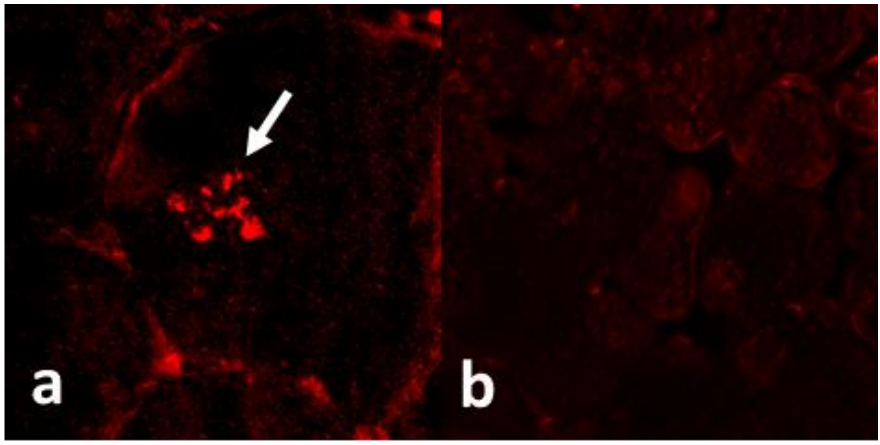

Figure 1.11 Immunofluorescence for amyloid, muscle,cows a. *Muscle; aged cow (group 2). Multiple intrasarcoplasmatic deposits of amyloid identified by Congo red (CR) fluorescence visualized through Texas red filters (arrow). CR stain.* ***b****. Muscle; young cow (group 1). Negative control. CR stain.*

1.3.2.1 Immunofluorescence and Immunohistochemistry

Lymphocyte subtypes were identified in the biopsies based on staining patterns of antibodies against cell surface proteins (Figs. 1.12 a-d). In all cases, the predominant cell populations were positive for CD3+, mostly CD8+ (Fig. 1.12 a), and rare CD4+ (Fig. 1.12 c), with an endomysial, perimysial, and, in some cases, perivascular distribution. No inflammatory cells were observed in the control group (Figs. 1.12 b 1.12 d). Scattered CD79α-positive cells were observed in only 2 cases of old cows.

MHC I–positive fibers were observed in 60% of biopsies from aged animals (Fig. 1.12 e). Percentage distribution of MHC I–positive fibers in studied groups was as follows: group 1, 45% mild and 5% moderate; group 2, 40% mild and 20% moderate; group 3, 40% mild and 30% moderate. There was a statistically significant positive association between age and presence of MHC I–immunopositive fibers ($G = 0.5114$; $P < .05$), and this relation was moderate (Somers $d = 0.3244$; $P < .01$).In biopsies from

control group stain with primary antibodies, anti–MHC I showed positive reaction only on vessels of perimysium and endomysium (Fig. 1.12 f).

Positively stained fibers containing β-amyloid were observed in 30% of biopsies from aged animals (Fig. 1.12 g). Percentage distribution of 6E10-positive fibers in studied groups was as follows: group 1, 15% mild and 5% moderate; group 2, 5% mild, 20% moderate, and 5% severe; group 3, 5% mild, 20% moderate, and 15% severe. There was a statistically significant positive association between age and presence of 6E10 immunopositive fibers ($G = 0.5075$; $P < .05$), and this relation was small (Somers $d = 0.2244$; $P < .05$). Stain with primary antibodies 6E10 showed no positive reaction for β-amyloid on biopsies in control group (Fig. 1.12 h).

There was a statistically significant positive association between presence of 6E10-immunopositive fibers and presence of inflammation ($G = 0.7172$; $P < .01$), and this relation was moderate (Somers $d = 0.4108$; $P < .001$). However, no statistically significant association between presence of MHC I–immunopositive fibers and presence of 6E10-immunopositive fibers was observed ($G = 0.4870$; $P = .079$).

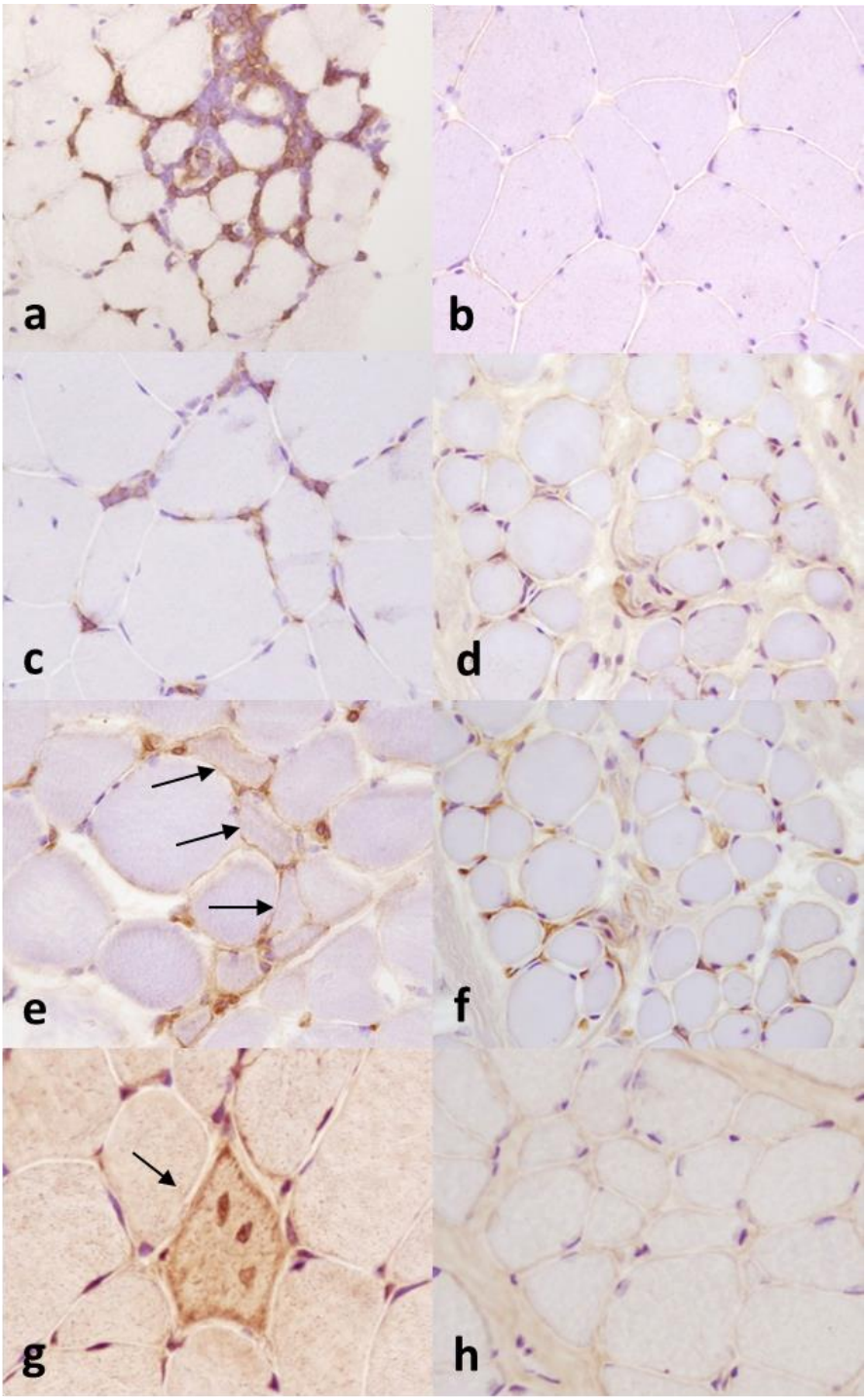
a
b
c
d
e
f
g
h

Fig. 1.12 Immunohistochemical analysis, muscle, cow a.*Muscle; aged cow (group 2). CD8 immunoperoxidase stain showing CD8+ T cells infiltrating the endomysium.*
b*Muscle; young cow (group 1). Lack of CD8+ cells. Immunoperoxidase stain.*
c.*Muscle; aged cow (group 2).CD4 immunoperoxidase stain showing scattered CD4+T cells infiltrating the endomysium.*
d. *Muscle; young cow (group 1). Lack of CD4+T cells. Immunoperoxidase stain.*
e. *Muscle; aged cow (group 2). MHC I immunoperoxidase stain showing abnormal positivity on the sarcolemma (arrows).*
f. *Muscle; young cow (group 1). Lack of MHC I expression. Immunoperoxidase stain.*
g*. Muscle; aged cow (group 2).Immunoreactive amyloid deposits within the sarcoplasm (arrow). 6E10 immunoperoxidase stain.*
h. *Muscle; young cow (group 1). Lack of amyloid deposits. Immunohistochemistry for β-amyloid (6E10).*

1.3.2.2 Western Blot

In the studied biopsies, AβPP, recognized by primary antibody 6E10, was revealed as a strong band at 130 kDa. Our results, normalized for actin, showed a significant increase in the oldest animals compared with young controls (P< .01vs control) for AβPP (Fig. 1.13).

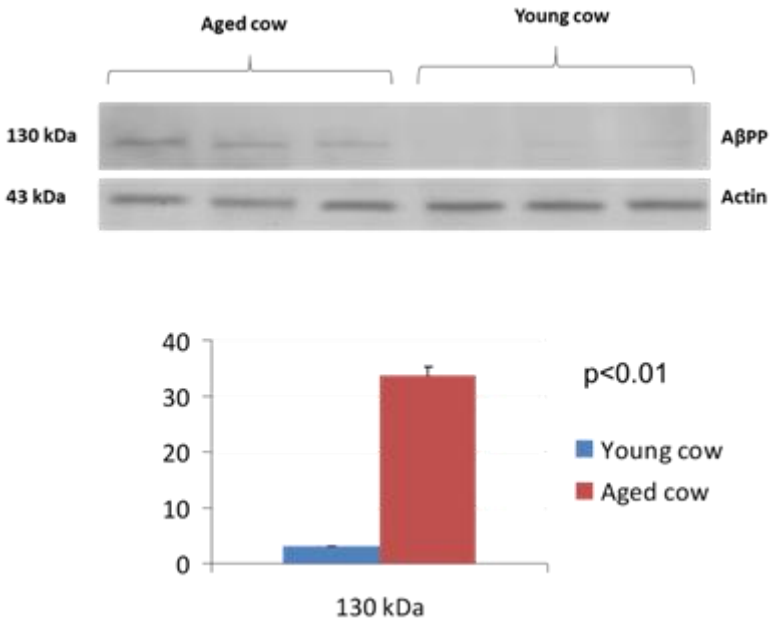

Figure 1.13. Western blot analysis for β-amyloid 1-16, muscle, cow. *Based on6E10 antibody, revealed a strong band at 130 kDa. Densitometric values of β-amyloid 1-16 show a significant increase in the older animals versus young controls. *P< .01 vs control. AβPP, β-amyloid precursor protein.*

1.4 DISCUSSION

Macroscopic examination of brains didn't reveal alterations neither for aged nor for young animals. Microscopic findings in the brains of our aged animals were similar to those previously described in old animals of other species as well as in elderly humans (Youssef et al., 2016). *Satellitosis* is generally the result of an altered cellular homeostasis leading to neuronal damage and depletion (Kiatipattanasakul et al., 1996; Summers et al., 1995). Specifically, satellitosis represents a response to primary neuronal degeneration (Kaufmann et al., 2012). Satellitosis increases in aged animals (Capucchio et al., 2010; Summers et al., 1995) and often portends to the imminent progression to *neuronophagia*, a process whereby the degenerated fragments of a necrotic neuron are removed piecemeal by macrophages.*Chromatolysis* is a prominent neuropathological feature generally induced by axonal injury, ischemia, neurotoxicity, and several neurodegenerative disorders such as Amyotrophic Lateral Sclerosis (ALS), spinal muscular atrophy, and Alzheimer's disease (Riancho et al., 2014). Chromatolytic dissolution of the rough endoplasmic reticulum (RER) is often seen also as a feature of aging and reflects a dysfunction of protein synthesis that most often precedes apoptosis (Martin, 1999).

In our study, one of the most consistent morphological aspect related to brain aging was the accumulation of intraneuronal *lipofuscin*. The age-dependent accumulation of lipofuscin in brain cells is one of the most consistent features of aging (Gray and Woulfe, 2005) and it has been known for more than 150 years (Brunk and Terman, 2002). Lipofuscin is a polymeric substance, formed due to iron-catalyzed oxidative processes and primarily composed of cross-linked protein residues, lipids, carbohydrates and traces of metals, especially iron (Jolly et al., 1995; Porta, 1991). Lipofuscin was generally thought to be an innocent end-product of oxidation which has no significant influence on cellular activities (Rubin et al., 1999), but recent evidences indicate that lipofuscin accumulation may have a detrimental effect to cellular functions (Brunk and Terman, 2002a) also decreasing the cellular autophagic capacity (Brunk and Terman, 2002).

Amyloid precursor protein (APP) is a single-pass transmembrane protein expressed at high levels in the brain and metabolized in a rapid and highly complex fashion by a series of sequential proteases, including the intramembranous γ-secretase complex, which also process other key regulatory molecules (O'Brien and Wong, 2011). Proteolysis of amyloid precursor protein (APP) with the sequential generation of the neurotoxic Aβ peptide appears to be a crucial step in the development of Alzheimer Disease (AD) in humans (O'Brien and Wong, 2011). One mechanism to eliminate extracellular Aβ in the brain includes the proteases neprilysin and insulin degrading enzyme (Selkoe 2001), the polyfunctional endothelial transport proteins P-glycoprotein, receptor for advanced glycation endproducts (RAGE), and low-density lipoprotein-like receptor (LRP1).One alternate explanation for Aβ accumulation in the elderly would be an alteration in the cleavage of APP. Excessive age-associated acetylation of the α-secretase gene may diminish non-amyloidogenic processing of APP (Donmez et al. 2010), whereas an increase in β-secretase1 (BACE1) activity, reported in early AD brain tissue, would increase amyloidogenic processing (Holsinger et al. 2002, Yang et al. 2003).

Although an AD-like condition has not yet been described in aged bovine, it is not surprising that an increased intraneuronal accumulation of APP is observed in aged brains. However, it is intriguing to question whether this accumulation may have a detrimental effect on cognitive functions in cattle and which is (or are) the pathway involved in the altered metabolism and subsequent accumulation of APP in bovine brains.

Cellular Prion protein (PrP^{c}) plays important physiological roles in CNS such as neuronal survival, neurite outgrowth, synapse formation/maintenance/functionality, and myelinated fiber formation/maintenance (Aguzzietal., 2008). Several studies have investigated a possible "*dangerous liason*" between Aβ and PrP with the subsequent accumulation of toxic proteins in the brain leading to AD or other neurodegenerative disorders. Whitehouse and colleagues suggest that BACE1 activity strongly increases during aging, thus enhancing Aβ production and the possibility of deposit formation (Whitehouse et al.,

2010). The reduction of PrP^c-mediated BACE1 inhibition due to the decrease in PrP^c levels may beacause of the enzyme activity elevation (Whitehouse et al., 2010). Our results showed that PrP^c was normally expressed both in young and aged bovine leading us to speculate that, in our cases, PrP^c preserved its role in protecting neurons from the aberrant proteolytic processing of APP by BACE1. These results may also indicate that APP is cleaved by α- and γ-secretase in a non-amyloidogenic pathway (Jacobsen and Iverfeldt, 2011) also justifying the absence of Congo Red positive amyloid senile plaques.

The accumulation of neurofibrillary tangles (NFTs) is a commonfeature of many neurodegenerative diseases such as Alzheimer's disease (AD) and of other diseases known as 'tauopathies' that include Pick's disease (PiD), progressive supranuclear palsy, corticobasal degeneration, argyrophilicgrain disease and familial frontotemporal dementiaand Parkinson's disease (Ferreret al., 2005). The self-assembly of NFTs results from the hyperphosphorylation of Tau protein, a highly soluble microtubule-associated protein (MAP) found in neurons. One of the most important function of Tau protein is to stabilize the axonal microtubulesthat are essential for fast axonal transport (Ferrer et al., 2005). In this study no neurofibrillary tangles were detected by theBielschowsky silver stain, similarly to Capucchio et al. observations on the brains of aged horses (2010). Moreover, immuno-labelled Tau hippocampal neurons observed in thestudy of Capucchio and colleagues (2010) did not express hyperphosphorylated Tau (AT8), indicating that the accumulated Tau wasnot hyperphosphorylated at position S202. Because we didn't perform an immunohistochemical analysis for Tau protein that confirm the presence of this protein in aged bovine brains, we can only report Capucchio and colleagues' assumption that non-phosphoryled Tau may accumulate insome hippocampal neurons in a non-neurofibrillary tangle manner, perhaps due to axonal transport deficiencies occurring in ageing (Capucchio et al., 2010).

Sarcopenia is a multifactorial condition that occurs in a variety of species, but only in humans and laboratory animals are extensive data available on its pathogenesis and morphologic features (Budford et al., 2010; Demontis

et al., 2013; Doherty et al., 2003; Evans, 1995; Pagano et al., 2015). In this work, we describe for the first time some of the most important consequences of muscle aging in cows, suggesting new insights for a comparative approach on the study of this concerning healthcare.

Our most relevant results indicated presence of statistically significant positive association between (1) age and increasing percentage of COX-negative fibers,(2) age and increasing percentage of angular atrophic fibers and fiber-type grouping, (3) increase of sarcoplasmic deposits of β-amyloid/AβPP and presence of lymphocytic inflammation, and (4) age and lymphocytic inflammation associated with MHC I sarcolemmal expression.

The irregular distribution of mitochondria evidenced at histochemical and histoenzymatic stains (ET, succinic dehydrogenase, and COX) and the presence of COX-negative fibers in a high number of biopsies from elderly cows suggest that, even in this species, sarcopenia is characterized by mitochondrial abnormalities and dysfunctions. In human medicine, age-related mitochondrial disorders have been associated with the accumulation of mitochondrial DNA mutations mainly induced by increased levels of ROS with aging (Aoi et al., 2011; Herbst et al., 2007) that contribute to the pathogenesis of age-related muscle atrophy (Hall et al., 2011); postmitotic tissues such as brain and skeletal muscle are very sensitive to the accumulation of ROS because of their high metabolic activity and their impossibility to counteract the ROS-induced damages with the generation of new cells (Harrison et al., 2003; Keller et al., 2004); and mutation and deletion of mitochondrial DNA created by excess ROS lead to the synthesis of defective mitochondrial proteins, decreased ATP production, and further generation of ROS (Herbst et al., 2007). This increase of ROS is involved in many age-related pathologies, such as atherosclerosis, diabetes mellitus, and Alzheimer disease (Aoi et al., 2011; Harrison et al., 2003; Su et al., 2008).

Another prominent finding in our study is the presence of neurogenic lesions, such as angular atrophy and fiber-type grouping. In human medicine and animal models, aging is associated with a gradual loss of motor neurons and neuromuscular junction dysfunction (Rowan et al.,

2012). Even though the pathogenesis of neuromuscular junction impairment is still poorly understood, many factors seem to be primarily involved, such as mitochondrial alteration, age-related chronic inflammation, and neurodegeneration (Gonzalez-Freire et al., 2014). Previous studies demonstrated an age-related remodeling of motor units leading to progressive phenomena of denervation, followed by reinnervation from remaining adjacent neurons (Deschenes et al., 2010); this aspect seems to be involved in the age-related loss of muscle strength and force-producing capacity (Doherty, 2003; Ryall et al., 2008). Denervation of skeletal muscle results in atrophic angular fibers scattered at random or in small or large groups within a biopsy; adjacent intact motor nerve may sprout and reinnervate clusters of denervated fibers resulting in fiber-type grouping (Dubowitz and Sewry, 2007). Thus, our results (fiber-type grouping) reflect the reinnervation process of muscle fibers.

Sarcoplasmatic deposits of congophilic material, mostly immunoreactive to 6E10 antibody, were detected in 30% of biopsies and strongly correlated to lymphocytic infiltrates. Age-related β-amyloid deposits in skeletal muscle are typical of s-IBM, the most common muscle disease of older persons(Askanas et al., 2012; Askanas et al., 2014). The characteristic features of s-IBM at light microscopy are the presence of vacuolated fibers detected on ET and identified as multiple or single foci of ß-plated sheet amyloid at Congo red fluorescence visualized through Texas red filter associated with extracellular T-cell inflammatory infiltrates (Askanas et al., 1993; Askanas et al., 2014). The pathogenesis of s-IBM is presumably very complex, but the accumulation of post translationally modified proteins, including β-amyloid, may be eliciting the T-cell inflammatory reaction (Vromman et al., 2013).

A critical issue in human s-IBM and Alzheimer disease is the relationship among cytokines, amyloid, and chronic inflammation. In s-IBM, cytokines such as IL-1β derived by macrophages and T cells are in excess and colocalize with β-APP. Furthermore, strong evidences indicated that β-APP enhances IL-1β production and IL-1β upregulates β-APP and β-APP gene expression, supporting an interaction between amyloid and

inflammatory mediators (Dalakas, 2004). Until now, s-IBM was the unique opportunity to study this relationship because of the accessibility of muscle specimens from which β–amyloid can be extracted and monitored; as such, we can offer a new model to investigate this relationship. The immunogenicity of β–amyloid was recently studied in healthy elderly subjects and patients with Alzheimer disease and compared with young/middle-aged adults (Dalakas, 2004). Strong β-amyloid reactive and HLA-restricted T-cell responses against the immunogenic β-amyloid 1–42 peptide were found in the elderly, suggesting that β-amyloid is presented as an antigen by antigen-presenting cells in the context of MHC–T-cell receptor interaction (Dalakas, 2004).

Aside from humans, s-IBM has been reported only once in a dog (King et al., 2009). To our knowledge, this is the first report of age-related muscle deposits of amyloid; thus, its causative factors are unknown. However, a common pathogenetic mechanism can be presumed.

Furthermore, we observed an age-related muscle inflammation, whereas lymphocytic infiltrates were observed in 40% of biopsies from aged animals and MHC I–positive fibers in 60%. There was a statistically significant positive association between age and presence of MHC I–immunopositive fibers ($G = 0.5114$; $P < .05$), and this relation was moderate (Somers $d = 0.3244$; $P < .01$).

What triggers T-cell activation in age-related bovine myositis as in human polymyositis and sIBM still remains unclear. In human polymyositis and sIBM, there is evidence of an antigen-directed and MHC I–restricted cytotoxicity mediated by CD8 T cells, as supported by the following: the cytotoxicity of endomysial T cells to autologous myotubes, the clonal expansion of autoinvasive Tcells and the restricted usage of T-cell receptor gene families, the upregulation of costimulatory molecules, and the release of perforin granules by autoinvasive CD8 cells to lyse muscle fibers (Dalakas, 2004).

Upregulated cytokines, chemokines, and adhesion molecules enhance the transmigration of T cells from the circulation to the muscle (Dalakas, 2004).

Immunohistochemical detection of sarcolemmal MHC class I is considered a valid test for immune-mediated idiopathic inflammatory myositis in humans (Das et al., 2013; Van der Pas et al., 2014) and dogs (Paciello et al., 2007), in the presence or absence of cellular infiltration. Muscle fibers do not normally express MHC class I antigens, but in human inflammatory myopathies and canine masticatory muscle myositis, MHC class I sarcolemmal expression has been found to be a valid diagnostic marker for skeletal muscle inflammation (Paciello and Papparella, 2009; Paciello et al., 2007).MHC I expression has been correlated to the active role of muscle fibers in antigen presentation and in initiating and maintaining pathologic events in immune-mediated myositis (Englund, 2001). The use of MHC I in bovine myositis has never been described so far; given our results, it could be considered a valid diagnostic tool even in this species.

Skeletal muscle atrophy statistically correlated with age in old animals versus young controls. This is a typical histologic finding of sarcopenia in all species. Muscle atrophy reflects a condition of unbalanced protein metabolism that, in sarcopenia, has been associated with a chronic low-grade systemic inflammation (called inflammaging) (Franceschi et al., 2007; Hall et al., 2011), increased levels of muscle-impairing inflammatory cytokines such as TNF-α, age-related hormonal changes, and an imbalanced protein synthesis/degradation (Buford et al., 2010; Combaret et al., 2009; Proctor et al., 1998; Ryall et al., 2008; Sakuma et al., 2012).

Selective type II fiber atrophy, even if not statistically confirmed, was more frequently observed in older animals versus young controls. This aspect of muscle atrophy has been already reported in transgenic mice and human sarcopenia, given to a more susceptibility of these fibers to oxidative stress (Ciciliot et al., 2013; Proctor et al., 1998; Sullivan-Gunn et al., 2013).

REFERENCES

1. Aoi W, Sakuma K. **Oxidative stress and skeletal muscle dysfunction with aging**. Curr Aging Sci. 2011;4(2):101–109.
2. Aguzzi,A, Baumann ,F and Bremer J. **The prion's elusive reason for being**. Annu. Rev. Neurosci. 2008;31:439–477.
3. Askanas V, Engel WK, Alvarez RB. **Enhanced detection of congo-red-positive amyloid deposits in muscle fibers of inclusion body myositis and brain of Alzheimer's disease using fluorescence technique.** Neurology. 1993;43(6):1265–1267.
4. Askanas V, Engel WK, Nogalska A. **Pathogenic considerations in sporadic inclusion-body myositis, a degenerative muscle disease associated with aging and abnormalities of myoproteostasis**. J Neuropathol Exp Neurol. 2012;71(8):680–693.
5. Askanas V, Engel WK, Nogalska A. **Sporadic inclusion-body myositis: a degenerative muscle disease associated with aging, impaired muscle protein homeostasis and abnormal mitophagy**. Biochim Biophys Acta. 2014;1852(4):633–643.
6. Brunk, UT, Terman A**. Lipofuscin: Mechanisms of age-related accumulation and influence on cell functions**. Free Radic. Biol. Med. 2002a;33:611–619
7. Brunk UT, Terman A. **The mitochondrial-lysosomal axis theory of aging: accumulation of damaged mitochondria as a result of imperfect autophagocytosis**. Eur J Biochem. 2002;269(8):1996-2002.
8. Buford TW, Anton SD, Judge AR. **Models of accelerated sarcopenia: critical pieces for solving the puzzle of age-related muscle atrophy**. Ageing Res Rev. 2010;9(4):369–383.
9. Capucchio MT, Márquez M, Pregel P, et al. **Parenchymal and vascular lesions in ageing equine brains: histological and immunohistochemical studies**. J Comp Pathol . 2010; 142 (1):61–73.

10. Ciciliot S, Rossi AC, Dyar KA. **Muscle type and fiber type specificity in muscle wasting**. Int J Biochem Cell Biol. 2013;45(10):2191–2199.
11. Combaret L, Dardevet D, Béchet D. **Skeletal muscle proteolysis in aging**. Curr Opin Clin Nutr Metab Care. 2009;12(1):37–41.
12. Dalakas MC. **Inflammatory disorders of muscle: progress in polymyositis, dermatomyositis and inclusion body myositis**. Curr Opin Neurol. 2004;17(5):561–567.
13. Das L, Blumbergs PC, Manavis J. **Major histocompatibility complex class I and II expression in idiopathic inflammatory myopathy.** Appl Immunohistochem Mol Morphol. 2013;21:539–542.
14. De Biase D and Paciello O. **Essential and current methods for a practical approach to comparative neuropathology** Folia Morphol. Vol. 74, No. 2, pp. 137–149
15. Demontis F, Piccirillo R, Goldberg AL. **Mechanisms of skeletal muscle aging: insights from Drosophila and mammalian models.** Dis Model Mech. 2013;6(6):1339–1352.
16. Deschenes MR, Roby MA, Eason MK, et al. **Remodeling of the neuromuscular junction precedes sarcopenia related alterations in myofibers**. Exp Gerontol. 2010;45(5):389–393.
17. Doherty TJ. **Invited review: aging and sarcopenia**. J Appl Physiol. 2003;95(4):1717–1727.
18. Dubowitz V, Sewry CA. **Muscle Biopsy: A Practical Approach**. 3rd ed. London, UK: Saunders Elsevier; 2007.
19. Englund P, Lindroos E, Nennesmo I. **Skeletal muscle fibers express major histocompatibility complex class II antigens independently of inflammatory infiltrates in inflammatory myopathies.** Am J Pathol. 2001;159:1263–1273.
20. Evans WJ. **What is sarcopenia?** J Gerontol A BiolSci Med Sci. 1995;50:5–8
21. Franceschi C, Capri M, Monti D, et al. **Inflammaging and anti-inflammaging: a systemic perspective on aging and longevity**

emerged from studies in humans. Mech Ageing Dev. 2007;128:92–105.

22. Gavier-Widen D, Wells GA, Simmons MM, Wilesmith JW, Ryan J. **Histological observations on the brains of symptomless 7-year-old cattle**. J Comp Pathol. 2001; 124(1):52-9
23. Gonzalez-Freire M, de Cabo R, Studenski SA, et al. **The neuromuscular junction: aging at the crossroad between nerves and muscle**. Front Aging Neurosci. 2014;6:208.
24. Gray DA, Woulfe J. **Lipofuscin and Aging: A Matter of Toxic Waste**. Sci. Aging Knowl. Environ 2005:re1
25. Hall DT, Ma JF, Marco SD, et al. **Inducible nitric oxide synthase (iNOS) in muscle wasting syndrome, sarcopenia, and cachexia.** Aging (Albany NY). 2011;3(8):702–715.
26. Harrison D, Griendling KK, Landmesser U. **Role of oxidative stress in atherosclerosis**. Am J Cardiol. 200;91(3A):7A–11A.
27. Herbst A, Pak JW, McKenzie D. **Accumulation of mitochondrial DNA deletion mutations in aged muscle fibers: evidence for a causal role in muscle fiber loss**. J Gerontol A BiolSci Med Sci. 2007;62(3):235–245.
28. Holsinger RM, McLean CA, Beyreuther K, Masters CL, Evin G. **Increased expression of the amyloid precursor beta-secretase in Alzheimer's disease**. Ann Neurol. 2002;51:783–86.
29. Jacobsen KT, Iverfeldt K **O-GlcNAcylation increases non-amyloidogenic processing of the amyloid-β precursor protein (APP).** Biochem Biophys Res Commun. 2011 Jan 21;404(3):882-6.
30. Jolly RD, Douglas BV, Davey PM, Roiri JE. **Lipofuscin in bovine muscle and brain: a model for studying age pigment.** Gerontology. 1995;41 Suppl 2:283-95.
31. Kaufmann W, Bolon B, Bradley A et al. **Proliferative and nonproliferative lesions of the rat and mouse central and peripheral nervous systems**. ToxicolPathol. 2012;40(4 Suppl):87S-157S.

32. Keller JN, Dimayuga E, Chen Q. **Autophagy, proteasomes, lipofuscin, and oxidative stress in the aging brain**. Int J Biochem Cell Biol. 2004;36(12):2376–2391.
33. Kiatipattanasakul W, Nakamura S, Hossain MM et al. **Apoptosis in the aged dog brain.** ActaNeuropathol. 1996;92(3):242-8.
34. King J, LeCouteur RA, Aleman M, et al. **Vacuolar myopathy in a dog resembling human sporadic inclusion body myositis**. Acta Neuropathol. 2009;118(5):711–717.
35. O'Brien RJ, Wong PC. **Amyloid Precursor Protein Processing and Alzheimer's Disease**. Annual review of neuroscience. 2011;34:185-204. doi:10.1146/annurev-neuro-061010-113613.
36. Paciello O, Shelton GD, Papparella S. **Expression of major histocompatibility complex class I and class II antigens in canine masticatory muscle myositis**. Neuromuscul Disord. 2007;17:313–320.
37. Paciello O, Papparella S. Histochemical and immunohistological approach to comparative neuromuscular diseases. Folia Histochem Cytobiol. 2009; 47 (2): 143–152.
38. Pagano TB, Wojcik S, Costagliola A, et al. Age related skeletal muscle atrophy and upregulation of autophagy in dogs. Vet J .2015; 206 (1):54–60.
39. Porta EA. **Advances in age pigment research.** Arch GerontolGeriatr. 1991;12(2-3):303-20.
40. Proctor DN, Balagopal P, Nair KS. **Age-related sarcopenia in humans is associated with reduced synthetic rates of specific muscle proteins**. J Nutr. 1998;128(2):351S–355S.
41. Riancho J, Ruiz-Soto M, Villagrá NT, Berciano J, Berciano MT, Lafarga M. **Compensatory Motor Neuron Response to Chromatolysis in the Murine hSOD1G93A Model of Amyotrophic Lateral Sclerosis**. Frontiers in Cellular Neuroscience. 2014;8:346. doi:10.3389/fncel.2014.00346.
42. Rowan SL, Rygiel K, Purves-Smith FM. **Denervation causes fiber atrophy and myosin heavy chain co-expression in senescent skeletal muscle**. PLoS One. 2012;7(1):e29082.

43. Rubin E., Farber JL **Cell injury**. In Rubin E, Farber JL, eds Pathology, Lippincott–Raven, Philadelphia; 1999:1–34.
44. Ryall JG, Schertzer JD, Lynch GS. **Cellular and molecular mechanisms underlying age-related skeletal muscle wasting and weakness.** Biogerontology. 2008;9(4):213–228.
45. Sakuma K, Yamaguchi A. **Molecular and cellular mechanism of muscle regeneration.** In: Cseri J, ed. Skeletal Muscle: From Myogenesis to Clinical Relations. Rijeka, Croatia: InTech; 2012: 3–18.
46. Selkoe DJ. **Clearing the brain's amyloid cobwebs**. Neuron. 2001;32:177–80
47. Serra F, Müller J, Gray J, Lüthi R, Dudas S, Czub S, Seuberlich T **PrP-C1 fragment in cattle brains reveals features of the transmissible spongiform encephalopathy associated PrPsc**, Brain Research (2017), doi: http://dx.doi.org/10.1016/j.brainres.2017.01.015
48. Seuberlich T, Botteron C, Benestad SL, Brünisholz H, Wyss R, et al. **Atypical scrapie in a Swiss goat and implications for transmissible spongiform encephalopathy surveillance**. J Vet Diagn Invest. 2007; 19:2–8.
49. Su B, Wang X, Nunomura A, et al. **Oxidative stress signaling in Alzheimer's disease**. Curr Alzheimer Res. 2008;5:525–532.
50. Summers BA, Cummings JF De Lahunta A. **Principles of neuropathology** In: Summers BA., Cummings JF. De Lahunta A.eds Veterinary Neuropathology. 1th ed.St Louis, US: Mosby; 1995:1-67
51. Sullivan-Gunn MJ, Lewandowski PA. **Elevated hydrogen peroxide and decreased catalase and glutathione peroxidase protection are associated with aging sarcopenia**. BMC Geriatr. 2013;13:104.
52. Tzaban S, Friedlander G, Schonberger O, Horonchik L, Yedidia Y, et al. **Protease-sensitive scrapie prion protein in aggregates of heterogeneous sizes**. Biochemistry 2002; 41: 12868–12875.

53. Van der Pas J, Hengstman GJ, ter Laak HJ. **Diagnostic value of MHC class I staining in idiopathic inflammatory myopathies**. J Neurol Neurosurg Psychiatry. 2004;75:136–139.
54. Vromman A, Trabelsi N, Rouxel C. **β-Amyloid context intensifies vascular smooth muscle cells induced inflammatory response and de-differentiation**. Aging Cell. 2013;12(3):358–369.
55. Yanai T, Masegi T, Kawada M et al. **Spontaneous vascular mineralization in the brains of cows.** J Comp Pathol. 1994;111(2):213-9.
56. Yang LB, Lindholm K, Yan R, Citron M, Xia W, et al. **Elevated beta-secretase expression and enzymatic activity detected in sporadic Alzheimer disease**. Nat Med. 2003;9:3–4.
57. Youssef SA, Capucchio MT, Rofina JE, Chambers JK, Uchida K, Nakayama H, Head E. Pathology of the Aging Brain in Domestic and Laboratory Animals, and Animal Models of Human Neurodegenerative Diseases. Vet Pathol. 2016 Mar;53(2):327-48.
58. Whitehouse IJ, Jackson C,Turner AJ and Hooper NM **Prion protein is reduced in aging and in sporadic but not in familial Alzheimer's disease.** J. Alzheimers.Dis. 2010;22:1023–1031.

Chapter 2

Neuronal lipofuscin storage and autophagy dysregulation in aged bovine brain

Based on manuscript:
De Biase D, Costagliola A, Pagano TB, Piegari G, Wojcik S, Dziewiątkowski J, Grieco E, Mattace Raso G, Russo V, Papparella S, Paciello O. **Amyloid precursor protein, lipofuscin accumulation and expression of autophagy markers in aged bovine brain.**BMC Vet Res. 2017 Apr 13;13(1):102.

2.1. INTRODUCTION

Lipofuscin, or age pigment, represents an intralysosomal polymeric material that cannot be degraded by lysosomal hydrolases, nor can be exocytosed (Terman and Brunk, 2004). It has been recently suggested that the continuous accumulation of lipofuscin, damaged proteins and organelles depends on the progressive age-related decline of autophagic and lysosomal activity (Cuervo et al., 2005). Long-lived post-mitotic cells such as neurons or cardiac myocytes cannot get rid of waste products by proliferation, which efficiently diminish the damaged structures through simple dilution, like actively proliferating cells do (Brunk and Terman, 2002a; Terman and Brunk, 2004). Thus, the age-dependent accumulation of lipofuscin in brain cells is one of the most consistent features of aging. Lipofuscin granules are detectable in a small percentage of neurons in young brains, but become progressively and markedly more abundant with age (Benavides et al., 2002). The rate of lipofuscin accumulation is the highest in the hippocampus and cerebral cortex among brain regions (Brunk and Terman, 2002a).Autophagy is a self-degradative, highly regulated process that involves the non-specific degradation of cytoplasmic macromolecules and organelles via the lysosomal system. There are three different autophagic pathways based on the mechanisms for delivery of cargo to lysosomes: macroautophagy, microautophagy and chaperone-mediated autophagy (CMA) (Wojcik, 2013). Macroautophagy (herein referred to as autophagy) is the major lysosomal pathway for the turnover of cytoplasmic components. Specifically, this process consists of the following steps: induction or initiation and cargo selection, vesicle nucleation and expansion, lysosome targeting, lysosome docking and autophagosome-lysosome fusion, vesicle breakdown and recycling. During Nucleation, the activity of specific autophagy effectors including Beclin-1 (Atg6 orthologue) and LC3 (microtubule-associated protein 1 light chain 3) generates an active phagophore (or isolation membrane) (Mizushima, 2007).The nascent membrane wraps around a portion of cytoplasm

(including the soluble proteins, aggregates, or organelle) to eventually form a double membrane-bounded structure called “autophagosome”. The nascent autophagosome subsequently fuse with lysosomes to form an autophagolysosome in which the cytoplasmic cargo is degraded by lysosome hydrolases; degradation products are recycled for the synthesis of new molecules (Mizushima, 2007). Emerging evidence indicates that autophagy protects cells by removing long-lived proteins, aggregated protein complexes, and excess or damaged organelles (Kim et al., 2008). Defects in autophagy, therefore, are associated to various pathological conditions within organisms, including tumorigenesis, defects in developmental programs and the build-up of toxic, protein aggregates involved in neurodegeneration (Kim et al., 2008) such as Amyloid precursor protein (APP). It has been recently suggested that the progressive age-related decline of autophagic and lysosomal activity may also be responsible for the continuous intraneuronal accumulation of lipofuscin, or “age pigment” (Cuervo et al., 2005). For this study, we aimed to investigate the expression of autophagic markers such as Beclin 1 and LC3 and the accumulation of pathologic proteins such as APP and lipofuscin in aged bovine brains. We also describe the possible relationship between lipofuscin accumulation, autophagy and increased Reactive oxygen species (ROS) production.

2.2. MATERIALS AND METHODS

2.2.1 Animals

For the present study, samples were collected from thirty Podolic dairy cattle (1–20 years old) in an abattoir in Campania Region, Italy, during post mortem inspection. Permission to obtain the samples was granted from the owner of the abattoir and from the veterinary inspector responsible for the sanitary surveillance. Each animal underwent a physical examination that did not report any apparent clinical illness or neurological sign (gait abnormalities, weakness and decreased mental status).

Afterward, the animals were slaughtered in strictly accordance with European slaughter regulations (CE n° 1099/2009). Moreover, the absence of prion diseases was confirmed in all animals by performing the rapid test recommended by European law. Animals were divided in two groups: group A (aged) comprised bovine aged more than ten years (n = 19) and group B (young) comprised bovine aged up to five years (n = 11) (table 2)

Bovine n°	**Breed**	**Sex**	**Age (years)**
1	Podolic	F	20
2	Podolic	F	16
3	Podolic	F	16
4	Podolic	F	13
5	Podolic	F	13
6	Podolic	F	13
7	Podolic	F	13
8	Podolic	F	13
9	Podolic	F	13
10	Podolic	F	13
11	Podolic	F	13
12	Podolic	F	12
13	Podolic	F	12
14	Podolic	F	12
15	Podolic	F	12
16	Podolic	F	11
17	Podolic	F	11
18	Podolic	F	11
19	Podolic	F	11
20	*Podolic*	*F*	*5*
21	*Podolic*	*F*	*5*
22	*Podolic*	*F*	*5*
23	*Podolic*	*F*	*4*
24	*Podolic*	*F*	*3*
25	*Podolic*	*F*	*2*
26	*Podolic*	*F*	*3*
27	*Podolic*	*F*	*2*
28	*Podolic*	*F*	*1*
29	*Podolic*	*F*	*1*
30	*Podolic*	*F*	*1*

Table 2. *Age, sex, and breed of the cases (Nos. 1– 19) and controls (Nos. 20–30) employed in this study*

2.2.2 Morphological analysis

At slaughterhouse, the brain was immediately removed and divided into two parts by a sagittal paramedian cut. The small part was frozen at −80 °C until further processing while the other part was fixed for 15 days in 10% neutral buffered formalin for histological and immunohistochemical examination. For the present study, transversal sections were taken from superior frontal gyrus and hippocampus (dentate gyrus). Precisely, for hippocampal formation we analysed pyramidal cells layer, Cornu ammonis (CA2, CA3 and CA4) fields. Sections were subsequently embedded in paraffin, sectioned at 4 μm and stained with haematoxylin and eosin (HE) and Periodic acid–Schiff (PAS). Histological specimens were examined and photographed with a light microscope (Nikon eclipse E600) associated to a microphotography system (Nikon digital camera DMX1200). Unstained sections from all cases were also evaluated with a fluorescence microscope (AxioSkop2 MOT, Zeiss) associated to a microphotography system (AxioCam MRc5, Zeiss) using blue light excitation (FITC filter; excitation, 455–500 nm; emission, 500–570 nm) in order to detect lipofuscin autofluorescence. The degree of lipofuscin accumulation was estimated as the quantity of neurons containing PAS positive storage material and scored as follows: absent, mild (less than one-third), moderate (between one-third and two-thirds), and high degree (more than two-thirds).

2.2.3 Double staining Immunohistochemistry-PAS

In order to investigate whether lipofuscin may be related to oxidative stress and impairment of autophagy, all the cases were stained with combined double immunohistochemical/histochemical methods following D'Andrea

et al. protocol (2002). The combined staining method consists of two steps: in the first step, an immunohistochemical staining was performed as previously described (Pagano et al., 2015). Primary antibodies used for this study included rabbit polyclonal Beclin-1 (BECN 1 H300: sc-11,427, Santa Cruz Biotechnology, Dallas, Texas, US) and rabbit polyclonal Superoxide Dismutase 1 (SOD1) (ab13498, AbCam, Cambridge, UK). To test the specificity of staining, two negative controls were simultaneously performed for each immunohistochemical run incubating one section with PBS (0.01 M PBS, pH 7, 2) and the other with an irrelevant and unspecific IgG.In the second step, a histochemical Periodic acid – Schiff (PAS) staining was performed. Briefly, sections were oxidized in 0,5% periodic acid solution for 5 min, rinced in deionized water, placed in Schiff reagent for 15 min, washed in tap water for 5 min, counterstained in Mayer's hematoxylin for 1 min and washed in deionizedwater. Finally, the slides were dehydrated, cleared and mounted.

2.2.4 Immunofluorescence

For all immunofluorescence experiments, 4-µm-thick sections of frontal cortex and hippocampus were mounted on positively charged glass slides (Bio-Optica, Milan). Antigen retrieval pretreatments were performed using a Heat Induced Epitope Retrieval (HIER) citrate buffer pH 6.0 (Bio-Optica, Milan, Italy) for 20 min at 98 °C. Primary antibodies used in this study included rabbit polyclonal Beclin-1 (BECN 1 H300: sc-11,427, Santa Cruz Biotechnology, Dallas, Texas, US) rabbit polyclonal LC3 (ab51520, Abcam, Cambridge, UK), mouse monoclonal APP (6E10) (SIG-39320, BioLegend, San Diego, California, US). The method was previously described (Paciello et al., 2010). Briefly, the primary antibody diluted inPhosphate Buffer Saline (PBS) was applied overnight at4 °C. Slides were washed two times, five minutes each,in PBS and incubated for two hours at roomtemperature with a Goat anti-Rabbit IgG (H + L) SecondaryAntibody (Alexa Fluor® 546 conjugate, A-11035,Thermo Fisher PO Box 117 Rockford, IL, USA) for Beclin 1, LC3 and a Goatanti-

Mouse IgG (H + L) Secondary Antibody (AlexaFluor® 546 conjugate, A11030, Thermo Fisher PO Box117 Rockford, IL, USA) for APP. Both secondary antibodies were diluted 1:50 in PBS. Slides were rinsed three times with PBS and coverslipped using Vectashield mounting medium containing 4′,6-diamidino-2-phenylindole (DAPI) (H-1200 Vector Laboratories, Inc., 30 Ingold Road, Burlingame, CA, USA).
For immunohistochemistry and immunofluorescence, the intensity grade of immunoreactivity was measured as the intensity of staining and percentage of positively stained cells referred to the entire studied sections and subsequently assessed as it follows:

- negative (0);
- mild (1);
- moderate (2) and
- high (3).

The degree of lipofuscin accumulation, the intensity grade of staining and the percentage of positively stained cells was scored by two independent observers (Prof. Orlando Paciello, Prof. Serenella Papparella) in each specimen, for each antibody and under blinded conditions as performed in a previous study (Pagano et al., 2015).

2.2.5 Western blot analysis

Samples of brain from elder cows and controls were cut at the cryostat at 20 μm and then lysed at 4 °C in 200 μL of TBS lysis buffer (Tris Buffer Saline, 20 mM Tris-HCl pH 7.6, 140 mM NaCl, 30 mM sodium pyrophosphate, 5 mM EDTA, 0.55% Nonident P40, 1% Triton X-100, 50 mM NaF, 0.1 mM Na3VO4, 1 mM PMSF, 1 mM benzamidine, 1 mM iodoacetamide, 1 mMphenantroline). Protein concentration in the supernatant was determined by Bicinchoninic Acid assay (BCA) protein assay (BCA: Pierce Biotechnology, Rockford, Illinois, US), and lysates were adjusted to equivalent concentrations with lysis buffer. Aliquots of 10 mg of total brain lysate were then separated on Sodium Dodecyl Sulphate -

PolyAcrylamide Gel Electrophoresis (SDS-PAGE). Proteins were transferred to Sodium Dodecyl Sulphate - PolyAcrylamide Gel Electrophoresis (PVDF) membranes that were blocked overnight at 4 °C with 5% non-fat dried skimmed milk in TTBS (TBS with 0.05% Tween 20). Incubation with primary specific antibodies against Beclin-1 (1: 500 dilution), LC3 (both isoforms, dilution 1: 3000) and mouse monoclonal APP (6E10) (dilution 1:2000) and horseradish peroxidase-conjugated secondary antibodies was performed in blocking solution for 1 h at room temperature. Immunoreactive bands were visualized by SuperSignal West Pico Chemiluminescent substrate kit (Pierce Biotechnology, Rockford, Illinois, US). The same blots were stripped and re-probed using anti-beta actin monoclonal antibody to confirm equal loading of proteins in all lanes. Bands intensities were quantified on scanned images using Image J software (National Institute of Health, USA) to determine average pixel intensity.

2.2.6 Statistical analysis

Data obtained from Western blots were analysed with Statview software (Abacus Concepts) by t-Student test. Blots were revealed by Enhanced chemiluminescence (ECL) and autoradiography using beta-actin as a loading control. The autoradiographs shown are representative of four independent experiments. Bars represent the mean ± SD of four independent experiments. The chi-squared test was used to assess differences between the studied groups of cows. We also performed Gamma statistic G (Siegel et al., 1988) in order to investigate for possible associations between immunohistochemical findings and age. Subsequently, d-Somer's statistics was performed to establish the relation of present association. P-values of <0.05 were considered statistically significant. Gamma statistic G (Goodman and Kruskal's gamma) measures the strength of association of the contingency table values when the variables are on an ordinal scale. Somers' D is closely related to the

gamma statistic and it's one of the most commonly used measures of association for doubly ordered contingency tables.

2.3. RESULTS

2.3.1 Histopathology

A detailed morphological evaluation of the bovine brains is reported in the Chapter 1 of this Ph.D thesis. The striking and constant finding in all aged brains (group A) was the accumulation of small perinuclear and granular yellow-brown, Periodic acid – Schiff (PAS) stain positive (Fig.2.1a) and autofluorescent deposits (Fig. 2.1b) consisting of lipofuscin. The amount of lipofuscin was moderate to severe, with a wide distribution in both cerebral cortex and hippocampus regions. Lipofuscin accumulation was found within the perikarya and sometimes the proximal dendritic tree of neurons and within the cytoplasm of astrocytes. No evidence of lipofuscin accumulation was observed in the neurons of young animals (Fig. 2.1c.Lipofuscin accumulation was significantly more noticeable among the older animals (group A) ($p < 0.001$). There was a statistically significant positive association between age and increase in severity of lipofuscin accumulation ($G = 0.7980$; $p < 0.001$) and this relation was strong (d Somer's statistics $=0.6611$; $p < 0.001$).

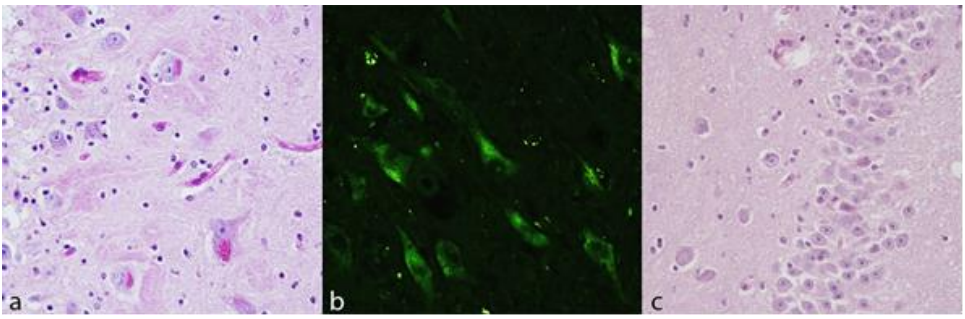

Fig. 2.1. ***Lipofuscin storage, hippocampus, dentate gyrus.****(a) Pyramidal neurons showing an abundant granular, PAS positive, intracytoplasmatic storage material. Periodic acid-Schiff (PAS) stain, 40X. (b) Intraneuronal storage material exhibits green-yellow autofluorescence by fluorescence microscopy. Fluorescence microscope; FITC filter (excitation, 455–500 nm; emission, 500–570 nm), 40X. (c) Neurons of young controls does not exhibit PAS positive and intracytoplasmatic storage material. Periodic acid-Schiff (PAS) stain, 40X.*

2.3.2 Double staining Immunohistochemistry-PAS

By using double staining IHC/PAS we observed a negative association between Beclin-1 expression and lipofuscin accumulation in neurons of the brain of aged animals (Group A). In young animals (Group B), neurons exhibited a prominent Beclin-1 immunolabelling, but lipofuscin accumulation was absent. Moreover, in aged brains (Group A), lipofuscin were present in cytoplasmic regions of neurons exhibiting prominent SOD 1 immunolabelling. Conversely, in the brain of young animals (Group B), SOD 1 was mildly expressed and no lipofuscin accumulation was detected.

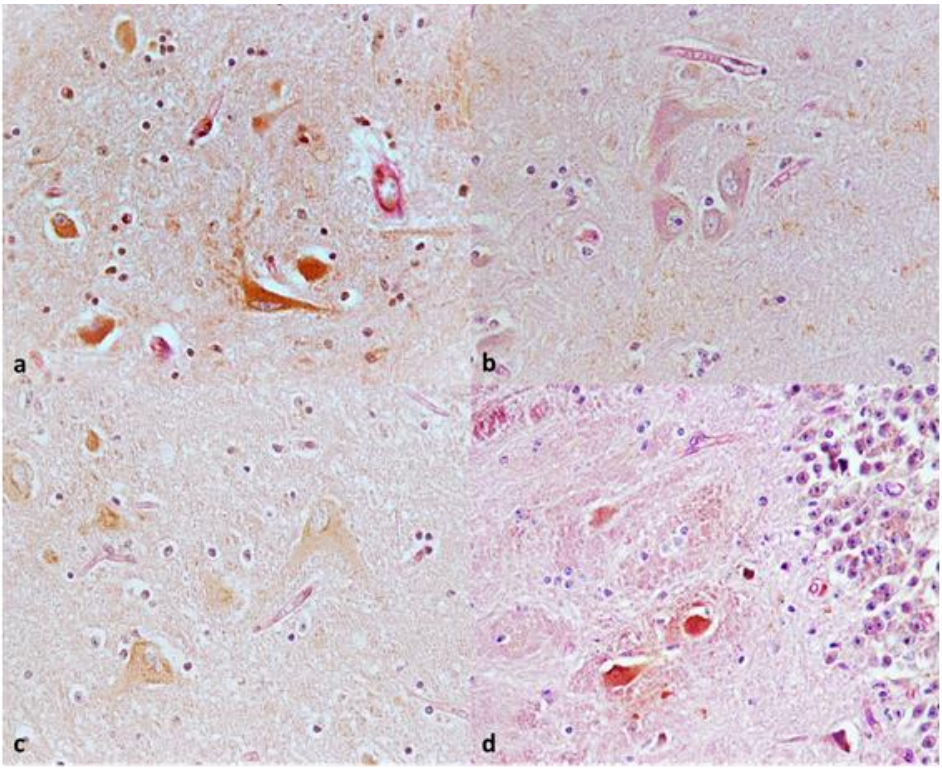

Fig. 2.2 Double staining Immunohistochemistry-PAS, hippocampus, dentate gyrus. *Beclin 1 expression is normally expressed in young (a), but not in aged bovine brain (b). Beclin 1 expression is inversely propotional to lipofuscin accumulation in neurons of aged brains. (c) SOD 1 neuronal expression and lipofuscin accumulation are mild in young bovine brains. (d) In aged bovine brains, SOD 1 strongly immunolabelled neurons have also a marked lipofuscin accumulation.*

2.3.3 Immunofluorescence

In all samples, autophagy induction was evaluated by Beclin-1 immunofluorescence and showed a progressive age-related decrease of intraneuronal Beclin-1 expression. In young animals (Group B), the percentage of Beclin-1 immuno-positive neurons and astrocytes as well as Beclin-1 staining intensity was of mild degree and widespread. Beclin-1 staining intensity as well as percentage of Beclin-1 immuno-positive cells

were significantly more noticeable among the young animals ($p < 0.01$and $p < 0.001$, respectively). On the contrary, in 76% (n = 14) of samples from aged cows (group A) no Beclin-1 positivity was detected (Fig. 2.3 a, b). In remaining 24% of cases percentage of Beclin-1 immuno-positive cells as well as Beclin-1 staining intensity was of mild degree. A Beclin-1 positivity was mainly observed in neurons in the hippocampus. There was a statistically significant negative association between age and increase of percentage of Beclin-1 immunoreactive cells ($G = -0.9521$; $p < 0.001$) and this relation was strong (d Somer's statistics = −0.6653; $p < 0.001$). There was also a statistically significant negative association between age and increase of staining intensity of Beclin-1 immunoreactivity ($G = -0.8523$; $p < 0.001$) and this relation was strong (d Somer's statistics = −0.6276; $p < 0.001$). Moreover, strongly LC3 immuno-positive neurons and astrocytes were observed in aged animals (Fig. 2.4a), indicating possibly an excessive accumulation of autophagosomes. In younger animals, LC3 staining intensity was mostly absent (Fig . 2.4b), even though a low percentage of LC3 widespread immune-positive neurons was rarely observed. These parameters were significantly more noticeable among the aged animals ($p < 0.01$and $p < 0.001$, respectively). There was a statistically significant positive association between age and increase of these parameters ($G = 1$; $p < 0.001$) and this relation was moderate (d Somer's statistics =0.5230; $p < 0.001$).Amyloid precursor protein (APP) positive immunoreaction was detected within the cytoplasm of neurons and astrocytes in the hippocampus and cerebral frontal cortex of all the aged animals (group A) (Fig. 2.5a), but never in young animals (Fig 2.5b). There was high degree of staining intensity of APP in all the cases of aged animals. Percentage of APP immuno-positive cells as well as their staining intensity were significantly more noticeable among the older animals ($p < 0.001$). There was a statistically significant positive association between age and increase in severity of APP positive immunoreaction ($G = 1$; $p < 0.001$) and this relation was moderate (d Somer's statistics =0.5230; $p < 0.001$).

2.3.4 Western blot analysis

We evaluated the expression levels of APP, Beclin-1, and LC3 in elder cows showing immunohistochemical positivity for APP (represented as 100 kDa band), Beclin-1(represented as 60 kDa band) and two isoforms of LC3 (represented as 18 kDa band for LC3-I and 16 kDa band for LC3-II) mainly to confirm the dysregulation of autophagy in brain from elder cows compared to young animals. Our results, normalized for actin, showed that Beclin-1 (60 kDa) was significantly reduced in the aged animals compared with the young animals (*** $P < 0,001$ vs control) (Fig. 2. 3c) and an increased LC3-II/LC3-I ratio ($P < 0,05$ vs control) (Fig. 2.4c). Moreover, a significant increase in the oldest animals compared to young animals ($P < 0,05$ vs control) (Fig. 2.5c) for APP was detected with a band approximatively to 100 kDa as previously described (Selkoe et al., 1988).

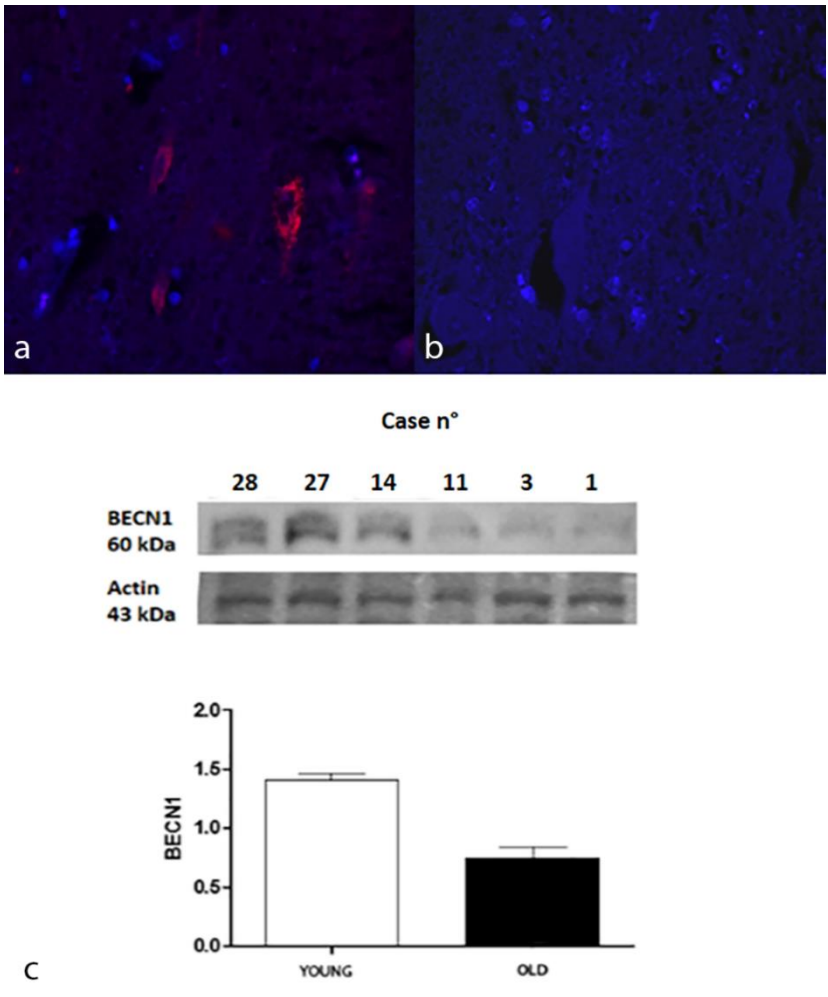

Figure 2.3. Beclin 1 expression, hippocampus, dentate gyrus. *(a)Immunostaining inyoung and (b) aged brain. TRITC filter (excitation, 543 nm; emission 560 nm). DAPI counterstain, 40X. (c) Protein expression in young and aged bovine brains. Densitometric values shows that BECN1 is expressed in higher amount in young controls when compared to aged brain samples (P<0,001 vs controls). Bars refers to mean values. Actin protein levels confirm the amount of protein loading in each lane.*

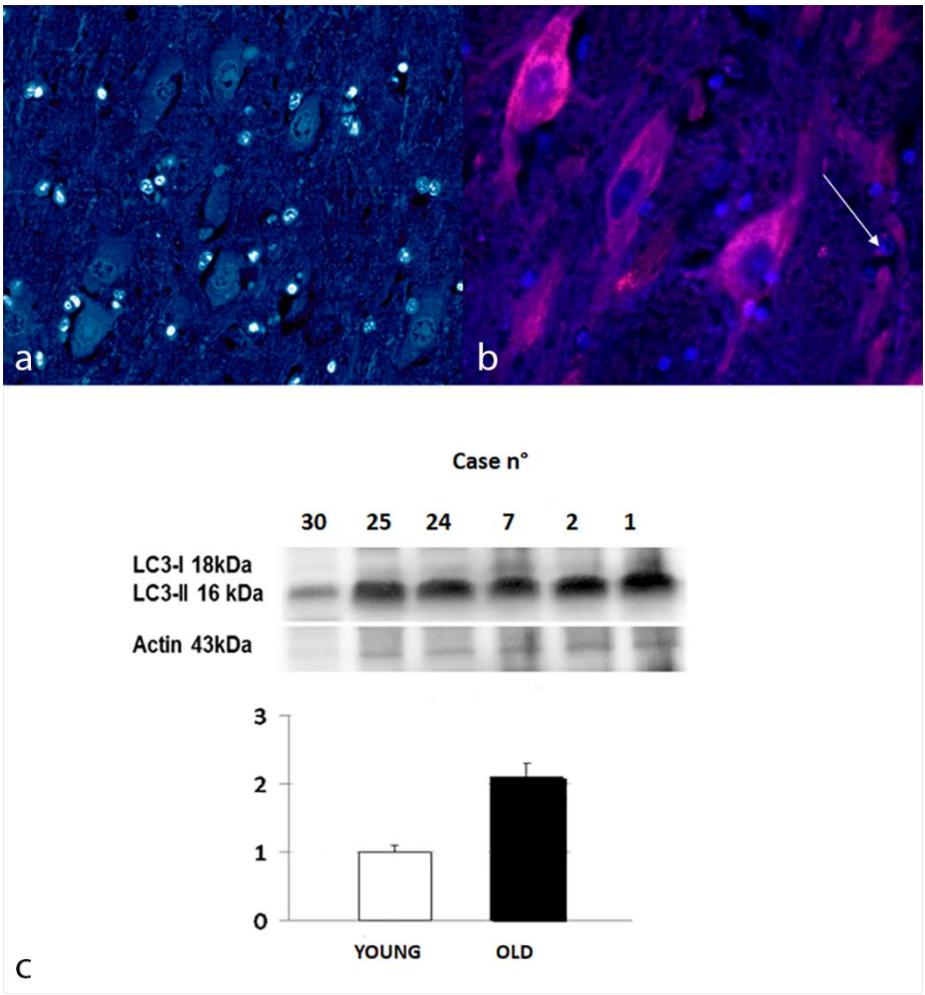

Figure 2.4. LC3 expression, hippocampus, dentate gyrus.*(a) Immunostaining in young and (b) aged brain.Immunoreaction for LC3 was detected also in astrocytes (arrow).TRITC filter (excitation, 543 nm; emission 560 nm). DAPI counterstain, 40X. (c) Protein expression in young and aged bovine brains. Densitometric values shows that LC3-II/LC3-I ratio is significantly increased in the aged animals compared to the young controls (P<0,05 vs control). Bars refers to mean values. Actin protein levels confirm the amount of protein loading in each lane*

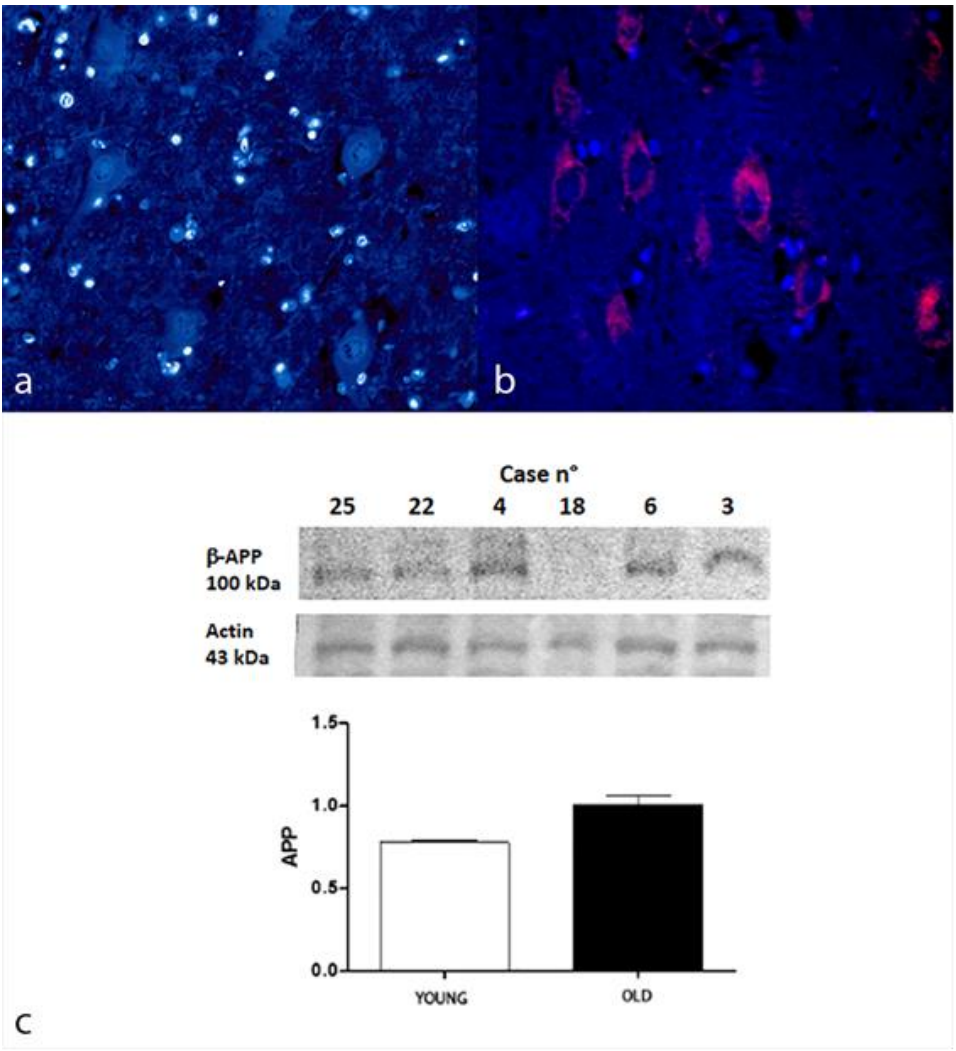

Figure 2.5. APP expression, hippocampus, dentate gyrus. *(a) Immunostaining in young and (b) aged brain. TRITC filter (excitation, 543 nm; emission 560 nm). DAPI counterstain, 40X. (c) Protein expression in young and aged bovine brains. Densitometric values shows that APP is expressed in higher amount in aged brains when compared to young controls (P<0,05 vs controls). Bars refers to mean values. Actin protein levels confirm the amount of protein loading in each lane.*

2.4. DISCUSSION

In this study, the age-dependent intraneuronal accumulation of lipofuscin is one of the most striking features of aged brains. This finding is not actually new, as it has been described for more than 150 years (Brunk and Terman, 2002b). In the past, lipofuscin was generally thought to be an innocent end product of oxidation which has no significant influence on cellular activities (Rubin et al., 1999), but in the last decade several authors have investigated about the possible detrimental and pathogenic potential of this material. Terman and Brunk, in a series of elegant experiments (Kurz et al., 2008; Brunk and Terman, 2002a and 2002b), hypothesized the so-called "mitochondrial–lysosomal axis theory of aging" that tries to explain the possible relationship between lipofuscin accumulation, decreased autophagy, increased Reactive Oxygen Species (ROS) production, and mitochondrial damage in senescent long-lived postmitotic cells. According to this theory, in senescent cells lysosomal enzymes are directed towards the plentiful lipofuscin-rich lysosomes and, subsequently, they are lost for effective autophagic degradation because lipofuscin remains non-degradable. The consequences are a progressive impairment of autophagy and the gradual accumulation of damaged mitochondria, other organelles and misfolded proteins that lead to neurodegeneration. Cytotoxic activity of lipofuscin consists also in its ability to incorporate redox-active transition metals (iron), resulting in a redox-active surface, able to catalyze the Fenton reaction: in presence of Fe^{2+}, H_2O_2 is decomposed forming hydroxyl radicals (OH). The resulting Fe^{3+} can be reduced by superoxide and the vicious cycle starts again (Kurz et al., 2008). Double staining Immunohistochemistry-PAS allowed us to suggest a direct relationship between lipofuscin accumulation, autophagy impairment and increased reactive oxygen species level in aged bovine brains. SOD1 is considered one of the key enzymes used by cells to protect themselves against oxygen free radicals (Fridovich, 1995). However, excessive dismutase activity may result in "overscavenging" of superoxide anion and in increased H_2O_2 formation, which in turn may facilitate deleterious peroxidative reactions and the production of highly

toxic hydroxyl radicals (Jaarsma et al., 2010).According to recent scientific literature, we can also hypothesize that progressive and severe lipofuscin accumulation may irreversibly lead to functional decline and death of neurons by diminishing lysosomal degradative capacity and by preventing lysosomal enzymes from targeting to functional autophagosomes. However, since lipofuscin progressively accumulates throughout the life of neurons, a combined immunohistochemical/histochemical protocol is not perfectly indicated to investigate the mechanism and relative timing of intraneuronal lipofuscin accumulation and the deposition of other proteins. Primary cultured neuronal cells exhibit, in vitro, a variety of features that are frequently observed in physiologically aged neurons in vivo, including lipofuscin accumulation (Mori, 2015). Thus, long-term aging culture of primary cultured neurons would be a remarkable model to unravel, at least in part, the molecular mechanisms behind lipofuscin accumulation and its pathological effects on neuronal cells. Further studies are indeed necessary to better understand how lipofuscin accumulation can influence oxidative stress and the neuronal autophagic pathway in bovine brains. To our knowledge this is the first study that describe the expression of autophagy markers in aged bovine brains. Our results suggest that in aged cow autophagy is significantly impaired if compared to young animals and they confirm that intraneuronal APP deposition increases with age. Beclin-1 and LC3 play a pivotal role in the autophagy process and their expression by immunoblotting, immunohistochemistry or immunofluorescence has become a reliable method for monitoring autophagy and autophagy-related processes (Pagano et al., 2015). Beclin-1 is a positive regulator of the autophagy pathway and promotes its induction whereas LC3 facilitates autophagosome elongation and closure [19]. During autophagic activity, the cytosolic form of LC3 (LC3-I) is conjugated to phosphatidylethanolamine to form LC3-phosphatidylethanolamine conjugate (LC3-II), which localizes to both the outside and the inside membranes of autophagosomes (Wong et al., 2010). Autophagosomes fuse with lysosomes to form autolysosomes and intra-autophagosomal components as well as LC3-II are degraded by lysosomal hydrolases.

Results from immunofluorescence and western blot analysis showed a progressive age-related decrease of intraneuronal Beclin-1 expression that most likely indicate a decrease in autophagy initiation. The increase of LC3 antibody expression detected by immunofluorescence may indicate an excessive accumulation of autophagosomes. Interestingly, western blot analysis showed an increased LC3-II expression that most likely indicate an impaired autophagosomal degradation resulting in the persistence of autophagic vacuoles that could interfere with intracellular trafficking promoting the presence of cytotoxic products [20]. Recently, Vallino Costassa et al. (2016) characterized the nature of Amyloid β (Aβ) deposits in aged bovine brains pointing out that they are similar to those in humans in early stages of aging. Consistent with these findings, we observed an age-dependent, intraneuronal accumulation of APP immuno-positive material. Furthermore, western blot analysis showed an increased level of APP in aged animal compared to young animals. Several authors suggested that autophagy dysregulation may alter APP metabolism and fail to clear aggregated Aβ via autophagy - lysosome system promoting the accumulation of misfolded proteins and subsequent neurodegeneration (Chang et al, 2005; Walsh et al., 2007). Moreover, we recently observed accumulation of APP in the sarcoplasm of some of the aged cows used for this study (Costagliola et al., 2016). The accumulation within abnormal muscle fibers of several pathologic and Alzheimer-related proteins such as beta-amyloid precursor protein (beta-APP), phosphorylated tau, alpha-1-antichymotrypsin, apolipoprotein E and presenilin-1 is an unusual feature of sporadic inclusion-body myositis (sIBM) (Askanas and Engel, 1998). We can speculate that same pathophysiological mechanism leading to the accumulation of APP can occur in the brain as well as in the muscle of old cows.However, molecular mechanisms underlying the progressive accumulation of toxic proteins during aging remain still elusive and unclear. In healthy individuals, APP is transcribed in the endoplasmic reticulum, modified by Golgi network and then shuttled to the cell surface through the secretory pathway (Kragh et al, 2012). APP can then either be degraded through the autophagy-lysosome system, or recycled by endosomes entering the cycle again (Kragh et al, 2012). An interesting

study of Pickford et al. (2008) contributed to clarify the association between autophagy impairment and neurodegeneration providing evidence that an essential component of the autophagy pathway, such as Beclin-1, is reduced in early Alzheimer disease promoting amyloid β accumulation in mice (Lee et al., 2008). Induction of autophagy and autophagosomal degradation seem to be impaired in Beclin-1 deficient cells. As a consequence, APP containing vesicles (endosomes, autophagosomes, and others) build up inside the cell. APP is increasingly cleaved by secretases generating Aβ that is possibly released from the cell (Kragh et al, 2012). Furthermore, the progressive accumulation of autophagosomes due to an impairment of autophagosomal degradation can serve as sites of Aβ generation, promoting the inhibition of APP turnover and degradation (Kragh et al, 2012). Nowadays, it's a firm belief that impairment and dysregulation of autophagy pathways is related to many neurological diseases both in humans and animals. To our knowledge, this is the first report concerning about the expression of autophagy markers Beclin 1 and LC3 in aged bovine brains. Our data show that autophagy is impaired in aged bovine brains and that intraneuronal accumulation of APP increases with age. According to our results, we also assume that the ineluctable formation and accumulation of lipofuscin in aged cow brains seems to be associated with an impaired function of autophagy and an increased oxidative stress. The indigestible nature of this material is associated with progressive diminution of lysosomal function, which has secondary effects on many different cellular activities. We thus believe that the accumulation of this age pigment is a very important—perhaps even central—aspect of the phenomenon of aging. Future studies, however, will allow to further understand the cellular and molecular events regulating the autophagy machinery.

REFERENCES

1. Askanas V, Engel WK. **Sporadic inclusion-body myositis and its similarities to Alzheimer disease brain.** Recent approaches to diagnosis and pathogenesis, and relation to aging. Scand J Rheumatol. 1998;27(6):389-405.
2. Benavides SH, Monserrat AJ, Farina S, Porta EA. **Sequential histochemical studies of neuronal lipofuscin in human cerebral cortex from the first to the ninth decade of life**. Arch. Gerontol. Geriatr. 2002;34:219-231
3. Brunk, UT, Terman A. **Lipofuscin: Mechanisms of age-related accumulation and influence on cell functions**. Free Radic. Biol. Med. 2002a; 33:611–619
4. BrunkUT, Terman A. **The mitochondrial-lysosomal axis theory of aging: accumulation of damaged mitochondria as a result of imperfect autophagocytosis**. Eur J Biochem. 2002b;269(8):1996-2002.
5. Chang KA, Suh YH **Pathophysiological roles of amyloidogenic carboxy-terminal fragments of the beta-amyloid precursor protein in Alzheimer's disease** J Pharmacol Sci. 2005;97(4):461-71.
6. Costagliola A, Wojcik S, Pagano TB, De Biase D, Russo V, Iovane V, Grieco E, Papparella S, Paciello **Age-Related Changes in Skeletal Muscle of Cattle**. Vet Pathol. 2016;53(2):436-46.
7. Cuervo AM, Bergamini E, Brunk UT et al. **Autophagy and aging: the importance of maintaining "clean" cells** Autophagy 2005;1:131-140
8. De Biase D, Paciello O **Essential and current methods for a practical approach to comparative neuropathology**. Folia Morphol (Warsz). 2015;74(2):137-49. doi: 10.5603/FM.2015.0024.
9. Fridovich, I. **Superoxide radical and superoxide dismutases**. Annu. Rev. Biochem. 1995;64:97–112.

10. Höhn A, Grune T. **Lipofuscin: formation, effects and role of macroautophagy**. Redox Biology. 2013; 1(1):140-144.

11. Jaarsma D, Haasdijk ED, Grashorn JA, Hawkins R, van Duijn W, Verspaget HW, London J, Holstege JC. **Human Cu/Zn superoxide dismutase (SOD1) overexpression in mice causes mitochondrial vacuolization, axonal degeneration, and premature motoneuron death and accelerates motoneuron disease in mice expressing a familial amyotrophic lateral sclerosis mutant SOD1**. Neurobiol Dis. 2000 Dec;7(6 Pt B):623-43.

12. Kim PK, Hailey DW, Mullen RT, Lippincott-Schwartza J. **Ubiquitin signals autophagic degradation of cytosolic proteins and peroxisomes** Proc Natl Acad Sci U S A. 2008;105(52):20567–20574
13. Kragh CL, Ubhi K, Wyss-Coray T, Masliah E. **Autophagy in dementias**. Brain Pathol. 2012;22(1):99-109.
14. Kurz T, Terman A, Gustafsson B, BrunkUT.**Lysosomes in iron metabolism, ageing and apoptosis**. Histochemistry and Cell Biology. 2008;129(4):389-406.
15. Lee JA, Gao FB. **Regulation of Aβ pathology by beclin 1: a protective role for autophagy?** J. Clin. Invest. 2008;118(6):2015-2018.
16. Mizushima N. **Autophagy: Process and function**. Genes Dev. 2007;21:2861–2873.
17. Paciello O, Wojcik S, Gradoni L et al. **Syrian hamster infected with Leishmania infantum: a new experimental model for inflammatory myopathies**. Muscle Nerve. 2010;41(3):355-61.
18. Pagano TB, Wojcik S, Costagliola A, De Biase D, Iovino S, Iovane V, Russo V, Papparella S, Paciello O. **Age related skeletal muscle atrophy and upregulation of autophagy in dogs**. Vet J. Vet J. 2015;206(1):54-60.
19. Pickford F, Masliah E, Britschgi M, et al. **The autophagy-related protein beclin 1 shows reduced expression in early Alzheimer**

disease and regulates amyloid β accumulation in mice. J. Clin. Invest. 2008;118(6):2190-2199.

20. Rubin E, Farber JL. **Cell injury**. In Rubin E, Farber JL, eds Pathology, Lippincott–Raven, Philadelphia; 1999:1–34
21. Selkoe DJ, Podlisny MB, Joachim CL, Vickers EA, Lee G, Fritz LC, Oltersdorf T. **Beta-amyloid precursor protein of Alzheimer disease occurs as 110- to 135-kilodalton membrane-associated proteins in neural and non-neural tissues**. Proc Nat Acad Sci U S A. 1988;85(19):7341-5.
22. Siegel S, Castellan Jr NJ. **Non parametric statistics for the behavioral sciences** 2nd ed. New York, McGraw Hill, 1988.
23. Terman A, Brunk UT. **Lipofuscin**. Int. J. Biochem. Cell Biol. 2004;36:1400–1404
24. Vallino Costassa E, Fiorini M, Zanusso G et al. **Characterization of Amyloid-β Deposits in Bovine** J Alzheimers Dis. 2016; 51(3): 875–887.
25. Walsh DM, Selkoe DJ. **Aβ oligomers - a decade of discovery**. J Neurochem. 2007;101(5):1172-84.
26. Wojcik S. **Crosstalk between autophagy and proteasome protein degradation systems: possible implications for cancer therapy**. Folia Histochem Cytobiol 2013;51(4):249–264
27. Wong E, Cuervo AM. **Autophagy gone awry in neurodegenerative diseases**. Nat Neurosci. 2010;13(7):805-11.

Chapter 3

Inflammasome and Autophagy cross-talk in bovine brains

3.1. INTRODUCTION

"*Immunosenescence*" is one of the most recognized effects of aging that consist in the dysregulation of the immune system as a result of defects in both initiation and resolution of immune responses (Lopez-Otin et al., 2013). Immunosenescence is accompanied by a low-grade and chronic pro-inflammatory environment in multiple tissues characterized by increased production of pro-inflammatory cytokines such as interleukin-6 (IL-6), tumor necrosis factor alpha (TNF-α), acute-phase proteins, reactive oxygen species (ROS), and autoantibodies. This pro-inflammatory environment has been defined as "***inflammaging***" and it has been linked to an increased incidence of several disorders, including neurodegenerative diseases (Franceschi et al., 2007; Montecino-Rodriguez et al., 2013). Microglia, the innate immune cells of the central nervous system (CNS), most likely contribute to the development of this age-related pro-inflammatory environment and it is speculated that any changes in microglial activities are key components in influencing the pathogenesis of neurodegeneration (Luo et al., 2010). Microglia normally keep in a quiescent state when not challenged, but rapidly transform to an activated state when triggered by appropriate stimulation showing a deramified shape and enhanced expression of activation-associated markers such as Major Histocompatibility Complex II (MHC II) (Sheffield and Berman, 1998). An emerging growing body of evidence in animal models sustains that inflammatory responses involving microglia and IL-1β secretion play a pivotal role in the progression of diseases of the Central Nervous System (CNS) (Glass et al., 2010). The molecular steps leading to IL-1β maturation take place in an intracellular complex known as ***"inflammasome"*** (Martinon et al., 2002). The inflammasome is a caspase-1 activating multiprotein platform that results from oligomerization of inactive monomeric proteins from the nucleotide-binding domain, leucine-rich repeat (NLR) protein family (Martinon et al., 2002). Different complexes have been described, but the most intensively studied is the **NLRP3** (or NALP3) **inflammasome** which is formed when NLRP3

associates with the adaptor protein ASC and procaspase-1 upon activation by different stimuli, such as pathogen associated molecular patterns (PAMPs), damage-associated molecular patterns (DAMPs), or endogenous danger signals such as increased reactive oxygen species (ROS) (Latz et al., 2013; Walsh et al., 2014). The precise mechanism of inflammasome activation is not fully understood. NLRP3 can sense a variety of molecular structures and it is thought that inflammasome activation occurs probably not through direct ligand-receptor interaction but rather the sensing of cellular homeostasis disruption (Ratsimandresey et al., 2013; Wen et al., 2013). Namely, several authors suggest that autophagy, a cellular mechanism of waste removal and recycle of cellular components, contributes as amacrophage-intrinsic negative regulator of NLRP3 inflammasome (Zhong et al., 2016). The last year of my Ph.D was dedicated to investigate the expression of the NALP3 inflammasome in bovine brains and its association with autophagy and increased ROS production.

3.2. MATERIALS AND METHODS

3.2.1 Animals

For the present study, samples were collected from forty-two Podolic dairy cattle (1–24 years old) in an abattoir in Campania Region, Italy, during post mortem inspection. Permission to obtain the samples was granted from the owner of the abattoir and from the veterinary inspector responsible for the sanitary surveillance. Each animal underwent a physical examination that did not report any apparent clinical illness or neurological sign (gait abnormalities, weakness and decreased mental status). Afterward, the animals were slaughtered in strictly accordance with European slaughter regulations (CE n° 1099/2009). Moreover, the absence of prion diseases was confirmed in all animals by performing the rapid test recommended by European law. Animals were divided in three groups: group A (aged) comprised bovine aged 15 to 24 years (n = 14), group B

(adult) comprised bovine aged 5 to 14 years (n=14) and group C (young) comprised bovine aged up to 5 years (n = 14) (table 3).

Group A	Group B	Group C
24	15	5
22	15	5
21	14	4
20	13	3
19	12	2
18	12	2
17	11	2
16	11	2
16	10	1
16	10	1
16	9	1
16	8	1
16	7	1
16	7	1

Table 3. *Age (in years) of the animals employed for this study. Group A (aged), Group B (adult) and Group C (young)*

3.2.2 Morphological analysis

At slaughterhouse, the brain was immediately removed and divided into two parts by a sagittal paramedian cut. The small part was frozen at −80 °C until further processing while the other part was fixed for 15 days in 10% neutral buffered formalin for histological and immunohistochemical examination. For the present study, transversal sections were taken from superior frontal gyrus and hippocampus (dentate gyrus). Precisely, for hippocampal formation we analysed pyramidal cells layer, Cornu ammonis

(CA2, CA3 and CA4) fields. Sections were subsequently embedded in paraffin, sectioned at 4 μm and stained with haematoxylin and eosin (HE) and Periodic acid–Schiff (PAS).

3.2.3 Immunohistochemistry

Immunohistochemistry (IHC) experiments were performed in order to evaluate the expression of NLRP3 and MHC II. For IHC, 4-μm-thick sections of hippocampus were mounted on positively charged glass slides (Bio-Optica, Milan). For antibodies detection, we used a well-established protocol described elsewhere (Pagano et al., 2015). Briefly, antigen retrieval pretreatments were performed using a HIER citrate buffer pH 6.0 (Bio-Optica, Milan, Italy) for 20 minutes at 98 °C. Following, endogenous peroxidase (EP) activity was quenched with 3% hydrogen peroxide (H2O2) in methanol and sections were blocked with a protein block (MACH1, Biocare Medical LLC, Concord, California, USA) for 30 minutes each. Slides were sequentially incubated overnight at 4 °C with primary rabbit polyclonal NLRP3 antibody (LS-B8262, LifeSpan BioSciences) diluted 1:400 in PBS (0.01 M PBS, pH 7,2) and mouse monoclonal MHC II antibody diluted 1:200 in PBS (clone H42A, VMRD). Antibody deposition was visualized using the DAB chromogen diluted in DAB substrate buffer and the slides were counterstained with hematoxylin. Between all incubation steps, slides were washed two times (5 minutes each) in PBS. In the corresponding negative control sections, the primary antibody was either omitted or replaced with normal serum from the same species of primary antibody (rabbit). As a positive control, we used an intestinal biopsy from a human patient affected by Crohn disease.

3.2.4 Double colour immunofluorescence

The pre-treatment steps were the same as those used for immunoperoxidase labelling and the procedure was described elsewhere

(De Biase et al., 2017). Primary antibodies used in this study included rabbit polyclonal Beclin-1 (BECN 1 H300: sc-11,427, Santa Cruz Biotechnology, Dallas, Texas, US), diluted 1:400 in PBS (0.01 M PBS, pH 7,2) and rabbit polyclonal Superoxide Dismutase 1 (SOD1) (ab13498, AbCam, Cambridge, UK) diluted 1:400 in PBS. Primary antibodies were applied overnight at 4°C. Slides were washed two times, five minutes each, in PBS and incubated for two hours at room temperature with a Goat anti-Rabbit IgG (H + L) Secondary Antibody (Alexa Fluor® 546 conjugate, A-11035,Thermo Fisher PO Box 117 Rockford, IL, USA)diluted 1 in100 in PBS, for two hours at room temperature. For NALP3 detection, after three washes in PBS, a rabbit polyclonal anti-NLRP3 antibody (LS-B8262, LifeSpan BioSciences) diluted 1:400, was applied and the sections were again incubated overnight at 4 °C. Slides were washed again three times in PBS and then incubated with a Fluorescein isothiocyanate (FITC)-conjugated pure goat anti-rabbit secondary antibody (Alexa Fluor® 488 conjugated, A-11034 Thermo Fisher PO Box 117 Rockford, IL, USA) diluted 1 in100 in PBS, for two hours at room temperature. Slides were rinsed with PBS and mounted with a solution of one part of glicerol/one part PBS. For scanning and photography, a laser scanning microscope (LSM 510; Zeiss, Göttingen, Germany) was used. The anti–NLRP3 polyclonal rabbit antibody bound to FITC was illuminated at 488 nm and read using a 505–560 nm band pass filter. Rabbit polyclonal anti-BECN1 and anti-SOD1 antibodies bound to TRITC were illuminated at 543 nm and then read with a 560 nm long pass filter. The different frames were scanned separately, with appropriate installation of the optical path for excitation and emission of each scan according to the manufacturer's instructions.

For immunohistochemistry and immunofluorescence analysis, the intensity grade of immunoreactivity was measured as the percentage of positively stained cells referred to the entire studied sections and subsequently assessed as it follows:

- Absent/none: negative (0);
- 1%-25%: mild (1);

- 26%-50%: moderate (2) and
- > 50%: high (3).

The percentage of positively stained cells was scored by two independent observers (Prof. Orlando Paciello, Dr. Davide De Biase) in each specimen, for each antibody and under blinded conditions as performed in a previous study with a concordance rate of 95% (De Biase et al., 2017).

3.2.5 Western Blot analysis

Samples of brain from elder cows and controls were cut at the cryostat at 20 µm and then lysed at 4 °C in 200 µL of TBS lysis buffer (Tris Buffer Saline, 20 mM Tris-HCl pH 7.6, 140 mM NaCl, 30 mM sodium pyrophosphate, 5 mM EDTA, 0.55% Nonident P40, 1% Triton X-100, 50 mM NaF, 0.1 mM Na3VO4, 1 mM PMSF, 1 mM benzamidine, 1 mM iodoacetamide, 1 mMphenantroline). Protein concentration in the supernatant was determined by Bicinchoninic Acid assay (BCA) protein assay (BCA: Pierce Biotechnology, Rockford, Illinois, US), and lysates were adjusted to equivalent concentrations with lysis buffer. Aliquots of 10 mg of total brain lysate were then separated on Sodium Dodecyl Sulphate - PolyAcrylamide Gel Electrophoresis (SDS-PAGE). Proteins were transferred to Sodium Dodecyl Sulphate - PolyAcrylamide Gel Electrophoresis (PVDF) membranes that were blocked overnight at 4 °C with 5% non-fat dried skimmed milk in TTBS (TBS with 0.05% Tween 20). Incubation with primary specific antibodies against NLRP3 (1: 1000 dilution) and horseradish peroxidase-conjugated secondary antibodies was performed in blocking solution for 1 h at room temperature. Immunoreactive bands were visualized by SuperSignal West Pico Chemiluminescent substrate kit (Pierce Biotechnology, Rockford, Illinois, US). The same blots were stripped and re-probed using anti-GABDH monoclonal antibody to confirm equal loading of proteins in all lanes. Bands intensities were quantified on scanned images using Image J software (National Institute of Health, USA) to determine average pixel intensity.

3.2.6 Statistical Analysis

Analyses were performed with GraphPad (version 5.03, GraphPad Software Inc., CA, USA). Statistical comparisons were made of each antibody by age group. A one-way analysis of variance (ANOVA) was performed to compare the overall level of MHC class II antigen and NLRP3 inflammasome labeling among age groups. The post-hoc tests employed were t tests for two samples assuming unequal variances. Data obtained from Western blots were analysed with Statview software (Abacus Concepts) by t-Student test. Blots were revealed by Enhanced chemiluminescence (ECL) and autoradiography using beta-actin as a loading control. The autoradiographs shown are representative of four independent experiments. Bars represent the mean ± SD of four independent experiments. The chi-squared test was used to assess differences between the studied groups of cows.

3.3. RESULTS

3.3.1 Morphology and Immunohistochemistry

The morphological findings were similar to those previously described (De Biase et al., 2017) and revealed mostly moderate to severe satellitosis and severe neuronal lipofuscin accumulation in aged brains. Immunohistochemistry was performed to show the expression and distribution of the NLRP3 and MHC II antibody in the brains of young and aged bovine. MHC class II staining pattern was localized to endothelial cells and microglial cells that displayed a ramified morphology (figure 3.1 a-c). The prevalence of MHC II–positive microglial cells in studied groups was as it follows: group A (aged): 80% high and 20% moderate; group B (adult), 15% high, 85% moderate and 5% mild; group C (young), 95% negative and 5% mild. There was a statistically significant positive

association between age and the presenceof MHC II–labeled microglial cells (p<0,0001) (fig. 3.3 a).

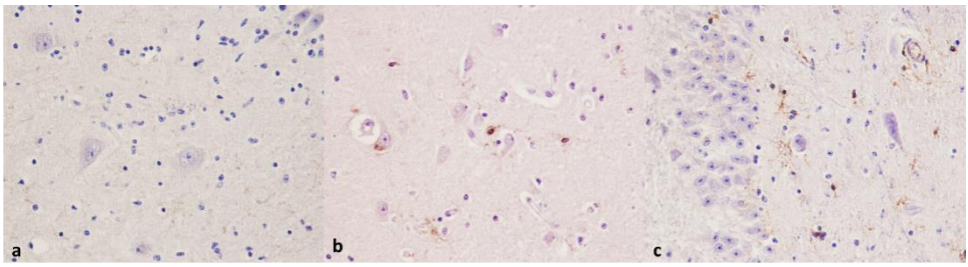

Fig. 3.1 Immunohitochemical expression of MHC II, hippocampus, dentate gyrus, cows. Young (a), adult (b) and aged animals (c)

NLRP3 immunoreactivity was nearly absent in young animals (group C) (fig 3.2 a). Conversely, NLRP3 immunoreactivity was detected in aged and adult animals (group A and B) as brown-ish intracytoplasmic granules mostly in neurons and microglial cells (fig 3.2 b and c). Similarly to MHC II expression, there was a statistically significant positive association between age and the presence of NLRP3-labeled cells (p<0,0001) (fig. 3.3 b). The prevalence of NLRP3–positive cells in the studied groups was as it follows: group A (aged): 90% high and 10% moderate; group B (adult): 30% high, 65% moderate and 5% mild; group C (young): 95% negative and 5% mild.

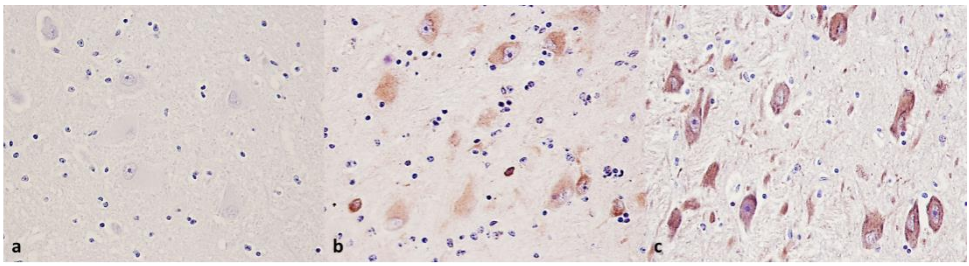

Fig. 3.2 Immunohitochemical expression of NLRP3, hippocampus, dentate gyrus, cows. Young (a), adult (b) and aged animals (c)

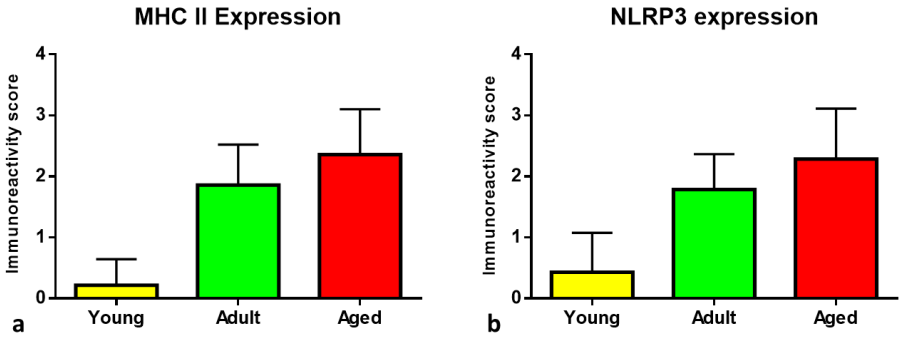

Fig. 3.3 ***Immunoreactivity score for (a) MHC II expression and (b) NLRP3 expression.*** *There is a statistically significant positive association between age and the presence of MHC II–labeled microglial cells and NLRP3 immunolabelled cells.Each value is* the mean ± SEM*(p<0,0001).*

Furthermore, we performed double-colour immunofluorescence in order to evaluate the possible association between NLRP3 expression, autophagy and increased ROS production. The overall expression of Beclin-1 as a marker for autophagy and SOD-1 as a marker for the antioxidant activity subsequent to ROS production was similar to what previously reported in this thesis (Chapter 2). TRITC-conjugated Beclin-1 expression appeared as a red, cytoplasmic fluorescence and it was significantly decreased in aged animals, but normal in younger animals. TRITC-conjugated SOD-1 expression apperared as a red, cytoplasmic, fluorescence and it was increased in the oldest animals while it appeared absent or mildly present in young animals. NLRP3 FITC-conjugated antibody was evident as a green, intracytoplasmic fluorescence and co-localization with either Beclin-1 or SOD-1 was evident as a yellow-orange fluorescence (fig 3.4 and fig 3.5).

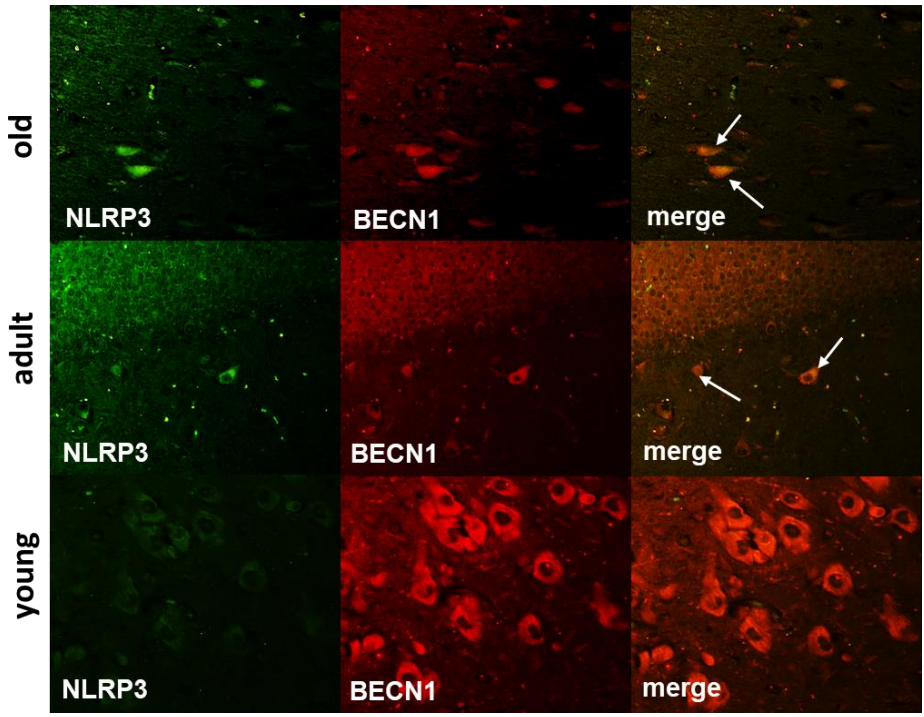

Fig. 3.4 Double color immunofluorescence, dentate gyrus, hippocampus, cow. *Green FITC immunofluorescence corresponds to NLRP3. Red TRITC immunofluorescence corresponds to Beclin 1 labeling. Yellow fluorescence indicates colocalization of NLRP3 and Beclin1 (arrows).*

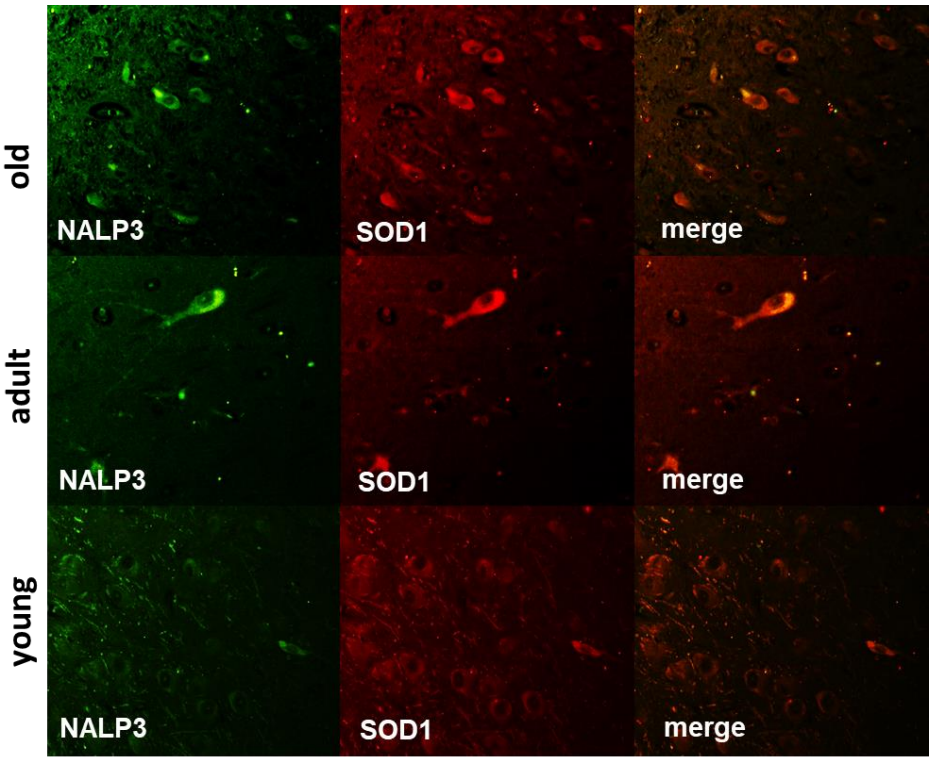

Fig. 3.5 Double color immunofluorescence, dentate gyrus, hippocampus, cow. *Green FITC immunofluorescence corresponds to NLRP3. Red TRITC immunofluorescence corresponds to SOD1 labeling. Yellow fluorescence indicates colocalization of NLRP3 and SOD1.*

3.2 Western blot analysis

We evaluated the expression levels of NLRP3 (represented as 118 kDa band) mainly to confirm an increased expression brain from elder cows compared to young animals. As expected, our results, normalized for GABDH, showed that NLRP3 expression was significantly higher in the aged animals (group A and B) compared with the young animals (group C) (*** $P < 0{,}001$ vs control) (Fig. 3.6).

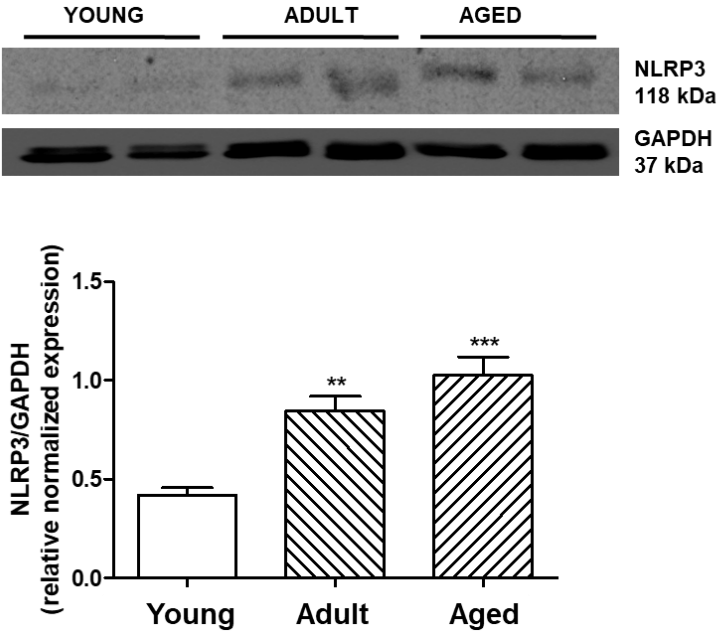

Fig. 3.6 Western blot analysis for NLRP3 expression. NLRP3 expression is significantly higher in the aged animals (group A and B) compared with the young animals (group C) (*** P < 0,001 vs control)

3.4. DISCUSSION

The term *neuroinflammation* is currently used to describe the inflammatory response originated in the CNS after suffering an injury (Morales et al., 2014). Neuroinflammation is characterized by an increase in microglial activation and by the upregulation of inflammatory cytokines such as interleukin-1β (IL-1β) (Deleidi et al., 2015). Albeit neuroinflammation plays an important role in the pathogenesis of many neurodegenerative diseases (Deleidi et al., 2015), it is widely accepted that neuroinflammatory changes also occur with age (Ward et al., 2015). Our results indicate an increased microglial activation in the hippocampus of aged cows that didn't show any apparent neurological disorder. Of the three age groups studied, the old and the adult one displayed a significantly higher level of MHC class II antigen expression. Microglia are often referred to as the resident innate immune cells of the CNS because, similarly to macrophages, they can provide the first and main form of active immune defense in the brain (Norden and Godbout, 2014).Microglia respond to and propagate inflammatory signals initiated at the periphery coordinating the immune response to infection (Hanisch and Kettenmann, 2007). When activated, microglia are capable of acquiring diverse and complex phenotypes which permits them to participate in the cytotoxic response, immune regulation and injury resolution (Ward et al., 2015). With normal aging, microglia develop an inflammatory phenotype revealing increased release of pro-inflammatory cytokines and an increased expression of MHC II and CD86, scavenger receptors (CD68), pattern associated recognition receptors, (e.g. toll-like receptors) and integrins (CD11b and CD11c) (Norden and Godbout, 2014). Interestingly, in the aged brain microglial activation is amplified and prolonged, which may be related to impairments in several key regulatory systems (Norden and Godbout, 2014). It has yet to be determined if the persistent activation of microglia is a normal aging event or it is due to a periodic stimulation of the immune system. However, several authors suggest that an increase in

activation level over time may severly alter the microglial responses to challenges, thus making the brain more susceptible to neurological damage and actively partecipating in the initiation and progression of neurodegenerative diseases (Fumagalli et al., 2011).The altered preservation ofcellular homeostasis is one of the most detrimental features of aging that lead to the activation of several defence systems. A recent growing body of evidence have suggested an instrumental role of inflammasomes in the pathophysiology of neuroinflammation during neuronal ageing, and its associated neurodegenerative diseases (Singhal et al., 2014).The NLRP3 inflammasome is by far the most widely studied complex in neurological diseases (as well as outside the CNS). Most studies have focused on NLRP3 function in microglia, although NLRP3 has also been proposed to function in neurons (Campan et al., 2012; Ramos et al., 2012). To our knowledge, this is the first study that investigate and describe the expression of NLRP3 inflammasome in bovine brains. Our results showed an increased expression of NLRP3 inflammasome in neurons and microglial cells of aged brains when compared with younger brains. These data are consistent with the recent scientific literature, indicating that the NLRP3 inflammasome is up-regulated in the brain as a result of aging (Singhal et al., 2014). We also investigated the potential interactions between NLRP3 inflammasome expression, ROS production and autophagy. SOD1 is an enzyme normally used by cells to protect themselves against oxygen free radicals (Fridovich, 1995). Consistent with previous findings (Chapter 2), we describe a neuronal overexpression of SOD1 in aged animals compared to younger animals. Moreover, double color immunofluorescence indicated an association between NALP3 and SOD1 expression. We suggest that the age-related overexpression of SOD1 may indicate an excessive dismutase activity due to an overproduction of ROS. The increased production of ROS may exceeds the antioxidant capacity of SOD1 resulting in deleterious peroxidative reactions, production of highly toxic hydroxyl radicals and ultimately oxidative stress-related injury (Chan, 1996; Jaarsma et al., 2000) and neuroinflammation (Singhal et al., 2014). Autophagy is an ancient, self-degradative, highly regulated housekeeping

mechanism which controls the non-specific degradation of cytoplasmic macromolecules and organelles via the lysosomal system. Autophagy preserves the cellular homeostasis by facilitating the removal of misfolded proteins and dysfunctional organelles (De Biase et al., 2017; Ravikumar et al., 2010). Normally, the autophagic uptake of dysfunctional mitochondria preventsthe excessive ROS production and the consequent activation of inflammasomes (Salimen et al., 2012). However, during aging, the autophagic capacity declines and increased ROS production may activate inflammasomes which provoke a low-grade inflammation inhibiting autophagy and accelerating the aging process (Salminen et al., 2012). For this study, Beclin 1 was used as a marker for autophagy and the results were similar to those previously described (De Biase et al., 2017). The overall expression of Beclin 1 was reduced in aged animals compared to younger animals. Surprisingly, several neurons of mature and aged animals showed an unexpected positive association between Beclin 1 and NLRP3 inflammasome expression. Our resultsjust apparently go against the grain, since several authors have recently suggested that the activation of inflammasomes lead to an induction of autophagy that work to limit inflammasome activity by physical engulfment (Martins et al., 2015). Although it is well estabilished that autophagy downregulates the inflammasome activity, their relationship may be more multifaceted (Salminen et al., 2012). In their pivotal work, Martins and colleagues realistically suggested that the role of autophagy in regulating the inflammasome may depend on time and context: in the absence of a danger signal, autophagy mayact to remove pro-IL-1β and inflammasome components from the cell, thus maintaining cellular homeostasis (Martins et al., 2015). The role of autophagy and inflammasomes in the aging of CNS and in CNS diseases has achieved substantial recognition and new researches are continually emerging (Walsh et al., 2014). Our study introduces intriguing observations, but it hasopened a plethora of research opportunities to investigate inflammasome and age-related changes in the bovine brain. Major steps forward would beto evaluate the peripheral and cerebral inflammatory and anti-inflammatory cytokines expression in order to determine the role of immune factors in the inflammasome activation

pathway; evaluate other autophagy markers such as LC3 or p62 to better define the relationship between inflammasome and autophagy machinery; investigate the possible association between the age-related accumulation of mutant protein aggregates such as Amyloid β or prion proteins and neuroinflammation. Therefore, it is of utmost importance a better understanding of the pathways by which microglia become dysregulated with age in order to improve our understanding of neuroinflammatory complications associated with age.

REFERENCES

1. Chan PH **Role of oxidants in ischemic brain damage.**Stroke 1996 Jun;27(6):1124-9.

2. Compan V, Baroja-Mazo A, López-Castejón G, Gomez AI, Martínez CM, Angosto D, Montero MT, Herranz AS, Bazán E, Reimers D, Mulero V, Pelegrín P **Cell volume regulation modulates NLRP3 inflammasome activation**. Immunity 2012; 37:487–500

3. De Biase D, Costagliola A, Pagano TB, Piegari G, Wojcik S, Dziewiątkowski J, Grieco E, Mattace Raso G, Russo V, Papparella S, Paciello O. **Amyloid precursor protein, lipofuscin accumulation and expression of autophagy markers in aged bovine brain**. BMC Vet Res. 2017 Apr 13;13(1):102.

4. Deleidi M,JäggleMandRubino G **Immune aging, dysmetabolism, and inflammation in neurological diseases.** Front.Neurosci. 2015; 9:172.doi: 10.3389/fnins.2015.00172

5. Glass CK, Saijo K, Winner B, Marchetto MC, Gage FH. **Mechanisms underlying inflammation in neurodegeneration**. Cell. 2010;140(6):918–34. pmid:20303880.

6. Franceschi C., Capri M., Monti D., Giunta S., Olivieri F., Sevini F. Panourgia MP, Invidia L, Celani L, Scurti M, Cevenini E, Castellani GC, Salvioli S. **Inflammaging and anti-inflammaging: a systemic perspective on aging and longevity emerged from studies in humans**. Mech. Ageing Dev. 2007;128:92–105.

7. Fridovich, I. **Superoxide radical and superoxide dismutases**. Annu. Rev. Biochem. 1995;64:97–112.

8. Fumagalli, M, Lecca D, Abbracchio MP. **Role of purinergic signalling in neuro-immune cells and adult neural progenitors.**Frontiers in Biosci 2011;16,:2326-2341

9. Hanisch UK, Kettenmann H. **Microglia: active sensor and versatile effector cells in the normal and pathologic brain**. Nat Neurosci. 2007;10:1387–1394.

10. Jaarsma D, Haasdijk ED, Grashorn JA, Hawkins R, van Duijn W, Verspaget HW, London J, Holstege JC.**Human Cu/Zn superoxide dismutase (SOD1) overexpression in mice causes mitochondrial vacuolization, axonal degeneration, and premature motoneuron death and accelerates motoneuron disease in mice expressing a familial amyotrophic lateral sclerosis mutant SOD1**. Neurobiol Dis. 2000 Dec;7(6 Pt B):623-43.

11. Latz E, Xiao TS, Stutz A. **Activation and regulation of the inflammasomes.** Nat Rev Immunol. 2013;13(6):397–411.

12. Lòpez-Otin C, Blasco MA, Partridge L, Serrano M, Kroemer G. The hallmarks of aging. Cell 2013; 153:1194–1217.

13. Luo XG, Ding JQ, Chen SD **Microglia in the aging brain: relevance to neurodegeneration**. Mol Neurodegener. 2010 Mar 24;5:12.

14. Martinon F, Burns K, Tschopp J. **The inflammasome: a molecular platform triggering activation of inflammatory caspases and processing of pro IL-beta.** Mol Cell. 2002;10(2):417–26.

15. Martins JD, Liberal J, Silva A, Ferreira I, Neves BM, Cruz MT. **Autophagy and inflammasome interplay.** DNA Cell Biol. 2015 Apr;34(4):274-81.

16. Montecino-Rodriguez E., Berent-Maoz B., and Dorshkind K. **Causes, consequences, and reversal of immune system aging**. J. Clin. Invest. 2013;123:958–965.

17. Morales I, Guzmán-Martínez L, Cerda-Troncoso C, Farías GA, Maccioni RB **Neuroinflammation in the pathogenesis of Alzheimer's disease. A rational framework for the search of**

novel therapeutic approaches. Front Cell Neurosci. 2014 Apr 22;8:112.

18. Norden DM, Godbout JP. **Microglia of the Aged Brain: Primed to be Activated and Resistant to Regulation.** Neuropathol Appl Neurobiol. 2013 Feb; 39(1): 19–34.

19. Ramos HJ, Lanteri MC, Blahnik G, Negash A, Suthar MS, Brassil MM, Sodhi K, Treuting PM, Busch MP, Norris PJ, Gale M Jr.**IL-1β signaling promotes CNS intrinsic immune control of West Nile virus infection.**PLoS Pathog. 2012 8, e1003039

20. Ratsimandresey RA, Dorfleutner A, Stehlik C. **An Update on PYRIN Domain-Containing Pattern Recognition Receptors: From Immunity to Pathology**. Front Immunol. 2013;4:440.

21. Ravikumar B, Sarkar S, Davies JE, Futter M, Garcia-Arencibia M, Green-Thompson ZW, Jimenez-Sanchez M, Korolchuk VI,Lichtenberg M, Luo S, Massey CO, Menzies FM, Moreau K,Narayanan U, Renna M, Siddiqi FH, Underwood BR, Winslow AR,Rubinsztein DC. **Regulation of mammalian autophagy in physiology and pathophysiology.** Physiol. Rev. 2010;90:1383-1436.

22. Salminen A, Kaarniranta K, Kauppinen A.**Inflammaging: disturbed interplay between autophagy and inflammasomes.**Aging (Albany NY). 2012 Mar;4(3):166-75.

23. Singhal G, Jaehne EJ, Corrigan F, Toben C, Baune BT.**Inflammasomes in neuroinflammation and changes in brain function: a focused review.** Front Neurosci. 2014 Oct 7;8:315.

24. Sheffield LG, Berman NE. **Microglial expression of MHC class II increases in normal aging of nonhuman primates**. Neurobiol Aging. 1998 Jan-Feb;19(1):47-55.

25. Walsh JG, Muruve DA, Power C. **Inflammasomes in the CNS**. Nat Rev Neurosci. 2014;15(2):84–97

26. Ward RJ, Dexter DT, Crichton RR.**Ageing, neuroinflammation and neurodegeneration.**Front Biosci (Schol Ed). 2015 Jun 1;7:189-204

27. Wen H, Miao EA, Ting JP**. Mechanisms of NOD-like receptor-associated inflammasome activation**. Immunity. 2013;39(3):432–41

28. Zhong Z, Sanchez-Lopez E, Karin M **Autophagy, NLRP3 inflammasome and auto-inflammatory/immune diseases** Clin Exp Rheumatol 2016; 34 (Suppl. 98): S12-S16.

Conclusions

Aging is the ineluctable, time-dependent, gradual and progressive impairment in physiological organ function and tissue homeostasis that eventually leads to death. Aging is a universal process, common among different species and probably with a similarly universal regulation mechanism. The understanding of the mechanisms underlying the cerebral and muscular aging in humans and in animals has progressed rapidly in recent years. Animal models have represented convenient and clinically relevant tools in this research field. Interestingly, large animals such as bovine are rarely used as animal models for aging study, even though they are more similar to humans in relation to brain size and lifespan and could be therefore essential to investigate complex patho-physiological mechanisms relating to neurodegenerative diseases, infectious neuropathologies and muscular disorders. In study n° 1 we aimed to describe the age-related morphological changes of bovine brains and skeletal muscle. Although the results regarding brain changes are similar to those previously described in other species, some of the most striking findings (i.e. the age-related lipofuscin accumulation) led us to further investigate the molecular pathways underlying these alterations. Moreover, we describe the first time some of the most important consequences of muscle aging in cows, suggesting new insights for a comparative approach on the study of this concerning healthcare. In study n°2 we aimed to define if the progressive age-related decline of autophagic and lysosomal activity may also be responsible for the continuous intraneuronal accumulation of lipofuscin, or “age pigment”. For this study, we surveyed the expression of autophagic markers, the accumulation of pathologic proteins and lipofuscin. We also investigated the possible relationship between lipofuscin accumulation and increased reactive oxygen species production. Our results showed that autophagy is impaired in aged bovine brains and that exist an age-dependent increase of intraneuronal accumulation of pathologic proteins. According to our results, we assume that the ineluctable formation and accumulation of lipofuscin in aged brains seems to be associated with an impaired function of autophagy and an increased

reactive oxygen species production. The indigestible nature of this material is associated with progressive diminution of lysosomal function, which has secondary effects on many different cellular activities. We thus believe that the accumulation of this age pigment is a very important—perhaps even central—aspect of the phenomenon of aging. In study n°3 we dedicated our researches to explore one of the most recognized effects of brain aging: the "***neuro-inflammaging***", an age-induced pro-inflammatory environment that have a critical role in the development of several neurodegenerative disorders. For this purpose, we evaluated the immunohistochemical and molecular expression of the inflammasome, a protein complex responsible for the inflammation and its relationship with autophagy and the increased ROS production. Our results revealed that aged bovine show an increased production of inflammasomes, probably due to an increased ROS production. Conversely, autophagy seems to have a protective role for the cell limiting inflammasome activity by physical engulfment. This thesis display results that are consistent with studies previously performed in other animal models as well as humans. However, we'd like to highlight that bovine may potentially be a pivotal animal model for brain aging studies. We also firmly believe that morphology always represents a crucial approach for any kind of interpretation of the lesions or to explain new molecular pathways of the diseases.